GEOPHYSICAL PROSPECTION AT CAISTEAL MAC TUATHAL, PERTHSHIRE,

SCOTLAND

by

MICHAEL ROBERT SAMUEL LUKAS

(Under the Direction of Ervan Garrison)

ABSTRACT

Topographic, magnetometry, and ground penetrating radar surveys were
conducted at the potential Iron Age hillfort of Caisteal Mac Tuathal in Perthshire,
Scotland to determine structural extents within, and propose areas of interest for future
studies at, the site This survey concluded the terrace at the base of the southern slope and
the area circumscribed by the visible rampart features and cliff faces to be void of
potential archaeological anomalies, and no potential structures or entrances were located
along the southwestern rampart. However, radar and magnetic anomalies interpreted as a
potential structure or "platform", and an entrance through the rampart, together with a
secondary structure were observed along the northwestern rampart. The details of these
potential structures are poorly understood because ground-truthing was not conducted
during this study. Regardless, this geophysical exploration of Caisteal Mac Tuathal has
improved our understanding of the site and structures therein.

INDEX WORDS: Shallow Geophysics, Archaeogeophysics, Ground Penetrating
                Radar, Magnetometry, General Packet Radio Service, Caisteal Mac
                Tuathal, Drummond Hill, Perthshire, Scotland, Iron Age, Hillfort

GEOPHYSICAL PROSPECTION AT CAISTEAL MAC TUATHAL, PERTHSHIRE,

SCOTLAND

by

MICHAEL ROBERT SAMUEL LUKAS

B.A., Willamette University, 2013

A Thesis Submitted to the Graduate Faculty of The University of Georgia in Partial

Fulfillment of the Requirements for the Degree

MASTER OF SCIENCE

ATHENS, GEORGIA

2016

GEOPHYSICAL PROSPECTION AT CAISTEAL MAC TUATHAL, PERTHSHIRE,

SCOTLAND

by

MICHAEL ROBERT SAMUEL LUKAS

Major Professor: Ervan Garrison

Committee: Jennifer Birch
               George Brook

Acknowledgements

First and foremost, I would like to thank Dr. Ervan Garrison[1], Dr. Nicholas Dixon[2], and Jackie Hoyt[3] for their assistance with data collection in Scotland. Gratitude is also owed to my academic and thesis advisory committee – Dr. Ervan Garrison, Dr. Jennifer Birch[4], and Dr. George Brook[5] – for their help in the development and pursuance of my thesis topic and studies at the University of Georgia, and to Dr. Dean Goodman[6] for his invaluable advice on, and help with, data processing with GPR_Slice.

This research was funded in part by the Joseph W. Berg Scholarship in Geophysics Fund and the Gilles and Bernadette Allard Geology Award Fund, both managed by the Department of Geology at the University of Georgia.

Table of Contents

List of Figures

List of Tables

Figure 1: Site location. (a) Map of the British Isles; (b) Loch Tay and Drummond Hill, Perthshire, Scotland; and (c) potential hillfort of Caisteal Mac Tuathal at Drummond Hill – yellow polygon high-lights the upper terrace (modified after Google, Inc., 2014. Compiled from Christison, 1900; RCAHMS, 1956; Dalland and Wessel, 2011).

1. Objectives

This research presents three topics regarding the unexcavated minimally surveyed site of Caisteal Mac Tuathal in Perthshire, Scotland (Fig. 1): a comprehensive literature review of the site's archaeological context; a study of remote sensing methods that could be utilized in studies of this shallow, remote, and topographically difficult to survey site; and a discussion of proposed structural extent and areas of interest for future studies within the site based on analyses of topographic, magnetometry, and ground penetrating radar data.

2. Archaeological Context

2.1. Pre-Roman Iron Age in Scotland

The Iron Age Celts in Scotland were insular groups of peoples who, along with

the rest of Britain and Ireland, became increasing isolated during the Early Iron Age. This

isolation is evident in the material remains and historical records of the British Isles

Celtic peoples – particularly their architecture, art (both decorative and utilitarian), and

warfare (Cunliffe, 2005:124). This cultural insulation and geographic isolation of the

British Isles from continental Europe resulted in a later transition from the Bronze Age to

Iron Age (Cunliffe, 1999; Harding, 2004; Armit, 2005; Cunliffe, 2005:32).

2.1.1. Celtic Culture

The insular nature of Celtic societies in Iron Age Scotland led to a piecemeal

adoption of technology, structural and artistic morphologies, and socioeconomic and

political structures only when needed or wanted – a phenomenon dependent upon the

social, economic, and political contexts of the indigenous groups (Cunliffe, 1999;

Harding, 2004). Consequently, Celtic culture in Iron Age Scotland developed uniquely in

comparison to southern Britain and continental Europe, and is commonly associated with

a long Iron Age (Table 1). The Scottish Long Iron Age is the timeline referenced in this

research.

2.1.1.1. Material Culture

Material culture in Iron Age Scotland was both utilitarian and decorative, despite

the prevalence of undiagnostic utilitarian artefacts throughout the Early Iron Age of

eastern Scotland (Harding, 2004:106-7). Pottery in particular proved especially undiagnostic with its coarse and undecorated typology and its sparseness across Early Iron Age eastern Scotland – an indication of its seemingly cultural insignificance (Harding, 2004:106; Cunliffe, 2005:118). However, the islands and islets of Scotland's Atlantic Façade contained a rich pottery tradition (Cunliffe, 2005:118), a likely continuance of its Neolithic grooved ware and Bronze Age beaker traditions (Fig. 2; Richards, 2005). In contrast, copper and bronze metalworking has proven culturally significant throughout Scotland, originating with the adoption of Hallstatt C_1 bronze

Table 1: Timeline of the European, Northern Britain, and Scottish Iron Ages
(Harding, 2004; Armit, 2005; Cunliffe, 2005, Noble et al., 2013).

	Europe	N. Britain (Pottery)	Scotland (The Long Iron Age)	Key Events:
800 B.C.	Hallstatt C	EIA-I	Late Bronze Age	A.D. 43 – Treaty between Roman fleet and Orcadian chieftans. (Cunliffe, 2005:219)
600 B.C.	Hallstatt D	EIA-II	Early Iron Age (EIA)	A.D. 79 – Roman invasion of Scotland begins under the direction of Gnaeus Julius Agricola. (Armit, 2005:95)
300 B.C.	La Tène I			
		MIA		A.D. 83 – Battle of Mons Graupius; terminus of Roman invasion. (Armit, 2005:102)
	La Tène II		Middle Iron Age (MIA)	
100 B.C.	La Tène III	LIA-I		A.D. 120s – Roman retreat to Hadrian's Wall. (Armit, 2005:103)
0	Roman	LIA-II		A.D. c.140 – Roman advance to the Clyde-Forth line; construction of the Antonine Wall. (Armit, 2005:103)
A.D. 79		Roman Iron Age	Late Iron Age (LIA)	
A.D. 400			Pictland	A.D. c.165 – Roman retreat to Hadrian's Wall. (Armit, 2005:103)

Gündlingen swords and horse gear, both of which spread throughout Scotland by c.800-750 B.C. (Cunliffe, 2005:449) and were quickly morphologically modified to suit indigenous needs – occurring in hoard deposits rather than accompanying inhumations (Cowen, 1967; Cunliffe, 2005:449).

Ironworking was not adopted in Scotland until c.450 B.C. at the earliest, and likely developed an insular La Tène technology in the same manner as the Gündlingen swords (Cunliffe, 2005:465-7). The Middle Iron Age saw increased Scottish trade with the continent, either directly or diffusively through southern Britain, resulting in the adoption of goods and wares of Mediterranean origin and style by the Scottish Celtic elite, with a particular preference for their use in feasting, drinking, and personal ornamentation. However, the lack of extensive trade routes throughout western and northern Scotland resulted in limited trade, and an extensive concentration of these goods and wares in eastern Scotland (Harding, 2004:192; Cunliffe, 2005:597).

2.1.1.2. Ritual and Religion

Ritual and religion in Early to Middle Iron Age Scotland likely differed greatly from that of southern Britain and continental Europe. However, little evidence for ritualistic or religious behavior has been recovered due to the rarity of recovered burials and ritual deposits in much of Scotland, and thus any claims of a difference is at present mere speculation (Harding, 2004:297; Armit, 2005:80; Cunliffe, 2005:597). This lack of direct evidence is paralleled by similar problems in studies of the Iron Age Ireland (McCormick, 2009:410).

Figure 2: Ceramic-rich regions of the British Iron Age (modified after Cunliffe, 2005:Fig. 5.10).

2.1.1.3. Warfare

Warfare among the Iron Age Celts in Scotland differed from the nature of warfare

on the continent. Despite the regular occurrence of swords, spears, and slings in the

archaeological records of Scotland and continental Europe (Armit, 2005:45), cavalry, body armor, and archery were used differently in Scotland. The Celts of Scotland and southern Britain continued to use chariots in warfare long after these were abandoned on the continent in favor of cavalry (Cunliffe, 1999). However, their use in battle has been questioned, with many concluding they were used only as a show of force prior to, and possibly during, battles; they likely were not used as weapons (Cunliffe, 1999:254-5; Armit, 2005:45). Seemingly in response to the overwhelming victories achieved by Agricola and his troops during the Roman Conquest, the last recorded use of chariots in Celtic Scotland conflicts was noted by Tacitus at the battle of Mons Graupius in A.D. 84 (Cunliffe, 1999:255). Continental Celts frequently used iron and bronze plate body armor and helmets, along with chainmail armor at later dates, and archery during conflict. However, there is little evidence suggesting the use of body armor by Scottish Celts and no evidence for their use of archery in conflict (Cunliffe, 1999:93-8; Armit, 2005:45).

2.1.2. Defensive Settlement Types

The Iron Age in Celtic Scotland presented differing settlement types (Fig.3). Of particular interest are those investigated here: crannogs, homesteads, hillforts, and brochs. Each of these settlement types exist in large numbers north of the Clyde-Forth line (the Antonine Wall) – a region of sociopolitical, economic, and geographic boundaries that was impacted by a Roman Conquest distinct and distant from that of Celtic societies in southern Britain and continental Europe.
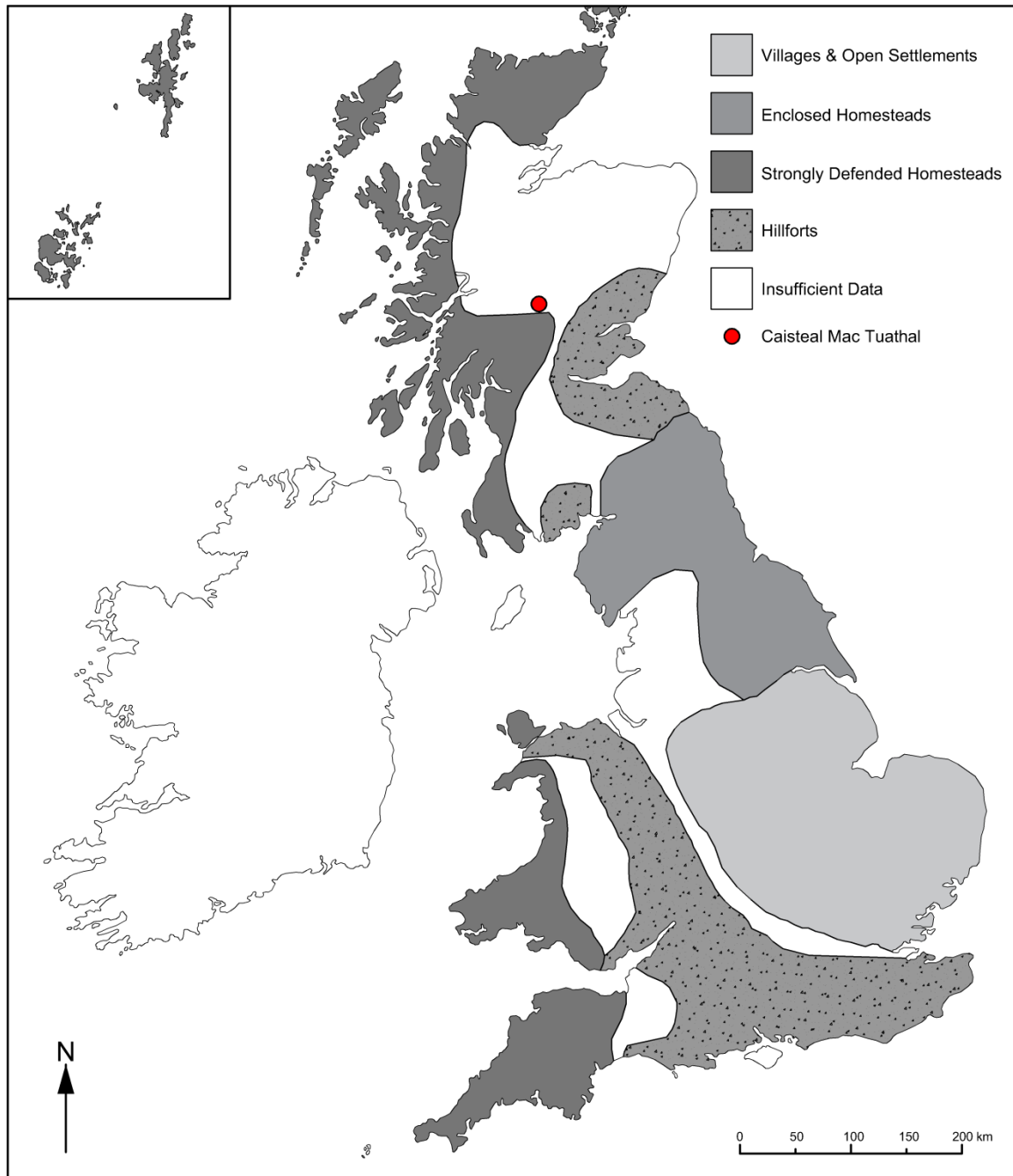
Figure 3: Predominate settlement types in Early Iron Age Britain, c.2150 BP (modified after Cunliffe, 2005:Fig. 21.6).

2.1.2.1. Crannogs

Crannogs are offshore, timber roundhouses typically constructed on artificial

islands or pilings and connected to the shoreline by defensible bridges (Fig. 4; Armit,

2005:33). Despite their expansive distribution through the Late Bronze through Early Historic (Middle Iron Age) periods in coastal and lacustrine Ireland and, more commonly, highland and southwest Scotland (Munro, 1882; Harding, 2004:106; Armit, 2005:33), their origins may lay in the Neolithic: Eilean Dòmhnuill in Loch Olabhat on North Uist

Figure 4: The Scottish Crannog Centre (reproduced with permission of the photographer, Nicholas Dixon).

in the Outer Hebrides, Scotland is one of the earliest known crannogs, dating to c.3,650 B.C. (Armit, 2005:33-4). Crannogs may have served as defensive homesteads designed to protect the semi-isolated, single-family domestic units common in the Late Bronze Age through Roman Incursion in Scotland, particularly between the Tabular Hills and Grampian Highlands (Cunliffe, 2005:322). However, compared to palisaded and ring-ditch homesteads, the required energy expenditure for their construction, along with their increased vulnerability to fire and siege due to shore proximity, undermine most security reasons for their construction (Armit, 2005:34).

In Scotland, lacustrine crannogs likely served as self-sufficient homesteads for farmers, herders, and gatherers, as demonstrated by the recovery of grains, seeds, nuts, animal dung, and insects during the excavation of Oak Bank in Loch Tay, Perthshire (Dixon, 1982; Armit, 2005:33-4), investigations into crannogs of Loch Awe (Harding, 2004:103), and palynological evidence for decreased forest cover in Scotland by c.300-200 B.C. (Dumayne-Peaty, 1998). Modern analogs at marine crannog sites (e.g.: on the

Beauly Firth; Hale, 2000) indicate tide levels made them susceptible to flooding, lending credence to their possible use for access to inlets and seas for fishing, trade, and travel (Harding, 2004:106).

2.1.2.2. Homesteads

Homesteads were particularly common during the Iron Age in central Scotland between the Tabular Hills and Grampian Highlands. With the single family unit being the most common social configuration, these roundhouse

Figure 5: Aisled roundhouse; *Machair Leathann. Excavation photograph. Site B fully excavated, looking S.* **(reproduced with permission: Copyright – Historic Environment Scotland; RCAHMS, 1957)**

homesteads were commonly long-lived and underwent multiple phases of construction, typically initially enclosed by palisades in early phases then shifting to bank and ditch enclosures in later phases (Fig. 5; Cunliffe, 2005:322). These homestead communities frequently belonged to subsistence economies based on agriculture and animal husbandry (Cunliffe, 2005:443), and have few archaeological indicators for social stratification or a centralized social structure, though invading Romans observed tribal confederacies – indicatory of common political and socioeconomic purposes – c. AD 79 (Armit, 2005:45; Cunliffe, 2005:322-3). Ring-ditch houses were common among Scottish homesteads, though it is possible they simply served as animal byres rather than places of residence (Reynolds, 1982:53-4).

2.1.2.3. Hillforts

Following Armit (2007:26) and Cook (2011:211), the term 'hillfort' is broadly defined in this research, encompassing a variety of enclosed hilltop sites, including duns ("dun" is Gaelic for fort [Lenfert, 2013:125]; e.g.: Dun Raouill [Raven & Shelley, 2003], Dun Geilbt [Graham, 1951]), promontory forts (e.g.: Burghead [Armit, 2003], Loch Knowe [RCAHMS, 1994]), and "traditional" hillforts (e.g.: Barra Hill

Figure 6: Hillfort; *Oblique aerial view of Woden Law centered on the fort* **(reproduced with permission: Crown Copyright - Historic Environment Scotland; RCAHMS, 2015b).**

[Cook, 2012], Dunsinane Hill [Christison, 1900]). Brochs will be discussed separately.

Hilltop settlements in Scotland continue the roundhouse tradition, and possibly appear as early as c.1,000 B.C. (Fig. 6; Armit, 2005:43). However, the first fortified hilltop occupation centers appear c.800-700 B.C., and frequently contain evidence for occupation and reoccupation through c. A.D. 100, though evidence for permanent occupation is often lacking (Cunliffe, 2005:364, 402). Hillfort use in Scotland was minimal in comparison to southern Britain (Harding, 2004:159). Ninety percent of known Scottish hillforts are located between the Rivers Tyne and Forth (Armit, 2005:46). Some Scottish hillforts evolved from palisaded enclosures, most initially developed as rubble-and-earth cored, drystone-walled ramparts bonded by horizontal timbers – the latter of which is distinctive to Scottish hillforts, despite the region's proximity to southern Britain

and continental Europe and their architectural influence. Hillforts in continental Europe and southern Britain utilized vertical timbers alongside horizontal timbers for structural support (Cunliffe, 2005:363). By c.400-300 B.C., many of Scotland's hillforts were abandoned, and those that remained occupied had expanded from the Early Iron Age's small, utilitarian defensive hillforts into developed hillforts similar to, though on a smaller scale than, oppida

Figure 7: Broch; *Oblique aerial view centered on the Broch of Gurness, taken from the NE* **(reproduced with permission – Crown Copyright – Historic Environment Scotland; RCHAMS, 2009)**

(Cunliffe, 2005:388). Most of these remaining hillforts were abandoned by c.200 B.C. (Armit, 2005:44), though by AD 79 occupied hillforts increased to approximately twenty percent of the known site assemblage (Armit, 2005:56; Cunliffe, 2005:401).

2.1.2.4. Brochs

Brochs are circular, multi-level drystone towers commonly found throughout the Scottish highlands and islands during the Iron Age (Fig. 7; Armit, 2005:35). Thought to have developed out of the Atlantic Roundhouse tradition, the earliest example of broch architecture appears c.600 B.C. in the Orkney Islands as thick-walled, single-level drystone roundhouse (Armit, 2005:37). The roundhouse at Bu, Orkney exemplifies the thick-walled architecture, but lacks the galleries, cells, stairs, and timber trusses for multilevel habitation associated with broch towers (Cunliffe, 1999: 161; Armit, 2005:37-

8). Broch towers appear in the Scottish archaeological record by c.400 B.C. (Armit, 1992; Armit, 2005:37) and likely originated in the Caithness-Orkney region, then spread south along the Atlantic Façade (Cunliffe, 2005:335) where they were readily adopted throughout the Scottish highlands and islands (Armit, 2005:37). It is thought that brochs initially developed as symbols of status – a statement supported by the heavy use of timber in Orkney brochs despite the archipelago's scant forests (Davidson & Jones, 1990: 26-7; Armit, 2005:37; Woodbridge et al., 2014).

Broch architecture evolved c.200-100 B.C. to include a more expansive settlement pattern, e.g.: the Broch of Gurness in Orkney and Old Scatness in Shetland (Armit, 2005:38-9). These broch villages were concentrated along the Atlantic Façade and northern islands, serving as evidence for a more centralized society with increased social controls (Armit, 2005:39). However, the defensive nature of brochs and broch villages was unlikely the result of conflict from population stressors, as evidenced by their typical self-sufficient nature and proximity to quality farmland and wild resources (Fojut, 1982; Cunliffe, 2005:335-7).

2.1.3. Evolution of Defensive Settlements in Celtic Scotland

The Late Iron Age in Scotland was typified by small, enclosed homesteads. However, this settlement type was prone to seemingly anomalous settlements such as the brochs and duns in lowland Scotland (Harding, 2004:187). These "anomalous" settlements appeared by the first and second centuries A.D., were likely constructed in response to Roman contact, and were possibly the result of a temporary economy based on prestige goods obtains from Romans and Romanized settlements south of Hadrian's Wall (Harding, 2004:187-8). North of the Clyde-Forth line, and later the Antonine Wall,

small, enclosed homesteads were common. Frequently associated with these homesteads were souterrains – underground structures that may have been used for defensive purposes (Warner, 1980; Watkins, 1980) or surplus storage (Armit, 1999). Despite their widespread use, souterrains in Scotland appear to have fallen into disuse or were infilled by the end of the second century A.D., although the lack of 3rd-4th century A.D. Roman material makes the establishment of a closed chronology difficult for the souterrains and their associated homesteads for this period (Harding, 2004:198).

The late Iron Age Pictish period c. 4th-5th centuries A.D. saw the return of hillfort settlements to Scotland, with refortification and expansion of Early Iron Age hillforts to nuclear forts common (Harding, 2004:233-5). Numerous hillforts and nuclear hillforts have been identified throughout western Scotland and Proto-Pictish in eastern Scotland (Noble et al., 2013:1141). However, little detailed research into proto- and later Pictish hillforts has been conducted, causing Pictish scholars to use those of the Scots in western Scotland, the coastal and promontory forts along the North Sea, and, more recently, the newly identified Pictish ringforts as contemporary analogs for sociopolitical analyses (Lane & Campbell, 2000; Noble et al., 2013:1141-2). However, it is of note the hillforts and nuclear hillforts of Pictland are significantly smaller than the hillforts and citadels in Scotland south of the Antonine Wall (Harding, 2004:232-3; Noble et al., 2013:1141). Crannogs are also present in Pictish archaeology in Scotland, though the research of them has suffered from lack of thorough excavation similarly to hillforts; radiocarbon dating has been pursued for a few of the identified sites, but the little thorough excavation that has occurred has precluded detailed sociopolitical analyses therein (Noble et al., 2013:1140). The radiocarbon dates, however, indicate that construction on these Late

Iron Age crannogs began during the 1st-2nd centuries A.D., and occupation in evident

through the 6th-7th centuries, though evidence for continual, permanent occupation of the

sites is lacking due to erosion or site reconstruction processes (Harding, 2004:211-2).

2.1.4. Pre-Roman Conquest Celtic Economy

The Scottish Celts, although insular throughout its prehistoric and historic

periods, maintained extensive trading with southern Britain and northern Europe – the

latter both directly and by diffusion through southern Britain. During continental

Europe's Hallstatt D period c.600-500 B.C., societies in the British Isles experience a

general decrease in trade with the continent (Cunliffe, 2005:462). However, by c.450

B.C., contact and trade had increased to where local British and Scottish artisans began

adopting La Tène metallurgical practices (Cunliffe, 2005:465-7). Continental La Tène

culture greatly influenced craft design and artistry, but a decrease in contact and trade

c.350-100 B.C forced the development and expansion of indigenous artefact

morphologies and artistry within assemblages (Cunliffe, 2005:470), promoted the further

development of an insular La Tène, particularly in Scotland.

The last century B.C. in the British Isles saw an increase in trade with continental

Europe, likely due to Rome's conquest of Celtic continental Europe, indicated by an

increase in concentrations of such artefacts as "Gallo-Belgic and Armorican coins,

northwest French pottery, and Italian and Spanish amphorae" concentrations in the

archaeological record (Cunliffe, 2005:474-5). However, the Roman Conquest of Gaul

initially proved detrimental to British trade routes, with a decrease in general trade

between 58-52 B.C. (Caesar, 1982). Soon after Caesar's conquest of Gaul, however,

Roman contacts and their allies re-established trade routes and increased trade with

Britain, until the Roman Conquest of the islands began in A.D. 43 (Cunliffe, 2005:484).

2.2. Celtic Scotland and the Roman Conquest

2.2.1. Conquest of Britain

Rome's conquest of Gaul and subsequent incursion into southern Britain was

initially of little note to Celtic Scotland, where a general shift from hillforts and fortified

settlements to more open settlements occurred during the two centuries preceding A.D.

79, indicating a time of relative peace for the previously conflict-ridden region (Armit,

2005:56-7). However, Gnaeus Julius Agricola led Roman troops north of the Tyne-

Solway line in A.D. 79, starting the Roman Conquest of Scotland (Armit, 2005:95).

Within five years Agricola successfully completed the campaign with the defeat of Celtic

forces at Mons Graupius in the northeastern coastal Grampian Mountains (Fig. 8; Tacitus,

1942). Despite being located a significant distance south of contiguous Scotland's extent,

Mons Graupius was the farthest north Agricola and his troops advanced. However, this,

along with Agricola's recall from the front soon after the battle, did not preclude a

successful completion of the Roman sphere of influence in Scotland: a treaty for trade

and cooperation had already been signed by Agricola and the Orcadian chieftans in A.D.

43 (Cunliffe, 2005:219). Roman troops withdrew from northern Scotland to the Tyne-

Solway line in the A.D. 120s (Armit, 2005:103) possibly to support the construction of

Hadrian's Wall, A.D. 122-130 (Dumayne, 1994:220). By c. A.D. 140 Roman troops had

returned to central Scotland, stopping at the Clyde-Forth line and constructing the

Antonine Wall. However, within 25 years the Roman military withdrew to Hadrian's
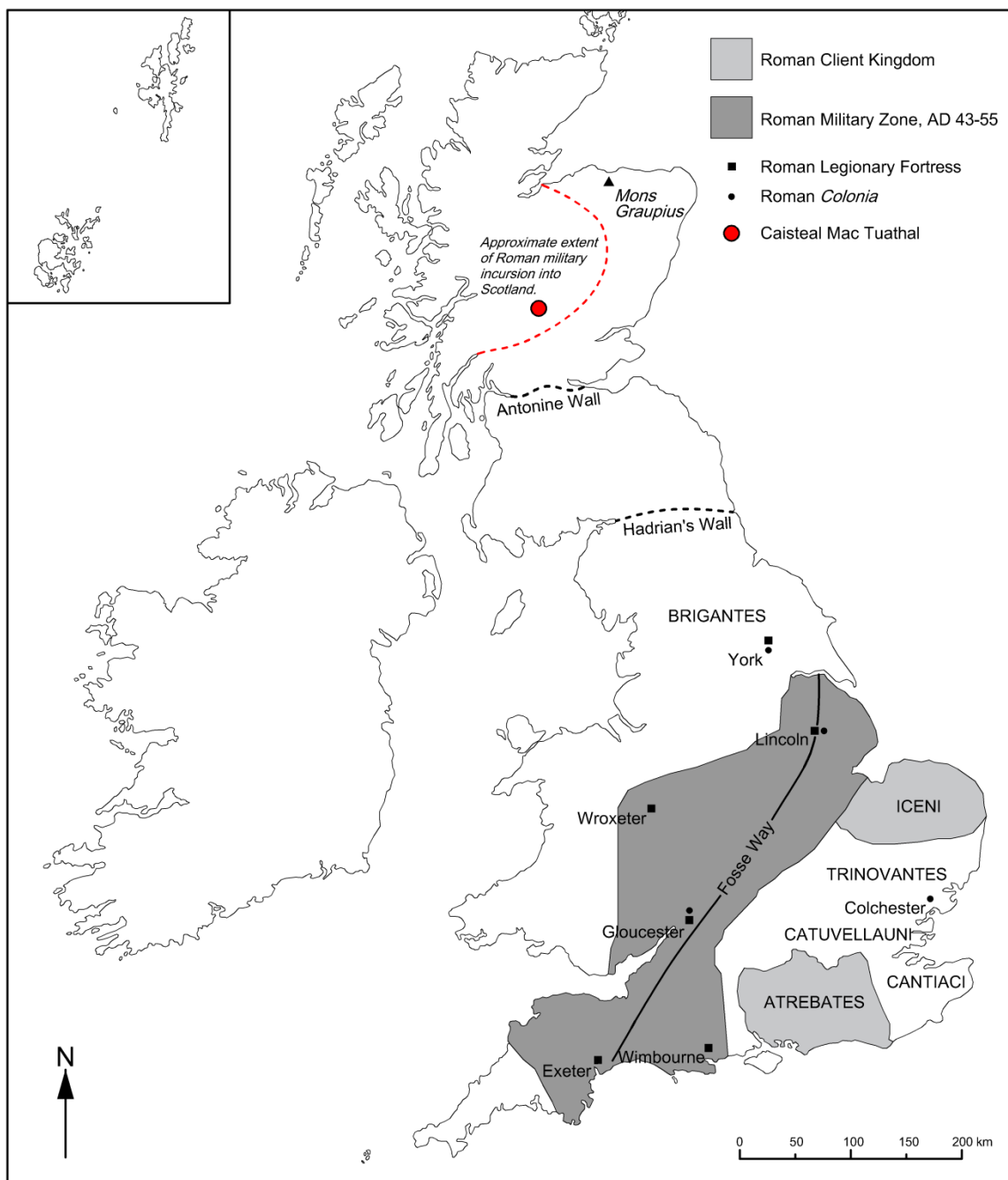
Figure 8: Roman conquest in Britain, 1st Century A.D. (modified after Cunliffe, 1999:Fig.198).

Wall for the last time, never again returning to the north as an occupation force (Armit, 2005:103).

2.2.2. Extent of Romanization

The Roman historian Tacitus accompanied Agricola during his campaign, writing about the Celtic peoples and Agricola's battles in *Agricola* (1942). He described a tribal Celtic society in Scotland, as evidenced by the number of indigenous chiefs directing combat during battle with Agricola and the Roman army (Armit, 2005:45). This historical notation provides greater detail of the sociopolitical environment in Middle and Late Iron Age Scotland than the presently known archaeological record (Cunliffe, 2005:322) – a characteristic that hinders archaeological corroboration of the historical record. The tribal nature of the Scottish Celts likely accounts for the distribution of elite settlements and imported goods throughout Scotland, with large concentrations of Roman artefacts at Trapain Law in East Lothian, Fairy Knowe in Perthshire, Leckie in Stirlingshire, and Hurley Hawkin in Angus indicating Romanization north of the Tyne-Solway line/Hadrian's Wall c. A.D. 79-165 (Harding, 2004:192). Proposed elite settlements at Torwoodlee, Selkirkshire (Piggott, 1951), Leckie (MacKie, 1982), and Fairy Knowe (Main, 1998) likely served as indigenous redistribution centers for Roman goods prior to the construction of the Antonine Wall (Macinnes, 1984). However, not every known elite settlement served as a redistribution center for Roman goods, as is evident by Edin's Hall in Berwickshire – a broch at where excavation have recovered few Roman artefacts (Harding, 2004:188).

This notion of varying intensities of Romanization in Britain and Scotland has been well documented (e.g.: Cunliffe, 1999, 2005; Harding, 2004; Armit, 2005). The highlands and Scotland were well insulated from the extensive Romanization and capitalism experienced by southern Britain. Despite the Roman military's impact during

the conquest (Cunliffe, 2005), the Celts in Scotland maintained much of their tribal social traditions; *loca* – tribal meeting places – were present in northern Britain through, and beyond, the 3rd century A.D. (Cunliffe, 2005:605). This is further supported by distinctly indigenous artefact hoards in Scotland north of the Antonine Wall dating to c. A.D. 84-165 – the period of regular Roman influence in the region (Hunter, 1997). Cunliffe (1999:260) aptly divided Roman Britain and Scotland into three impact zones: (1) the Romanized core in southeast Britain around London; (2) the Roman-controlled periphery north to the Clyde-Forth line; and (3) the un-Romanized, uncontrolled extremity in Scotland north of the Antonine Wall, and Ireland. This variance in Romanization was also documented by Tacitus in *Agricola* (1942:21), where he observed Romanization in southeast Britain to be little more than subversive enslavement.

2.3. SM 9156 – Caisteal Mac Tuathal

2.3.1. Topography, Geology, and Climate

Historic Scotland scheduled monument 9156 (Historic Scotland, 2001) – Caisteal Mac Tuathal – is located approximately 7.4 kilometers west-southwest of Aberfeldy, Scotland. The site is in the heart of the Tay Valley beneath a dense bracken blanket on the steep terrain (Dalland and Wessel, 2011) of Drummond Hill's heavily forested northeast promontory (RCAHMS, 1956), along the northern shore of Loch Tay – a finger lake relict of the last British Ice Sheet (Craig, 1991:508; Hughes et al., 2014). The geology underlying Caisteal Mac Tuathal is comprised of Late Proterozoic to Early Ordovician amphibolites and the Pitlochry Schist Formation (Fig. 9; British Geological Survey, 2000), and the overburden is brown forest soil of humus-iron podzols and humic gleys (Fig. 10; Grant, 1981; The Macaulay Institute for Soil Research, 1984). The

Drummond Hill - North Terminus
Subset of BGS Schiehallion, Sheet 55W

KEY

Southern Highland Group

S_{SH} Pitlochry Schist Formation

Argyll Group
Tayvallich Subgroup

J_{T} Loch Tay Limestone Formation

Intrusive Igneous Rocks
Dikes, sheets, and veins

F Felsite: Late Silurian

Metamorphosed Intrusive Ingeous Rocks

D_{1} Amphibolite: Late Proterozoic to Early Ordovician

——— Geological boundary, solid
—⊣— Fault, tick mark on downthrow
-—♦—- Major antiform trace
-—Ɪ—- Major synform trace,②,ⓔ, and③ are second, Errochty, and third phase folds, respectively
^{40}⟋ Inclined strata, degrees dip
^{85}⟋ S_3 inclined cleavage, degrees dip
^{10}⟋ D_2 lineation, degrees plunge; ^ direction of vergence of S_2
^{5}⟋ Axis of D_2 minor fold, degrees plunge; ^ direction of vergence of minor fold

Subset Location

1 ¾ ½ ¼ 0 miles
1 0 kilometres
50 m contour interval from mean sea level
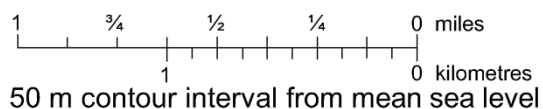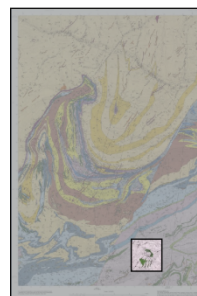
Notes on North:
At the center of sheet:
• true north is 1° 43' E.
• magnetic north is 4° 59' W as of July 2001, with annual change ~13' E.

References:
BRITISH GEOLOGICAL SURVEY. 2000. Schiehallion. Scotland Sheet 55W. Solid Geology. 1:50 000 (Keyworth, Nottingham: British Geological Survey)

Figure 9a: Geologic Map of the Drummond Hill northern terminus (KEY).

regional climate is temperate, with rainfall averaging[7] ~475mm in winter and ~305mm in summer (Met Office, 2013).

2.3.2. Archaeological Context

Perthshire was different in character during the Scottish Iron Age through the Pictish Period. Located less than 25 km north of the Antonine Wall, the county served as a borderland between the Romans and indigenous north, and between three major tribes:

---

[7] 1981-2010 (Met Office, 2013)
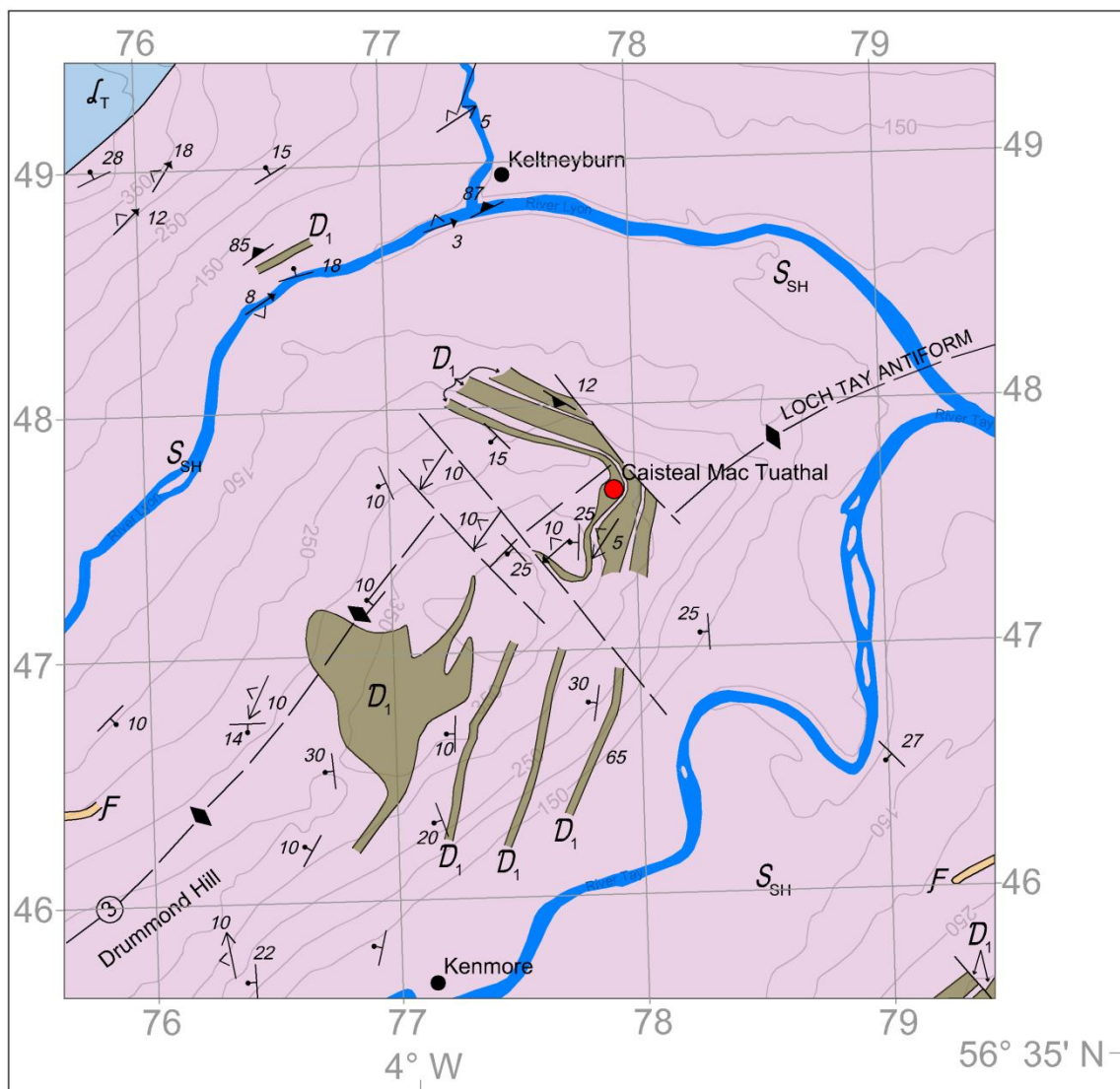
Figure 9b: Geologic map of the Drummond Hill north terminus (MAP).

the Caledones of the Highland Massif, the Venicones of the eastern coastal region, and

the Vacomagi of the northern Grampian Mountains (Fig. 11; Cunliffe, 2005:218).

Because borderlands are inherently volatile regions (Sinopoli, 1994; LeBlanc, 1999,

2006; Birch, 2010), Perthshire underwent numerous changes through the Scottish Iron

Age and Pictland. These changes are best illustrated by the previously stated shifting

settlement patterns in eastern Scotland (refer to section 2.1.2) due to the current poor
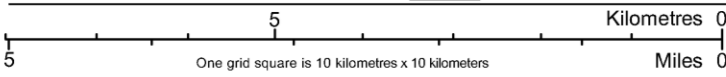
Loch Tay - North Terminus
Subset of MISR, Eastern Scotland Sheet 5, Soil Map

Soil Associations	Parent Materials		Component Soils	Landforms	Vegetation
Organic Soils	e - Eroded peat Organic deposits	4	Blanket peats	Uplands and northern lowlands with gentle and strong slopes	Blanket and flying bent bog Upland and mountain blanket bog Deer-grass bog. Sedge mires
Aberlour	Drifts derived from acid schists and granitic rocks	6	Humus-iron podzols; brown forest soils and gleys	Hills and valley sides with gentle and strong slopes; non-rocky	Arable and permanent pastures Dry Boreal heather moor
		11	Peaty gleys, peat; peaty podzols and peaty rankers	Undulating hills with gentle and strong slopes; moderately rocky	Moist Boreal heather moor Blanket and upland blanket bog Bog heather moor
Corby/ Boyndie/ Dinnet	Fluvioglacial and raised beach sands and gravels derived fron acid rocks	97	Humus-iron podzols; gleys	Undulating lowlands, mounds and terraces with gentle slopes	Arable and permanent pastures Oak and birchwood Rush pastures and sedge mires
		98	Humus-iron podzols, alluvial soils	Valley floors, terraces, and mounds with gentle and strong slopes	Arable and permanent pastures Oak and birchwood Rush pastures and sedge mires
Strichen	Drifts derived from arenaceous schists and strongly metamorphosed argillaceous schists of the Dalradian Series	497	Noncalcareous gleys, humic gleys; some peaty gleys and humus-iron podzols	Undulating lowlands and valley sides with gentle and strong slopes; non-rocky	Rush pastures and sedge mires Arable and permanent pastures Acid bent-fescue grassland
		498	Humus-iron podzols; brown forest soils and gleys	Undulating lowlands and valley sides with strong and steep slopes; non-rocky	Arable and permanent pastures Boreal and Atlantic heather moor Acid bent-fescue grassland
		499	Peaty podzols, humus-iron podzols; gleys	Hills and valley sides with strong and steep slopes; non-rocky	Boreal and Atlantic heather moor Bog heather moor Blanket and upland blanket bog
		501	Peat, peaty gleys, some peaty podzols	Undulating lowlands and hills with gentle and strong slopes; non-rocky	Blanket and upland blanket bog Bog heather moor Boreal and Atlantic heather moor
		503	Humus-iron podzols and brown forest soils; some gleys and peat	Hummocky valley moraines	Acid bent-fescue grassland Arable and permanent pastures Oak and birchwood
		504	Peaty podzols, peaty gleys, peat	Hummocky valley and slope moraines	Boreal and Atlantic heather moor Bog heather moor Blanket and upland blanket bog
		505	Brown forest soils, humus-iron podzols, humic gleys	Hill and valley sides with strong to very steep slopes; slightly and moderately rocky	Bent-fescue grassland Broadleaved woodland Rush pastures and sedge mires
		506	Brown rankers, brown forest soils; some humus-iron podzols and gleys	Hills and valley sides with steep and very steep slopes; very rocky	Dry Boreal and Atlantic heather moor. Blaeberry heath Acid bent-fescue grassland
		508	Rankers, peaty podzols; humus-iron podzols and peaty gleys	Rugget hills with strong and steep slopes; very rocky	Boreal and bog heather moor Upland bent-fescue grassland Blaeberry heath
		509	Rankers, peaty podzols; humus-iron podzols and peaty gleys	Rugged hills with strong and steep slopes; very rocky	Boreal and bog heather moor Upland bent-fescue grassland Blaeberry heath
		512	Subalpine soils; rankers and peat	Mountains with gentle to very steep slopes; non- to very rocky	Alpine lichen heath Lichen-rich Boreal heather moor Mountain blanket bog
		514	Alpine soils	Mountain summits with gentle and strong slopes; non- and slightly rocky	Alpine lichen heath Stiff sedge - fescue grassland Alpine club-moss snow-bed

Location of Subset

Kilometres 0
5
5
One grid square is 10 kilometres x 10 kilometers
Miles 0

References:
Grant, R. (1981). Eastern Scotland. Soil Survey of Scotland. Sheet 5. 1:250 000. [Map]. Aberdeen: The Macaulay Institute for Soil Research

Figure 10a: Soil Map of the Loch Tay north terminus (KEY).

understanding of sociopolitical characteristics therein (Harding, 2004; Armit, 2005; Cunliffe, 2005:216). Of particular interest to this study, however, are the Tay Valley and Glen Lyon around Drummond Hill due to their proximity in the aforementioned borderland.

2.3.2.1. Tay Valley and Glen Lyon

The Early Iron Age in the Drummond Hill area was characterized by enclosed and defended homesteads. Several duns and hillforts are also present in the surrounding
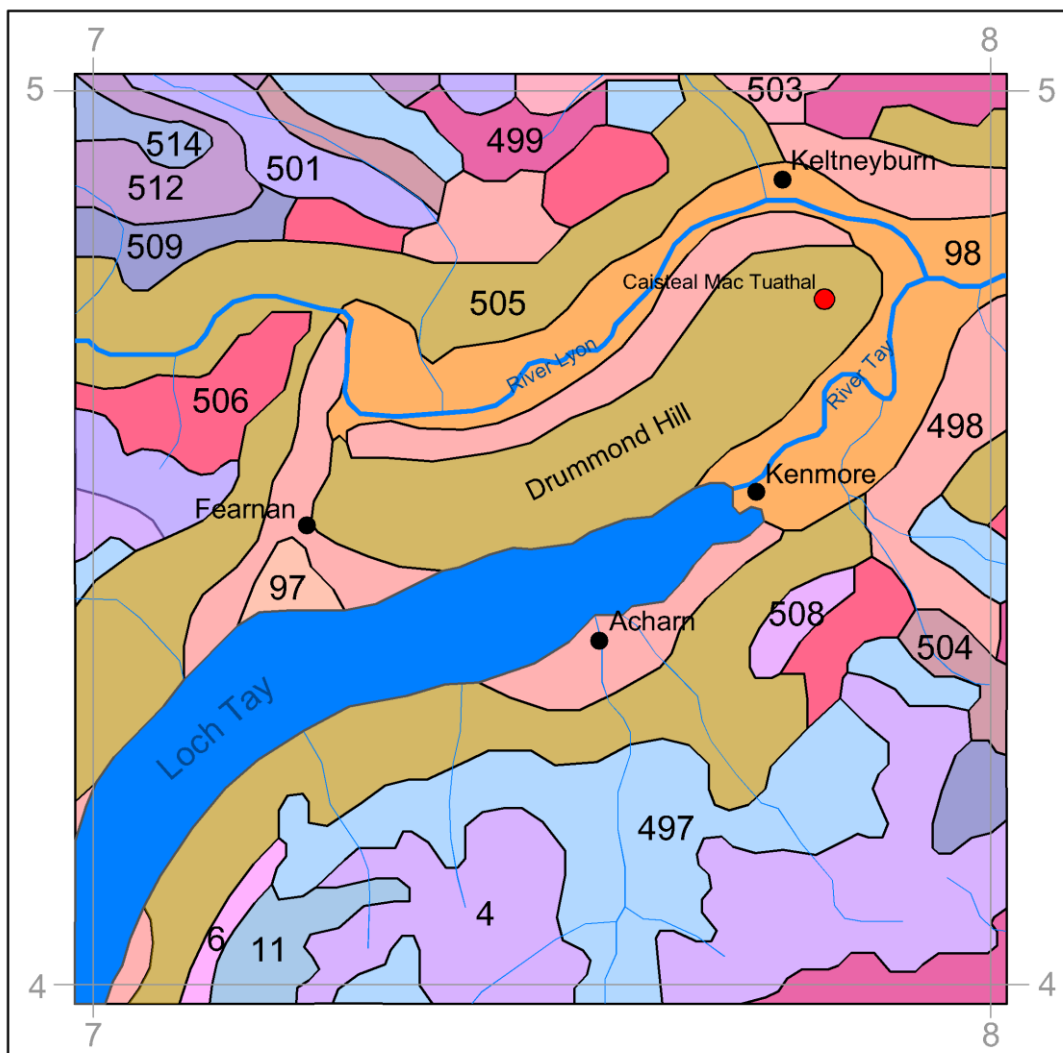
Figure 10b: Soil map of the Loch Tay north terminus (MAP).

area, though a lack of radiocarbon dating limits our understanding their chronology

(RCAHMS, 2015), as does extensive historic and prehistoric quarrying at several of the

sites (e.g.: Casteal Baraora [RCAHMS, 1979] and The Dun [NSA, 1834-35; Christison,

1900]). Souterrains (e.g.: Castle Menzies [RCAHMS, 2015]) and several possible

settlements of "ring-fort" morphology (e.g.: Castle Menzies Home Farm [Clark, 1970],

Caisteal Dubh [Watson, 1915; RCAHMS, 1950-9], and Easter Croftintygan [RCAHMS,
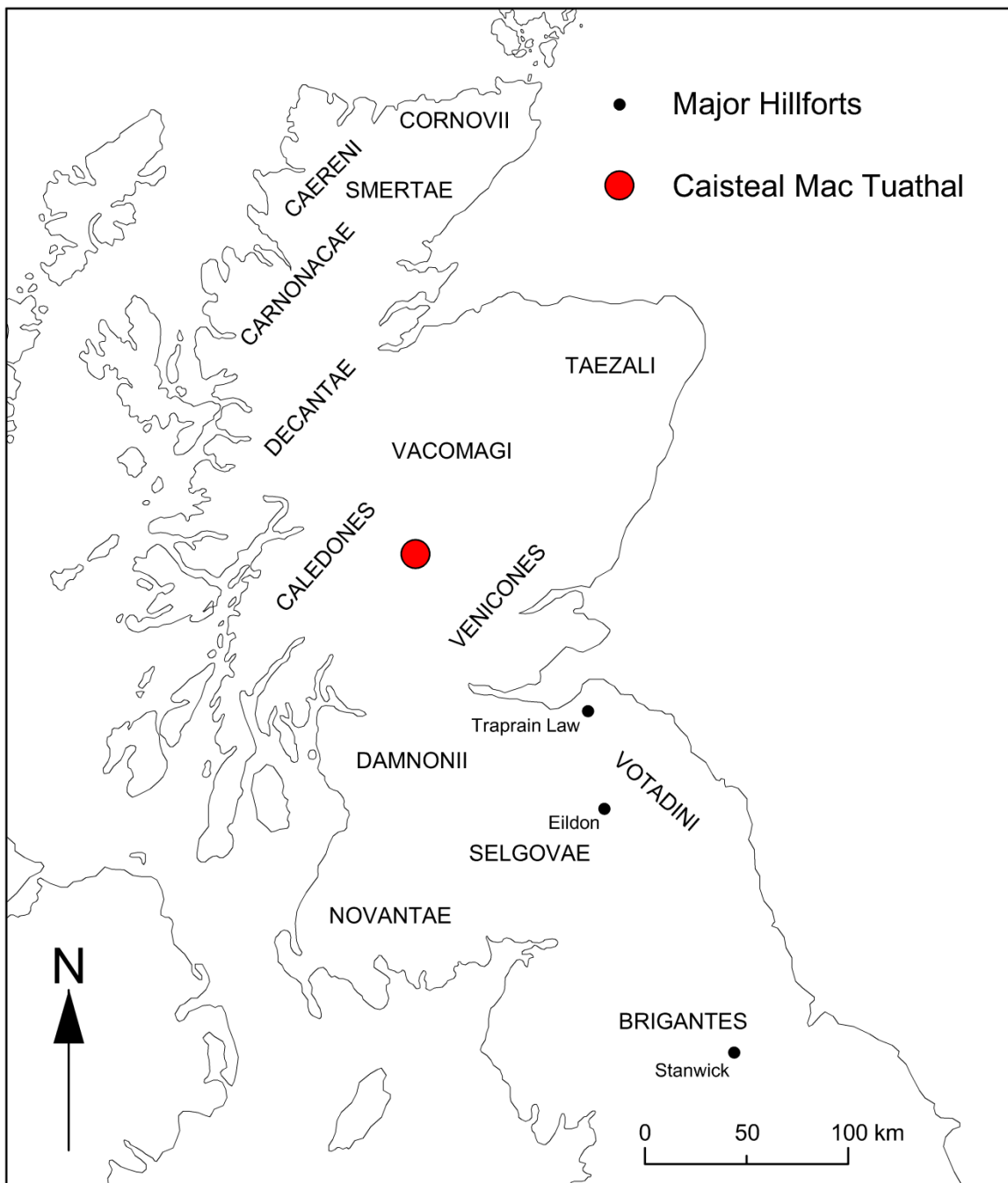
Figure 11: Major Celtic tribes of Northern Britain (modified after Cunliffe, 2005:Fig. 9.6).

2015]) are also present in the valleys, indicating indigenous habitation during the Scottish

Late Iron Age and Pictish Period.

2.3.2.2. Loch Tay Crannogs

Crannogs are particularly abundant in the Loch Tay, with 17 confirmed and 1 potential crannog identified thus far (Fig. 12; RCAHMS, 2016), at least three of which were potentially visible from Caisteal Mac Tuathal prior to Drummond Hill's initial reforestation from 1583-1631, further silviculture efforts during the Victorian Era, and transfer to state management in 1922 (Murray, 1935; Batcheler, 1960; Gillies, 2005). Radiocarbon dates indicate crannogs first appeared in the region c. 788-697 cal. B.C. (Dixon, 1981:346-7) and continued in use throughout Pictland (Dixon et al., 2007).

2.3.3. Archaeological Studies

Several surface surveys conducted during the past 116 years all located the best preserved site feature: the western rampart (Hutcheson, 1889; Christison, 1900; RCAHMS, 1956; Feachem, 1963; Dalland & Wessel, 2011; Rubicon Heritage, 2014). However, only the most recent surveys that have revealed an extension to the western rampart, an annex immediately north of the rampart (cf. Fig. 37), and a potential entrance along the northernmost point of the projected site (Dalland & Wessel, 2011; Rubicon Heritage, 2014). However, good preservation of these potential site features is questionable due to extensive bioturbation from tree growth. The site was heavily forested for over 100 years prior to the recent clear-cutting of trees within the boundaries of this Historic Scotland scheduled monument (Dalland & Wessel, 2011:2).
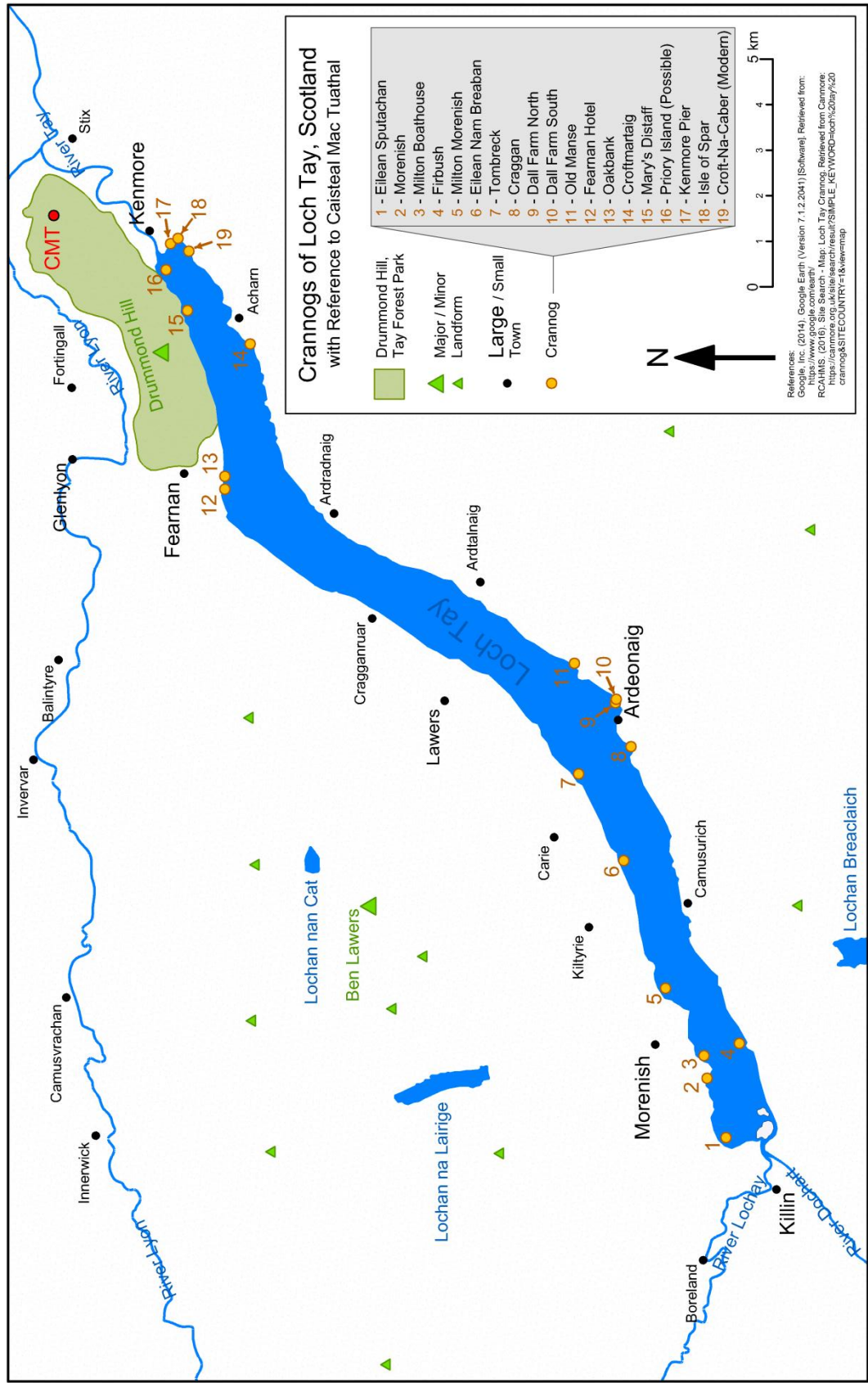
Figure 12: Crannogs of Loch Tay, Scotland.

3. Field Conditions

Field conditions were typical of a mild Scottish highland summer – sub-18°C, frequent misting, occasional downpours, and windy. Meteorologically, the geophysical survey of Caisteal Mac Tuathal was impeded when heavy or long-duration rains precluded safe access to the site along the gravel and dirt forest service roads. If heavy rains occurred while the GPR survey was being conducted then the survey was paused until the rain ceased; the survey team had to scramble to protect the water-sensitive SIR-2000 control unit and the data ports on the GSSI 80 MHz MLF transmitter and receiver. On the first day of the GPR survey it was unknown that the data ports on antenna would flood when it was raining, and as a result the heavy rains that day flooded the data port, forcing a cancellation of the day's survey, and requiring overnight drying to mitigate any potential electrical shorts.

The site of Casteal Mac Tuathal, was covered by a dense, approximately 2 m high growth of bracken that required three days of strimming and hand-clearing to make geophysical surveys feasible. Once the bracken had been cleared, numerous tree piles, tree stumps, and boulders were exposed, resulting in the application of spatial constraints for each utilized geophysical methodology. Furthermore, uneven terrain persisted despite clearing the overgrowth, thus forcing the survey team to proceed at a more careful pace to minimize the risk of injury.

4. Methods and Research Design

Due to insufficient LiDAR data coverage of the site, and the availability of elevation point data from a recent site survey, topographic data for Caisteal Mac Tuathal was not collected during this study, but rather obtained from an existing archive and reprocessed for use in topographic corrections for geophysical data. Furthermore, the shallow soil profile of Caisteal Mac Tuathal precluded the use of resistivity methods, and the rough, steep terrain precluded a conductivity survey as well. The terrain conditions favored the use of three geophysical survey techniques – magnetometry, ground penetrating radar (GPR), and conductivity. However, only magnetometry and GPR methods were used in this studies survey of the upper (UT) and lower (LT) terraces (Fig. 13) due to limited access to appropriate conductivity equipment.

4.1. General Packet Radio Service Rover and Global Positioning Systems

On behalf of Forestry Commission Scotland, Enda Flaherty and her team at Rubicon Heritage collected topographical data of Caisteal Mac Tuathal in 2014 using a general packet radio service (GPRS) rover. These data were provided to the author and used to produce a 1 m contour map of the site (Plan 1) and a 0.5 m contour map of the upper terrace (Plan 2). Datums for the geophysical survey grids were collected by Dr. Nicholas Dixon using a Magellan 5000 Pro global positioning system (GPS) unit.

4.2. Magnetometry

Localized variations in the Earth's magnetic field, as measured at the ground surface, correspond to changes in magnetic susceptibility of soils, sediments, and
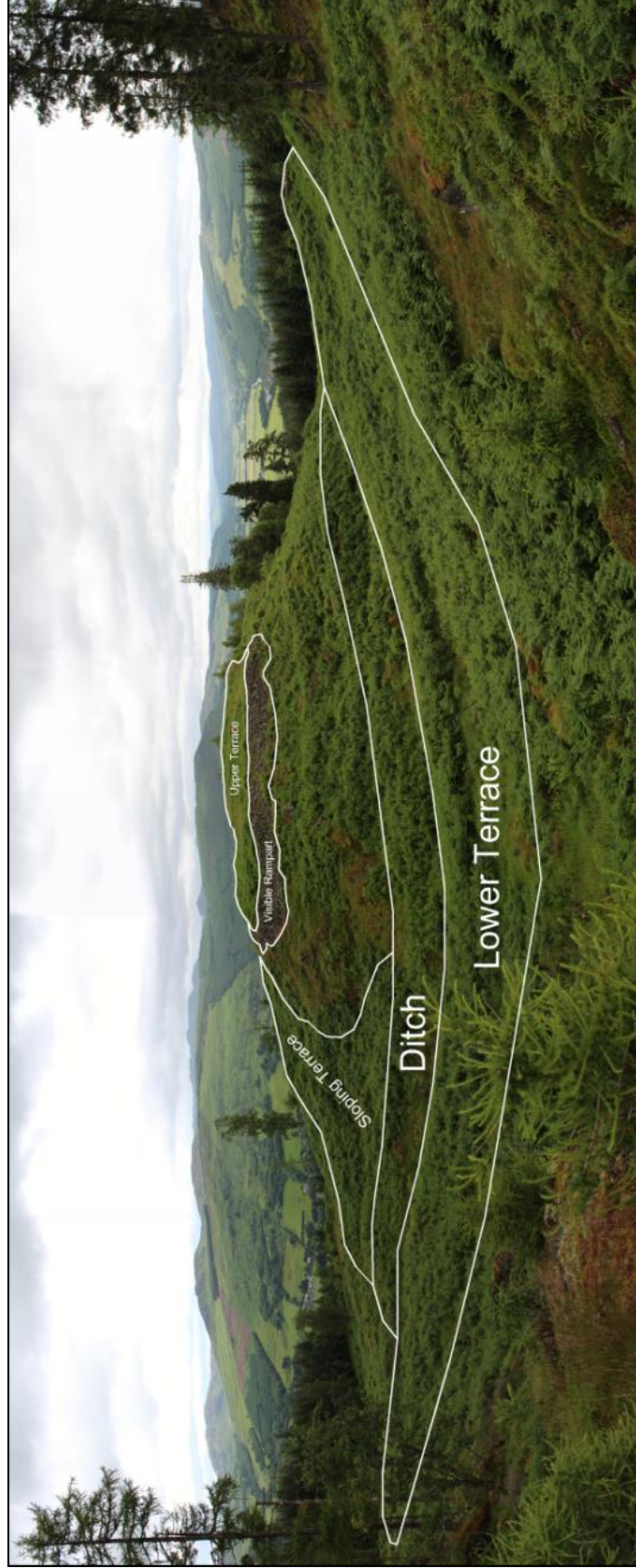
Figure 13: Annotated photograph of Caisteal Mac Tuathal illustrating site areas, looking north from the cup-marked rock.

anthropogenic deposits in the subsurface (Batayneh et al., 2007; Leopold et al, 2010).

Magnetometry measures relative magnetic susceptibility and thermo-remnant magnetism

at points or along transects, permitting the construction of a 2D or 3D plot for visual

analysis of subsurface features. Unlike GPR, a magnetometer is more easily utilized in

vegetated environments (Dirix et al., 2013). However, a magnetometer cannot easily

distinguish between distinct stratigraphic layers of magnetically congruent sediments

(Murdie et al., 2003a), although it can definitively assess and characterize a horizontal

stratigraphy that may represent walls and in-filled trenches (Rego and Cegielski, 2014).

4.2.1. Utilized Magnetometry Equipment and Methods

A Bartington Grad-601 fluxgate magnetometer (Fig. 14) was used to measure

relative magnetic susceptibility and thermo-remnant magnetism along transects spaced

0.5 m across thirteen 20 m x 20 m grids, each oriented N30°E, S60°E (Fig. 15). Fluxgate

magnetometers have been used extensively in the study of magnetic susceptibility and

thermoremnant magnetism of archaeological sites (Milsom, 2003; Asăndulesei, 2011).

An advantage of the Fluxgate design is that it can be used to rapidly traverse a survey

grid in a paced and timed fashion.

4.2.1.1. Magnetometry Data Processing

Magnetometry data were processed using TerraSurveyor version 3.0.27.0 to

permit the educing of tree stumps and fells, boulders, bedrock, and archaeological

features from the raw data. The LT composite (Plans 3 & 4) was destriped[14], clipped

from -14.00 to 7.00 nT, and graduated (grad.) shaded; the western LT and swale

composite (Plan 5) was destriped[6], clipped from -9.00 to 5.00 nT, and grad. shaded; the

UT composite (Plans 6 & 7) was destriped[6], clipped from -40.00 to 20.00 nT, and grad.

---

[14] Applied to traverses, mean methodology, X orientation, threshold of 1.5σ.

Figure 14: The author operating a Bartington Grad-601 fluxgate gradiometer along line 2 in grid 5 (reproduced with permission of the photographer, Ervan Garrison).

shaded; and the UT circular anomalies composite (Plan 8a) was destriped[6], clipped from -

50.00 to 15.00 nT, and grad. shaded. Cyan and green color alteration was applied to the

UT circular anomalies composite (Plan 8b, c) to illustrate that observed patterns were not

color-shade specific. The UT southwestern rampart composite (Plan 9) was destriped[6],

clipped from -35.00 to 20.00 nT, and grad. shaded.

4.3. Ground Penetrating Radar

Ground penetrating radar (GPR) is an electromagnetic (EM) technique that can be

used for both archaeological site prospection and characterization by identifying changes

in permittivity and conductivity (Milsom, 2003) that could be the result of constructed

Figure 15: CMT 2015 magnetometry grids with selected topography.

features. These changes in permittivity and conductivity can be used to detect anthropogenic and environmental stratigraphic anomalies (Murdie et al., 2003a; Gaffney, 2008; Asăndulesei, 2011). Site prospection is typically conducted using a series of transects to locate subsurface anomalies, while site characterization can involve surveys in both transect or grid form[15]. Archaeological surveys tend to use the grid approach, comprised by transects typically spaced 0.5-1m apart depending upon the antenna frequency used and desired survey resolution (Leopold et al., 2011; Böniger & Tronicke, 2014).

GPR transmitters vary in frequency output from less than 20MHz to over 2GHz. Lower GPR antenna frequencies penetrate the ground deeper than high-frequency antennae, though they produce lower resolution scans than those attainable with higher frequency antennae. Additionally, GPR surveys of saturated soils and sediments result in a lower resolution than can be obtained under dry conditions due to increased attenuation of the radar waves. Due to these GPR system characteristics, antenna units typically employed in archaeological prospection and characterization can vary from under 100MHz to 400MHz (Murdie et al., 2003a; Milsom, 2003; Linford & Linford, 2004; Böniger & Tronicke, 2014). When feasible, surveys should be conducted during the dry season. However, GPR surveys can also be fruitful in damp-to-saturated soils, identifying the boundary between the zones of percolation and saturation as well as non-sediment anomalies such as stone structures, stone-lined trenches, and metal pipes (Milsom, 2003; Murdie et al., 2003a; Ruffell et al., 2004). Furthermore, the digital nature of GPR data requires further processing to produce evaluable visualizations.

---

[15] Refer to Linford and Linford (2004: Fig.2, 3) for line scan (transect) and 3D GPR visualizations.

4.3.1. Utilized GPR Equipment and Methods

Multi-frequency unshielded, non-ground contact horn GPR antennas are rarely

used in geophysical surveys today due to their unwieldiness for extensive non-motorized

surveys of even, level, and/or graded terrain when compared to ground-coupled GPR

antennas. Furthermore, their use, licensing, utilized frequencies, and radiated emissions

in the United States of America have been restricted by Federal Communications

Commission (FCC) Code of Federal Regulations (CFR) report 47 CFR Part 15 Subpart F

(2002) and it's 2002, 2003, 2005, and 2007 amendments (CFR, 2015). Shielding has been

applied to minimize radiated emissions by GPR antennas whose construction postdates

the enactment of these FCC rulings. Since the possession and operation of unshielded,

non-ground coupled horn GPR antennas may only occur under FCC permit and/or waiver

(cf. requests for waivers in FCC, 2004), shielded, ground-coupled GPR antennas have

become the norm for GPR investigations (E. Garrison, pers. comm., 2015). The

possession and use of unshielded, non-ground contact horn GPR antennas manufactured

prior to the enactment of these FCC rulings, including the Geophysical Survey Systems

Incorporated (GSSI) 16-80 MHz multiple low-frequency (MLF) system owned and

operated by the University of Georgia, was grandfathered into the legislation.

The University of Georgia-owned GSSI 16-80 MHz MLF unshielded GPR antenna

operating at 80 MHz and SIR-2000 control unit connected by a 30 m armored data cable

(Fig. 16) was used to collect geophysical data at the site. Changes in permittivity and

conductivity allow for the detection of anthropogenic and environmental stratigraphic

anomalies (Murdie et al., 2003a; Gaffney, 2008; Asăndulesei, 2011). The GPR survey

utilized the 80 MHz unshielded, non-ground contact horn antenna rather than the 100

Figure 16: Jackie Hoyt and Dr. Nicholas Dixon maneuvering the 80 MHz MLF GPR antenna and armored data cable along Line 15 (reproduced with permission of the photographer, Ervan Garrison).

MHz ground-coupled antenna available through the University of Georgia because the

steep, uneven terrain of Caisteal Mac Tuathal precluded the safe and effective handling of

the 100 MHz antenna (cf. Fig.s 16, 17, & 26). The GPR survey was conducted within the

area circumscribed by the UT magnetometry grids, with 1 m spaced lines (Fig. 18), to a

time-depth of 500 ns – the SIR- 2000's default for an 80 MHz antenna, and a time-depth

that would permit a complete scan of potential archaeological deposits by penetrating

bedrock despite the GPR antenna not being ground-coupled. A GPR survey was not

conducted within the LT area due to the terrain's impassability with the equipment (cf.

Fig. 26), and data collection of the UT was interrupted within two hours of the survey

Figure 17: The author (right) and Nick Dixon (left) carrying the GPR antenna and associated equipment up the SW slope of Caisteal Mac Tuathal (reproduced with permission of the photographer, Ervan Garrison).

start on Day 1 due to a 1-hour downpour flooding the data ports on the antenna – an incident that required overnight drying to rectify. Day 2 of the GPR survey proceeded without further incident.

4.3.1.1. GPR Data Processing

The GPR data were processed using GPR_Slice version 7.0 to identify environmental and potential archaeological anomalies in profile (radargrams) and in plan (grids sampled at multiple depths; time-slices).
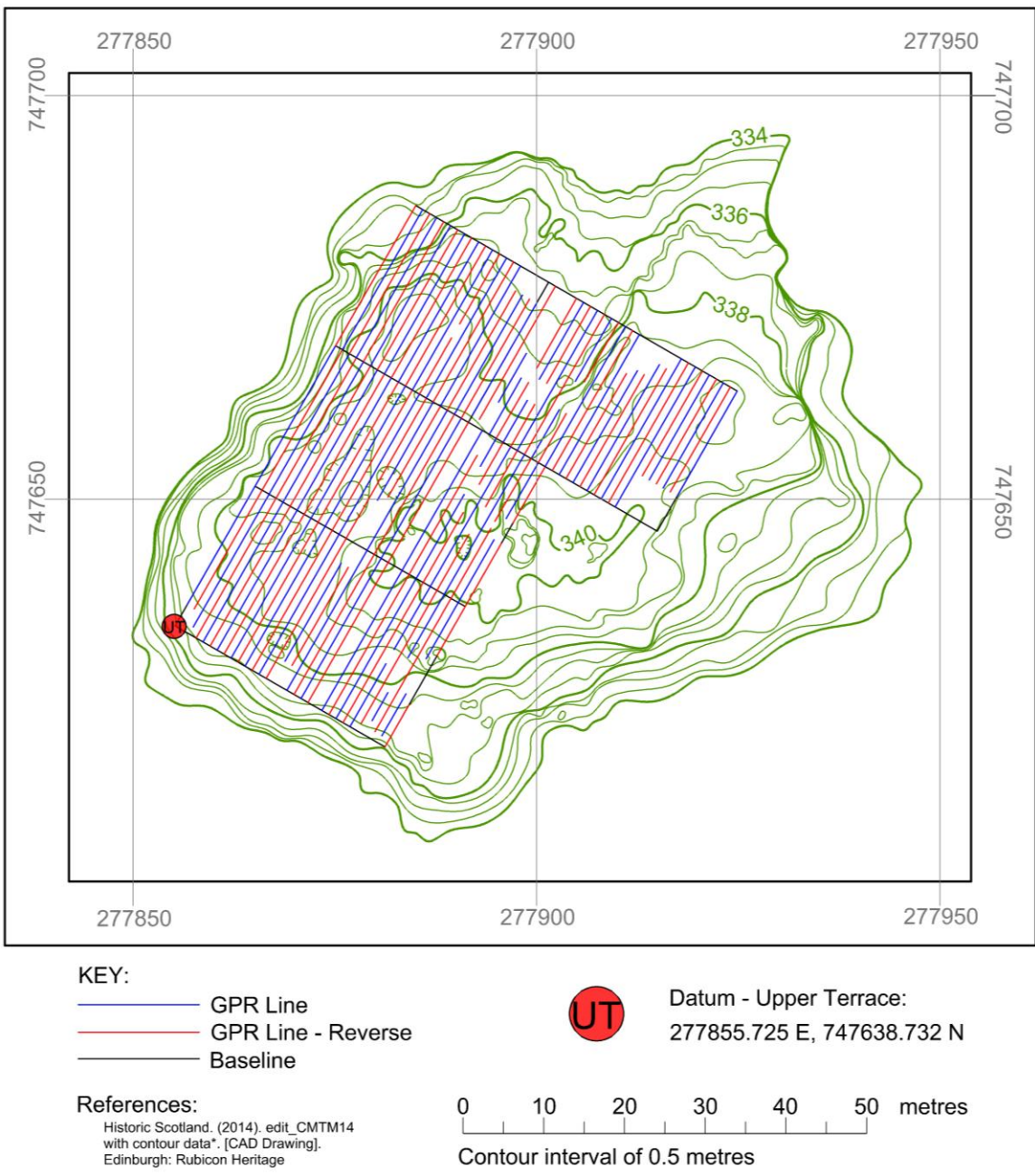
Figure 18: Map of GPR lines with selected topography.

4.3.1.1.1. Radargrams

GPR radargrams – the first observed format for modern GPR data – are profiles of

a radar signal along a continuous scan between two points – start of line (SOL) and end
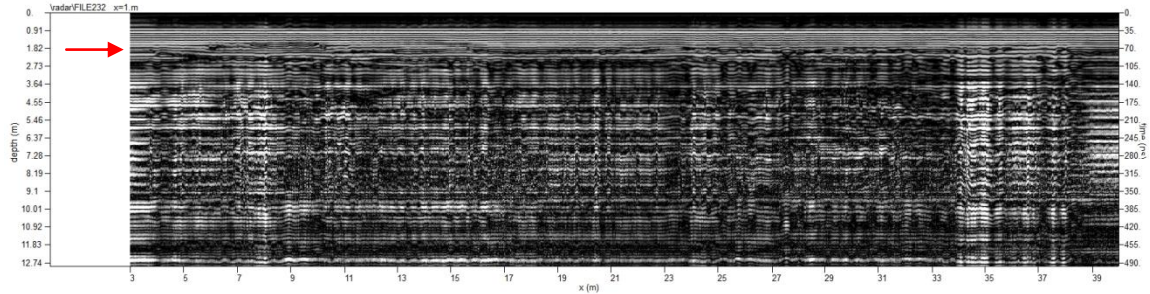
Figure 19: Example of a gain-adjusted radargram (line 1 of this study). The red arrow points to the base of the Fresnel zone at a range of ~70 ns.

of line (EOL) – within a survey. The x-axis is line length in metres, and the y-axis is depth. The observed depth, or range, of each radargram is initially measured innanoseconds (10^{-9} seconds; ns) – frequently referred to as the time window – and is determined prior to the survey and input into the GPR controller alongside other survey parameters (e.g. samples per scan, vertical high- and low-pass filters, and scans per second). Depth measurement in a distance metric is not determined or estimated until ground-truthing or migration analysis occurs, respectively. Most GPR control units, including the GSSI SIR-2000 utilized in this survey, have pre-programmed settings for the various compatible GPR antennas (GSSI, 2001; GSSI, 2009).

In order to process and interpret GPR data, it is important to determine where the ground surface is recorded in the radargrams, and then adjust, or time-zero, the radargrams to reflect the true ground surface. The first waveform visible in the wiggle traces of the radar signal is not the ground surface, but rather the start of the Fresnel Zone – the region within the first emitted or refracted radar waveform where the observed signal is comparatively weak (low amplitude reflections) to those in subsequent waveforms (Fig. 19; Malyshkin et al., 2011). With long wavelength antenna[17], such as the

---

[17] Wavelengths greater than or equal to 1 m.

80 MHz antenna used in this study, the ground surface may be included within and thus obscured by the Fresnel Zone, and must therefore be identified during processing.

The GPR data were processed in two grids due to program limitations in compiling a montage of differently-gained GPR data: Day 1 was composed of lines 1-20; and Day 2 was composed of lines 21-77. The radargrams for each grid had their time/depth adjusted (refer to section 2.2.3.1.3 for further details) and were batch gain-wobbled, time-zeroed, resampled, background filtered, and topographically corrected (refer to section 2.2.3.1.4 and Plan 14 for further details) to draw out the geophysical anomalies from the raw data and background noise. The radargram images for lines comprised of multiple scans were spliced together to permit better visual analysis of the processed radargrams (Radargrams 1-10).

4.3.1.1.2. Time-slices

Plan views of GPR data – frequently called time-slices – are arbitrarily spaced slices at consistently spaced time-depths across gridded, interpolated GPR radargrams. This permits the visualization of the radar data at sequentially shallower-to-deeper radar surfaces. Each GPR grid for this survey was time-sliced 40 times during the slice/resample/XYZ processing, had search and blanking radii of 2.5 applied during gridding, and was interpolated 4 times between slices to produce high-resolution plans and three-dimensional models of each grid at regular depths (cf. Plans 10-13 & Fig.s 31-33). A complete list of processing applied to the GPR data is located in Appendices A and B. Time-slices for topographically corrected data were produced using the *extract 3D volume XYZ planes to 2D*.grd format* program to minimize data distortion produced when utilizing *slice/resample/XYZ*.

4.3.1.1.3. Migration Analysis

Ranges of acceptable dielectric constants and radar wave velocities rather than exact values were determined for migration analysis due to density of bracken and sedge at the surface, and the uneven distribution of the humus-iron podzol overburden atop the amphibolite bedrock within the geophysical survey grids at Caisteal Mac Tuathal (Table 2; Shukla, 2014). However, complete migration analyses were not conducted for the GPR grids due to the significant vegetation cover and shallow soils at site; the GPR_Slice "search" function for migration analysis data was used to extrapolate each grid's dielectric constant and average radar wave velocity from hyperbolas within the soil profile. The dielectric constant and radar wave velocity were input into the GPR_Slice plot options for relative depth; the radar wave velocity and dielectric constant for the bedrock was not included because this survey was not interested in depth to bedrock at the site. The objective of this research was to identify structural extent of the site, not the stratigraphy of any potential structures identified therein – something the comparison of unmigrated and migrated GPR data would permit (Conyers, 2013:140).

Table 2: Relative dielectric constants and radio wave velocities for selected geological materials at Caisteal Mac Tuathal.

Material	ε_r	Velocity (m/ns)	Source
Fine-grained soils	41-49	0.043-0.047	Reynolds, 2011
Amphibolite	8	*N/A*	Simmons et al., 1981; Parkhomenko, 1967
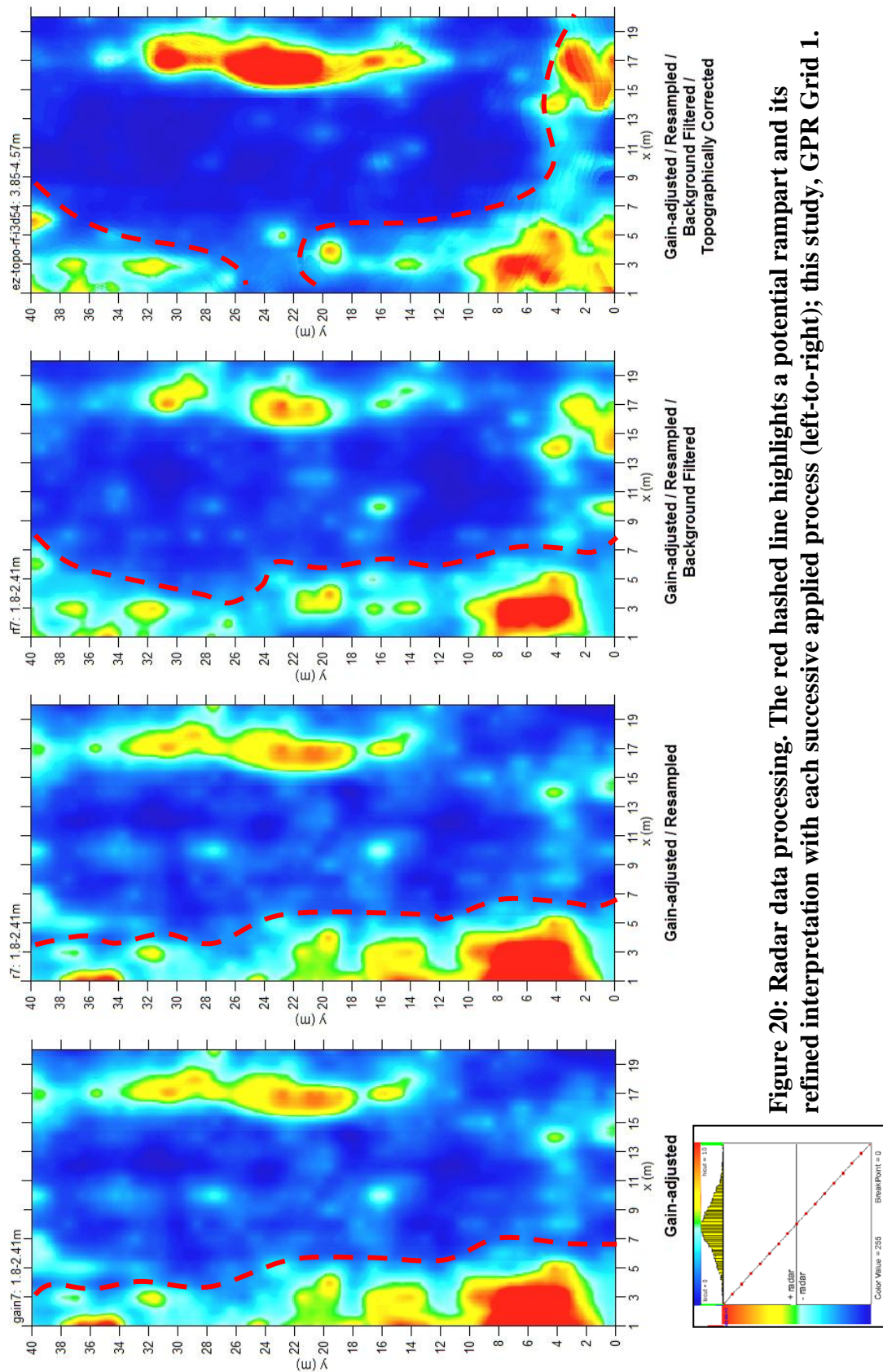
Figure 20: Radar data processing. The red hashed line highlights a potential rampart and its refined interpretation with each successive applied process (left-to-right); this study, GPR Grid 1.

4.3.1.1.4. Topographic Corrections

When conducting geophysical investigations – especially when the techniques utilized image the subsurface through a range of depths – it is important to topographically correct data to improve site interpretations (Goodman & Piro, 2013). For GPR investigations, topographic corrections involve two primary processes: surface elevation correction and correcting for antenna tilt.

Correcting surface elevation for each line of the GPR survey is beneficial because it aligns anomalies that are along the same

Figure 21: Uncorrected, topo-corrected, and topo/tilt-corrected radar wave ray diagrams (after Goodman et al., 2006)

contour, correctly repositioning those with more, or less, overburden than other anomalies along the same contour (Fig. 20). Correcting for antenna tilt is important because the recorded data are observations of the subsurface perpendicular to the motion of the antenna, thus tilting the antenna results in repeated measurements when traversing a mound and gaps in the record when traversing a ditch (Fig. 21). However, tilt corrections need only be applied if the utilized antenna is actually tilted during the survey – something ground-coupled antennas are highly susceptible to while unshielded, horned antennas are portaged and only susceptible to tilt if the operator physically adjusts the angle of the antenna. In this study, tilt corrections were not applied to the topographic

corrections of GPR data because a non-ground-coupled 80 MHz unshielded, horned antenna was used.

4.4. Ground-truthing

Ground-truthing observed geophysical anomalies is important not only to identify the causes of the anomalies, but also to determine their exact depths and adjust the radargrams accordingly. Ground-truthing was not conducted in this survey except for magnetometry and GPR anomalies resulting from visible surficial features (e.g. trenches and holes, tree stumps and fells, boulders, outcropping bedrock). The absence of thorough ground-truthing is primarily due to restrictions placed on the survey by the Historic Scotland geophysical survey permit application process, and also by the time available to conduct the surveys.

Figure 22: Upper terrace southern baseline, looking N60°W (reproduced with permission of the photographer Ervan Garrison).

6. Results

Prior to discussion of the lower and upper terrace results it is important to note that a strong positive anomaly can be produced in magnetometry data by any rapid increase in distance between the sensor and the ground. This is particularly evident in the compilation of upper terrace grids, where strong positives are recorded along the steep slope and at foliage-covered pits and ditches along the western and southern baselines (Fig. 22), and in the center of grid 10 where a trench formed by an uprooted tree was encountered (Fig. 23). Both magnetometer and GPR anomalies within the UT surveys are

Figure 23: Bedrock outcrops and hidden boulders, tree stumps and fells in magnetometry Grids 9, 10, 12, and 13 (reproduced with permission of the photographer Ervan Garrison; modified by the author).

more easily identifiable as environmental or potentially archaeological due to the more open, generally less obstructed terrain (cf. Fig.s 23 & 24).

6.1. Lower Terrace

No potential archaeological geophysical anomalies were identified within the lower terrace (datum: 277803.499 E, 747602.825 N) magnetometry data.

6.1.1. Magnetometry

The LT magnetometry data (Fig.s 25 & 27) included anomalies bordering the (20 m, N30°E) baseline are resultant from the steep slope into the ditch, tree fells and stumps, and boulders. The general evenness along the southwestern baseline was caused by shallow bedrock. Shallow bedrock is also visible along the data gap in Grid 5, and was

CMT 2015 Geophysical Survey Surface Features w/Selected Topography

KEY:

Environmental Features

- Gentle Slope
- Slope off Outcrops
- Visible Bedrock
- Rock/Boulder
- Treefell
- Tree Stump
- Multiple Treefells
- Ditch from Uprooted Tree
- Standing Water
- Ditch/Gully

Geophysical Survey Features

- Survey Grid Extents:
  All grids along N30°W, S60°W
- LT Datum - Lower Terrace:
  277803.499 E, 747602.825 N
- UT Datum - Upper Terrace:
  277855.725 E, 747638.732 N

Archaeological Features

- Visible Rampart
- Potential Structural Feature

Contour interval of 1 metre

Figure 24: Surface features of the LT and UT grids.

Figure 25: Processed LT magnetometry composite. The areas constrained by the red-dashed lines and grid boundaries have been interpreted as shallow bedrock.

confirmed as this due to bedrock outcropping in the area (cf. Fig. 18). This conclusion is

further verified by observations in the UT magnetometry data. The southwestern gaps in

data within Grids 3 and 4 are due to impassable terrain caused by tree piles (Fig. 26). The

northeastern gap in the Grid 3 and 4 data is due to impassable steep terrain.

Grids 1 and 5 of the LT magnetometry data were composited and enlarged for

better interpretations (Fig. 27). The southwestern third of this composite illustrates

shallow bedrock. The anomalies bordering the 20 m, N30°E baseline are resultant from

tree piles, tree stumps, and large boulders. There was approximately 20 cm of standing

water was also present in this region during data collection. The large dipoles at

coordinates (12, 18) and (5, 33) are large boulders. The gaps in Grid 1 data are due to

impassable terrain caused by piles of felled trees, and the gap in Grid 5 data is due to

impassable steep outcropping bedrock.

6.1.2. Ground Penetrating Radar

The interpretation of the lower terrace archaeogephysical data was developed

solely from processed magnetometry data rather than the multi-technique study applied to

the upper terrace. This is because of the aforementioned shallow bedrock, and terrain too

strewn with logging debris, too steep, and too unstable to properly and safely conduct a

survey with the 80 MHz MLF GPR antenna.

6.2. Upper Terrace

The upper terrace (datum: 2778550725 E, 747638.732 N) has numerous

environmental, and many potential archaeological and geophysical anomalies. Of

particular interest is the rubble stratum visible along the western and southern borders of

48
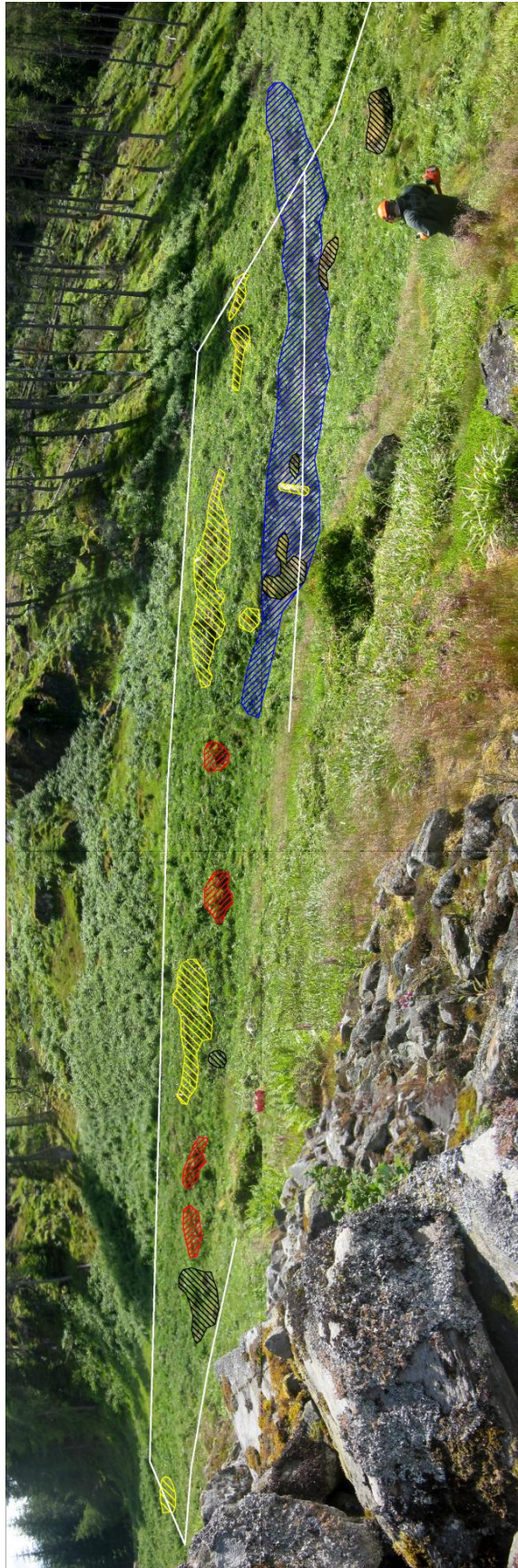
Figure 26: Annotated photograph of the lower terrace looking south. The white lines are baselines for Grids 1-5, the blue hatch is a region with 20 cm of standing water, the yellow hatches are tree fells and stumps, the black hatches are boulders greater than 1 m in diameter, and the red hatches are 1+ m drop-offs hidden by foliage (reproduced with permission of the photographer Ervan Garrison; annotations by the author).
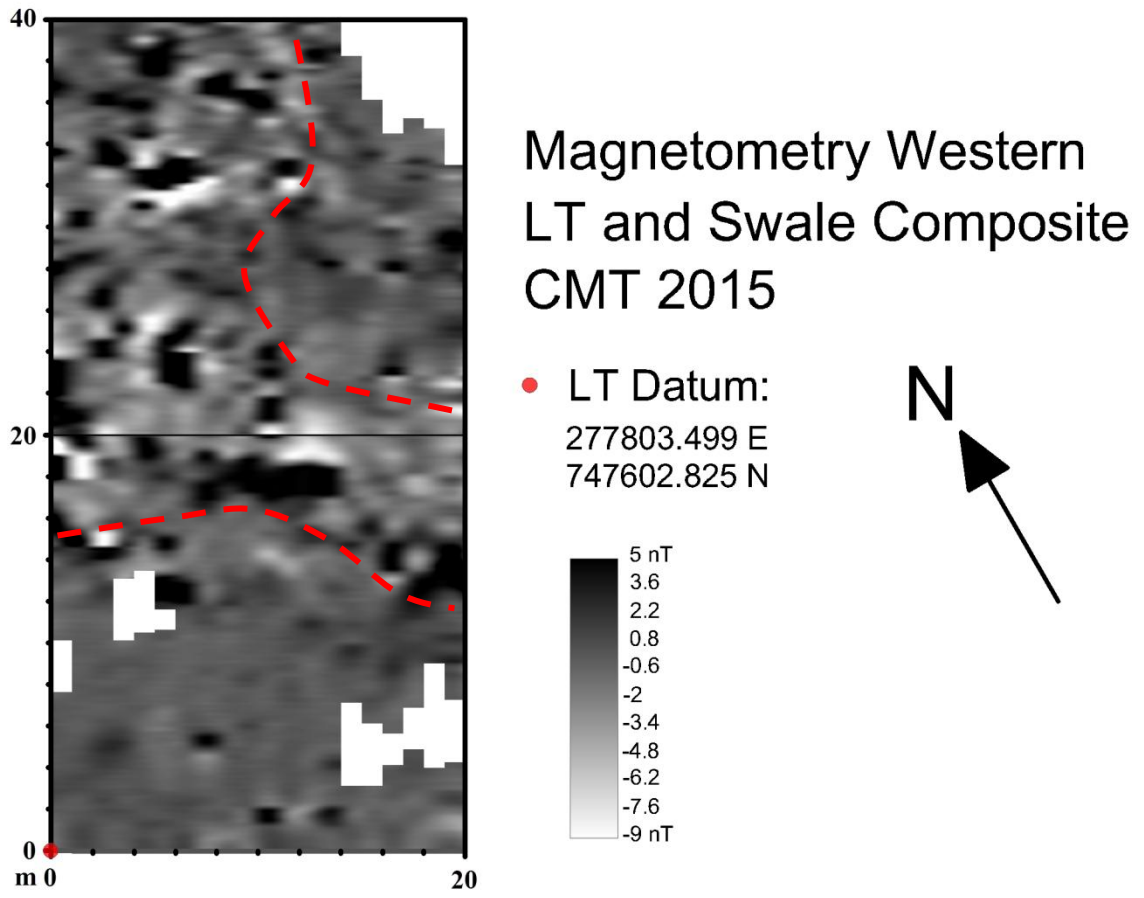
Figure 27: Reprocessed western LT and swale composite. The areas constrained by the red-dashed lines and grid boundaries have been interpreted as shallow bedrock.

the upper terrace survey area that is likely debris remaining from the collapse of Caisteal

Mac Tuathal's former ramparts.

6.2.1. Magnetometry

In the UT magnetometry data (Fig. 28), the strong positive anomaly between the

data gaps in Grid 10 is resultant from a ditch formed by a large uprooted tree trunk; the

positive anomalies in northeastern Grid 11 are due to the surveyor climbing over a tree

fell while collecting data; and the strong dipole in the northeastern corner of Grid 9 is due

to surface metal. The strong positive anomaly along the southwestern baseline in Grid 7

is caused by the exposed southwest rampart, while the general smoothness of the

magnetometry data in the northeastern half of Grid 7 is due to shallow bedrock – the

same as that observed in the lower terrace grids along the (20 m, N30°E) baseline.

Shallow bedrock is also evident along the UT (20 m, N30°E) baseline in Grids 6 and 8,

and throughout Grids 10-13. The square-shaped anomaly in Grid 12 is likely caused by a

large uprooted tree trunk (cf. Figs. 23 & 24), and the apparent semi-circular anomaly in

Grid 13 is caused by the boundary between exposed bedrock and soils. The small

anomaly in the northwestern part of this semi-circle is due to a surficial rock.

The two semi-circular anomalies in Grids 6, 8, and 9 (Fig. 29) were reprocessed

and color-treated to allow for further distinction between potential environmental and

archaeological anomalies. These two anomalies bulge from the (0 m, N30°E) baseline,

each respectively centered on 17 m and 39 m N30°E from the UT datum. The

southwestern of these two anomalies is likely the collapsed remains of a structure

attached to the rampart. The northeastern anomaly is more difficult to interpret due to an

increase in environmental anomalies caused by several tree trunks and uprooted trees (cf.
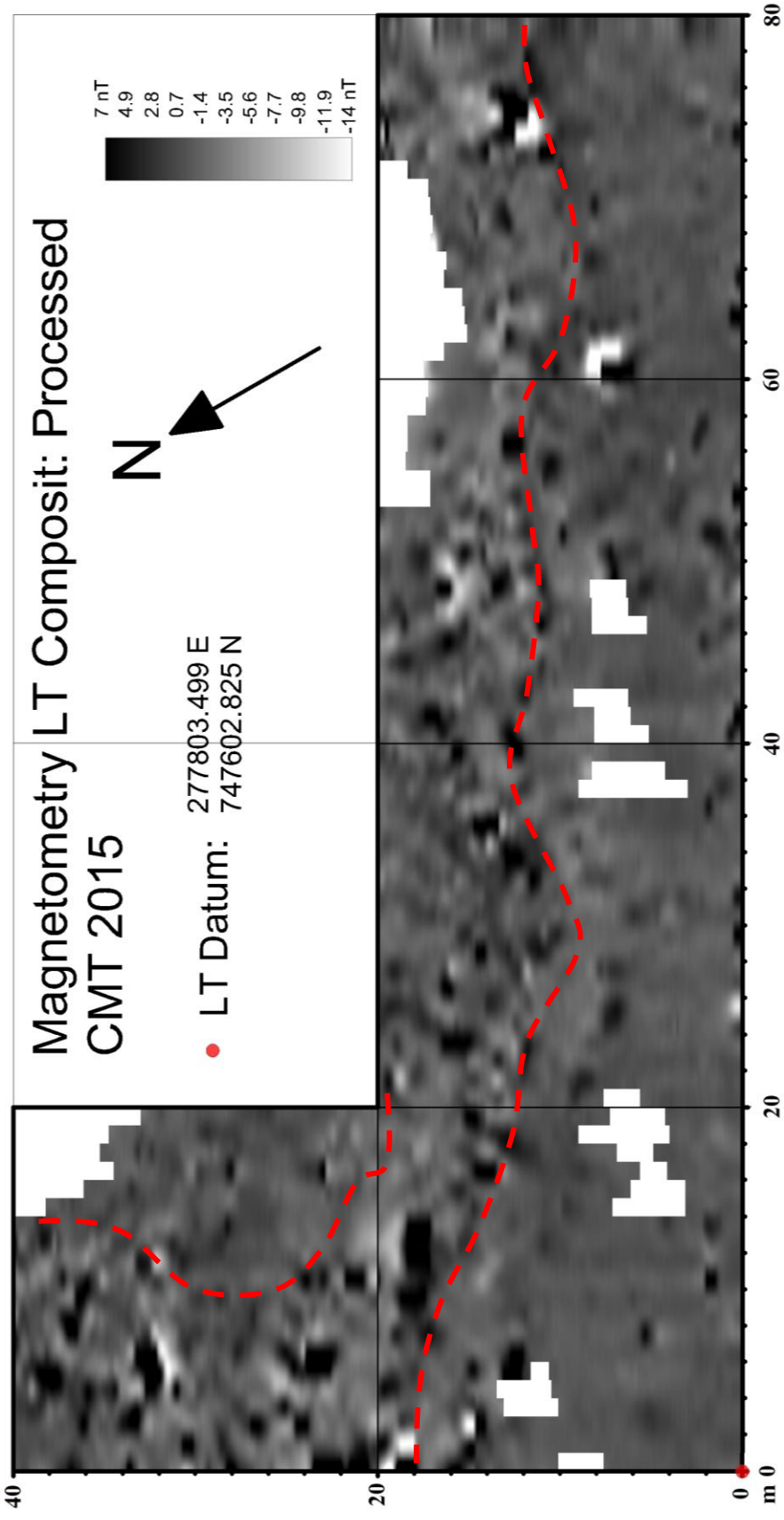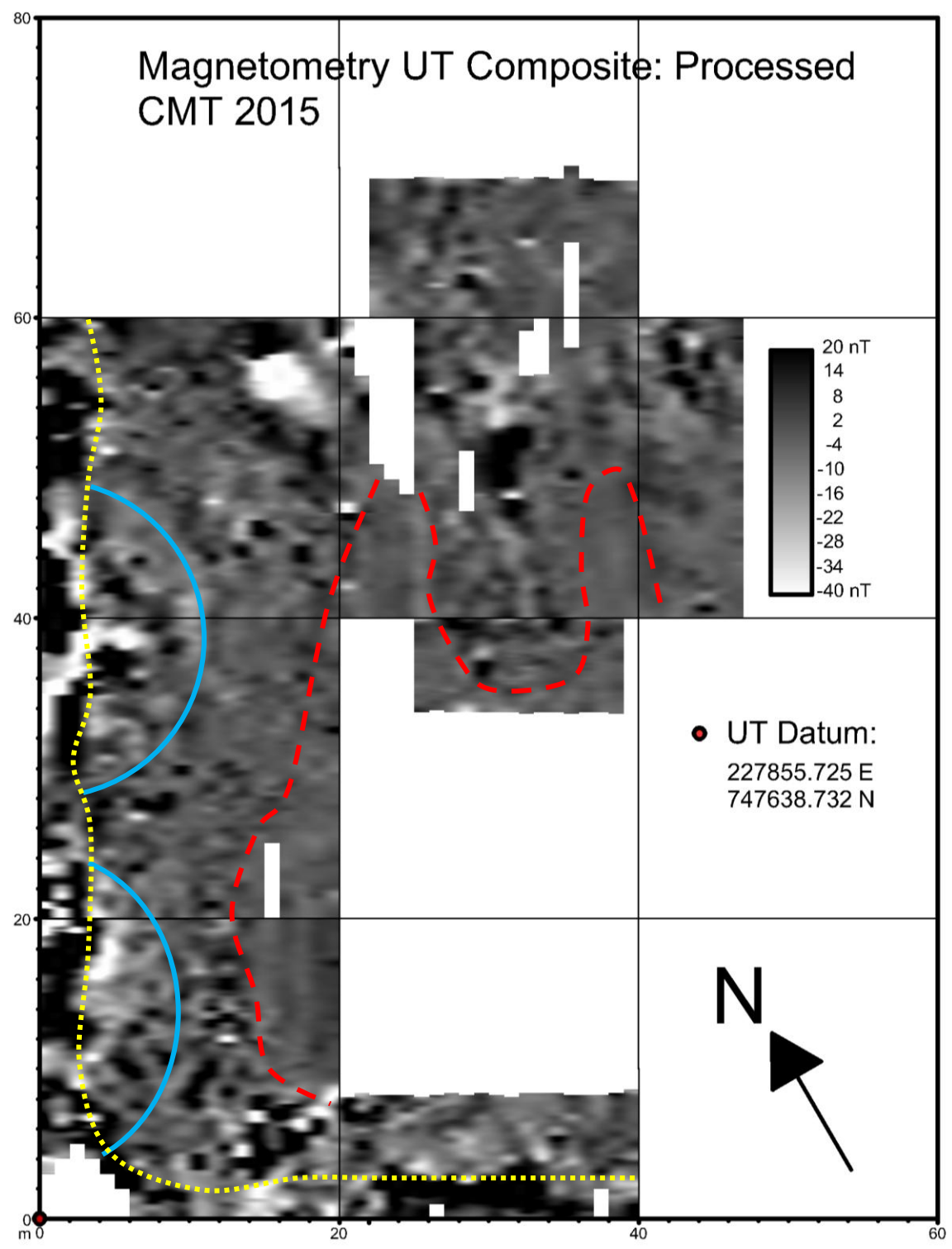
Figure 28: Processed UT magnetometry grid composite. The areas constrained by the red-dashed lines and grid boundaries have been interpreted as shallow bedrock, the blue arcs circumscribe the semi-circular anomalies, and the yellow-dotted line outlines the rampart's interior face.
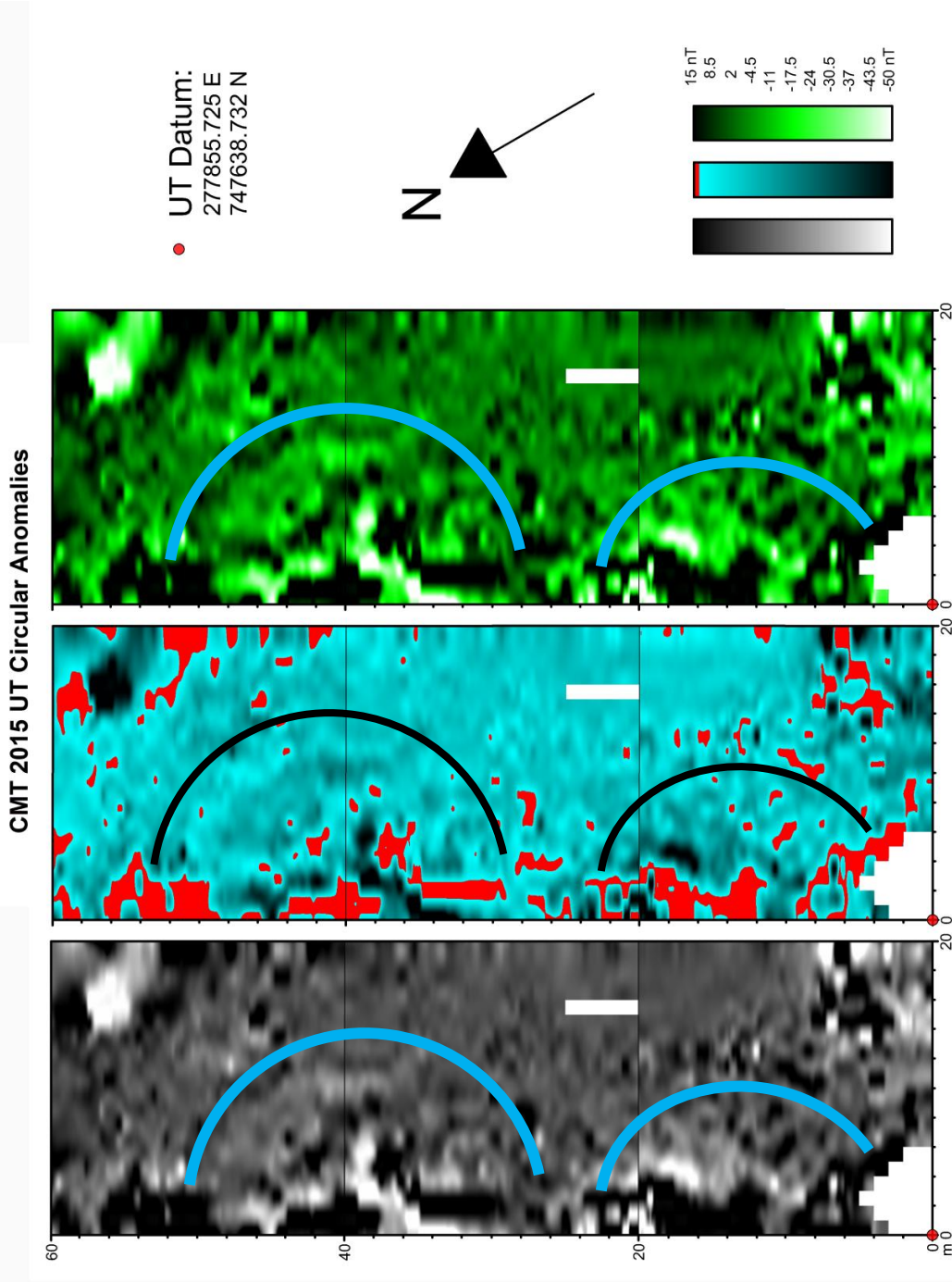
Figure 29: Reprocessed and color altered UT circular anomalies (Grids 6, 8, & 9 composite). The blue (and black) arcs circumscribe the semi-circular anomalies

Figs. 23 & 24). The strength of the northwestern rampart anomaly decreases between the two circular anomalies, and is likely the location of an entrance to the site.

6.2.2. Ground Penetrating Radar

Several environmental and potential archaeological anomalies were identified within the GPR data (Figs. 30-32); a few distortions resultant from the processing techniques applied to the data were noted, including the strong positive anomalies in Grid 1 at (16, 18-26) and in Grid 2 at (38, 55-60), both of which result from data extrapolation across line breaks. Data along the southwestern border have also been distorted due to processing. Confirmed environmental anomalies include the three positive anomalies along x = 36 (Figs. 30-32) – reflections resultant from uprooted tree trunks – and the arc opening west centered on (31, 25) (Fig. 32) – reflections resultant from the bedrock surface (southeastern reflections) and a tree trunk (northeastern reflections). The moderate positive, arcing anomaly (Figs. 30-32) in Grid 2 centered on (16, 50) is resultant from a large overturned tree trunk which the antenna was swung around rather than lifted over. Furthermore, the isolated, positive anomalies (Figs. 30-32) at (25, 15), (22, 38), (27, 40), (27, 48), and (31, 45) correlate to surficial tree stumps and boulders, and the positive anomalies centered on (21, 10) and (29, 9) correlated to steep slopes and outcropping bedrock.

The semi-circular anomalies in the magnetometry data along the western rampart are also observable in the GPR data (Figs. 30 & 31). The northern semi-circular anomaly is still obscured in the GPR data due to the overlying tree trunks and rough terrain. However, the southern semi-circular anomaly was further resolved – a circle of six strong positive anomalies was elucidated, although two of these anomalies may simply be radar
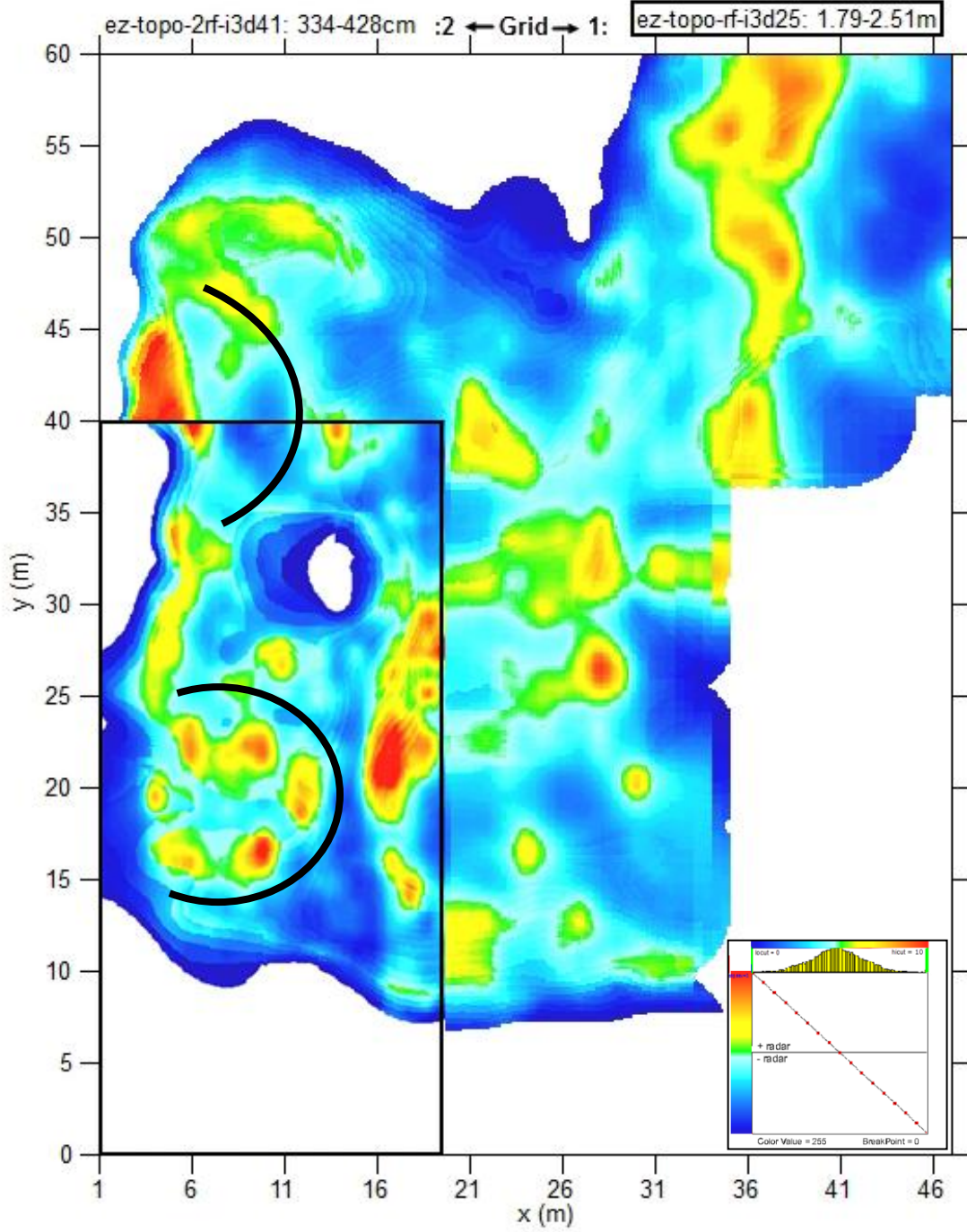
Figure 30: Gain-adjusted, resampled, background filtered, and topographically corrected composite of GPR Grids 1 and 2 at an approximate depth of 3.34-4.28 m below site maximum elevation (341.5 m a.m.s.l.). The depth for each grid differs due to different surface elevations used as time-zero – a 2 m-offset between the two. The black arcs highlight the semi-circular anomalies.
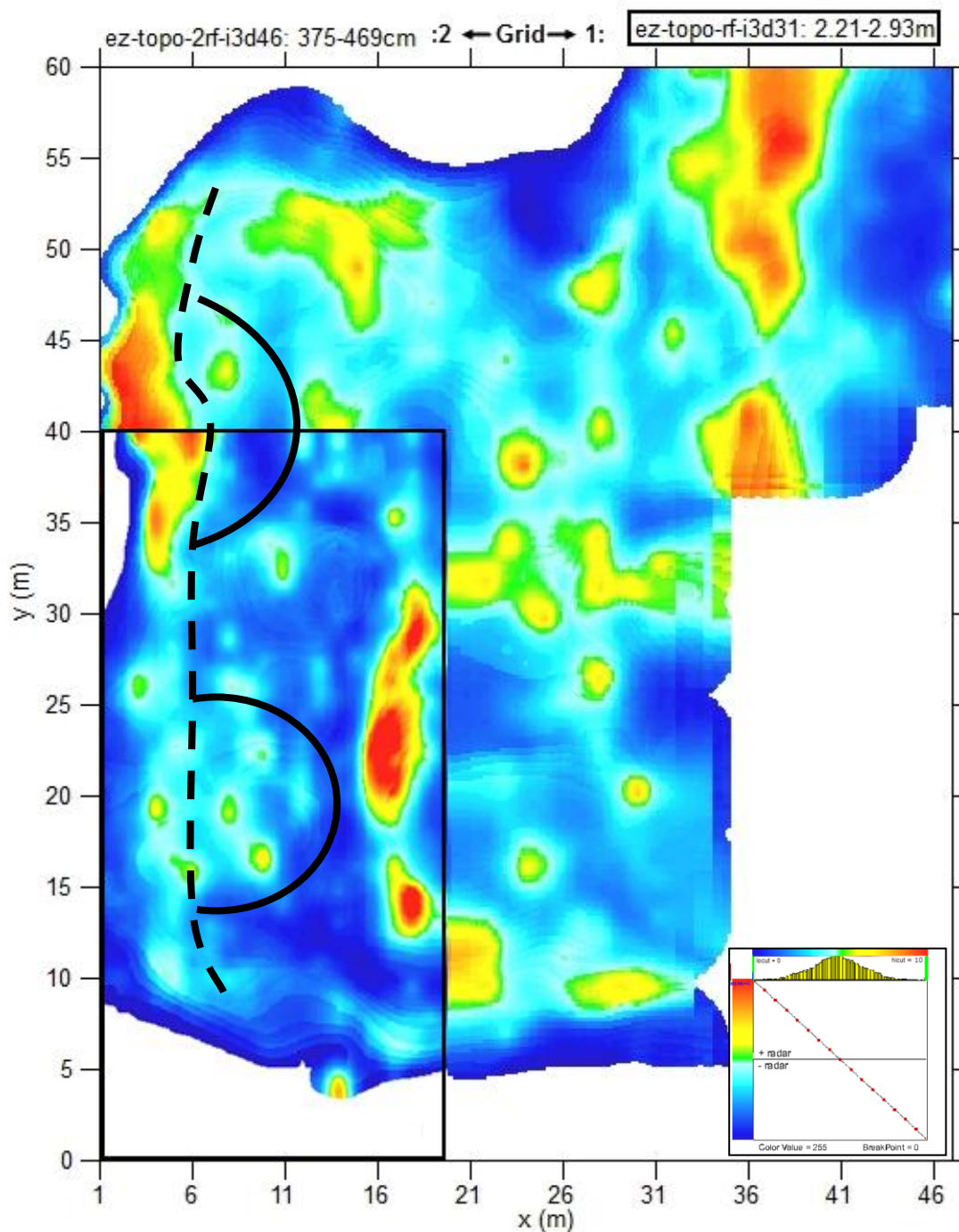
Figure 31**: Gain-adjusted, resampled, background filtered, and topographically corrected composite of GPR Grids 1 and 2 at an approximate depth of 3.75-4.69 m below site maximum elevation (341.5 m a.m.s.l.). The depth for each grid differs due to different surface elevations used as time-zero – a 2 m-offset between the two. The black arcs outline the semi-circular anomalies, and the black dashed line outlines the interior of the rampart.**
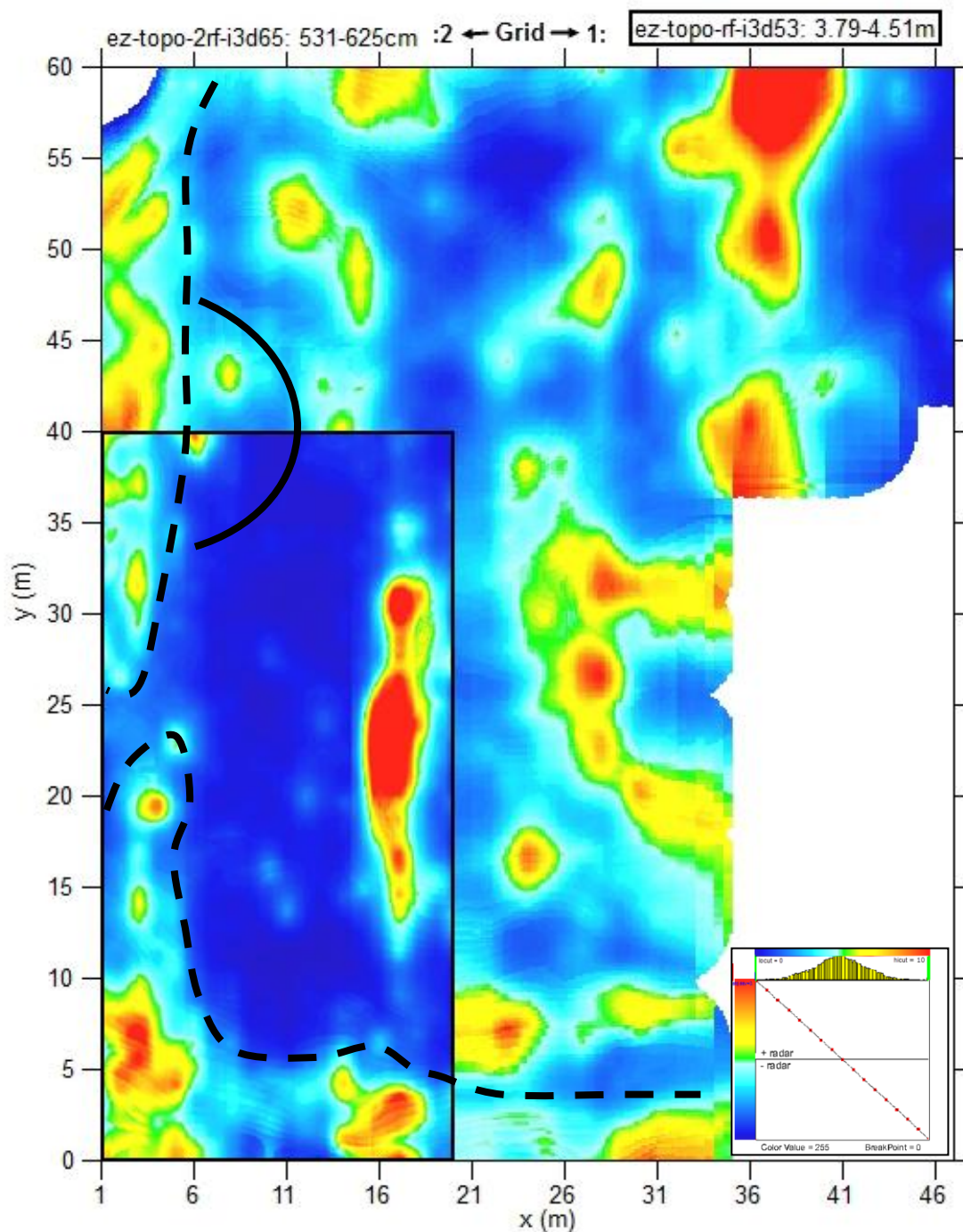
Figure 32**: Gain-adjusted, resampled, background filtered, and topographically corrected composite of GPR Grids 1 and 2 at an approximate depth of 5.31-6.25 m below site maximum elevation (341.5 m a.m.s.l.). The depth for each grid differs due to different surface elevations used as time-zero – a 2 m-offset between the two. The black arc outlines the northern semicircular anomaly, and the dashed black line outlines two sections of the observed ramparts and defines the gap within them.**
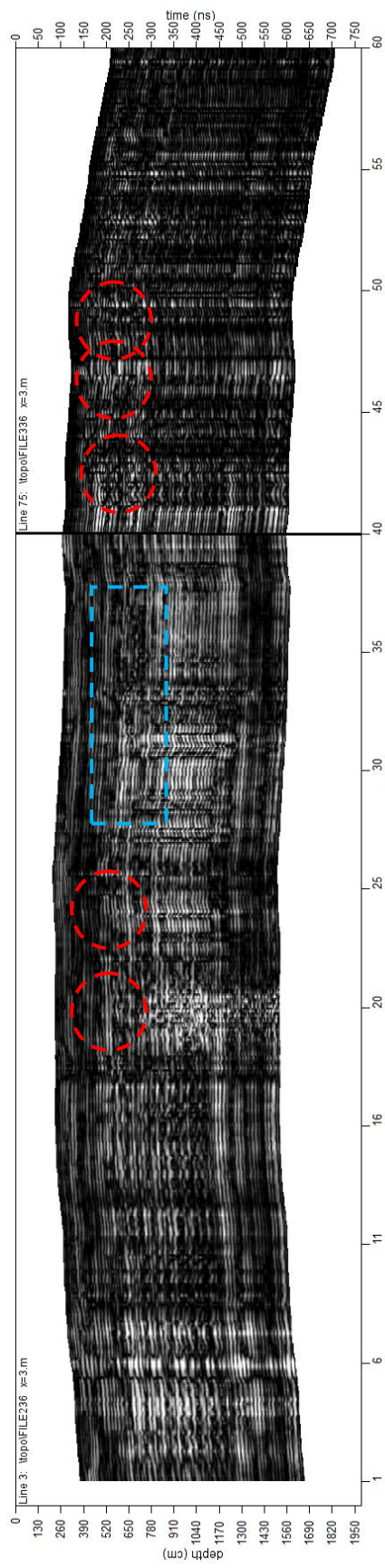
Figure 33: Composite radargram of lines 3 and 75. The dashed red circles highlight potential archaeological anomalies along the rampart and the dashed blue box highlights the possible gap in the rampart.

Figure 34: Composite radargram of lines 7 and 71. The dashed red circles highlight potential archaeological anomalies along the semi-circular anomalies.
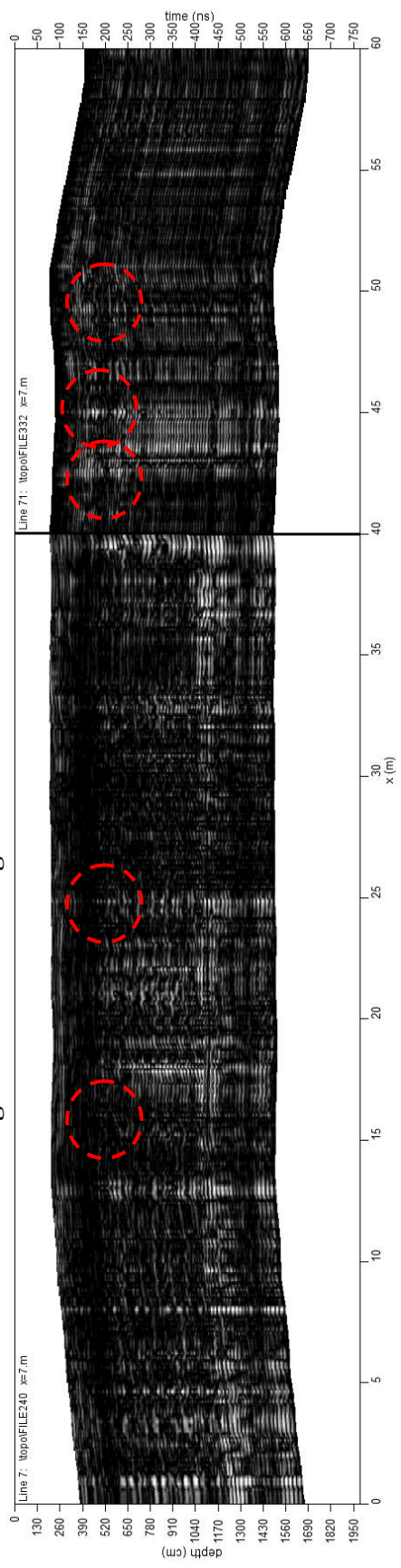
reflections from tree trunks (cf. Figs. 24, 30, & 31). These two circular anomalies cease approximately 5.31-6.28 m below site maximum elevation.

The rampart observed on the surface and in the magnetometry data is also clearly defined in the GPR survey, with the location and potential characteristics of buried portions identified. The rampart is clearly visible in the radar reflections along the western and southern baselines (cf. Fig.s 32 & 33). At y = 20-25 m, between the two semi-circular anomalies at shallower depths, a gap in the rampart is evident by the decreased reflection strength – a potential entrance (cf. Figs. 30-34). This gap aligns with the sloping terrace (cf. Fig. 14) that connects the LT to the rampart from the southeast.

7. Discussion and Pre-Ground-truth Conclusions

7.1. Comparison to Previous Surveys and New, Pre-ground-truth Conclusions

Rubicon Heritage (2014) proposed site features for Caisteal Mac Tuathal after conducting a surface and GPRS rover survey (Fig. 35). The 2015 topographical and geophysical survey discussed here did not locate the southern annex or possible entrance proposed by Rubicon Heritage, but did locate two potential structures and an entrance along the northwestern rampart instead (Fig. 36). The northern annex and possible entrances proposed by Rubicon Heritage were not explored due to time limitations on the survey and the need for extensive site clearing.

Interpretations of topographic, magnetometry, and GPR data from the July 2015 survey of Caisteal Mac Tuathal have revealed a potential entrance through, and potential structural elements along, the western rampart. These potential structures along the interior to the western rampart include a potential platform/lookout tower (southern semicircular anomaly) and a potential residence and/or small byre (northern semicircular anomaly), with more confidence placed upon the interpretation of the southern anomaly due to numerous tree trunks atop the northern semicircular anomaly inhibiting a thorough analysis of the potential structure. Apart from the magnetometry anomaly in Grid 13, there are no geophysical data indicating other features inside the surveyed hillfort/upper terrace or along the lower terrace. However, this lack evidence is not unexpected due to the shallow soil profile encountered at the site precluding extensive preservation of archaeological material *in situ*. Any archaeological materials or features that have
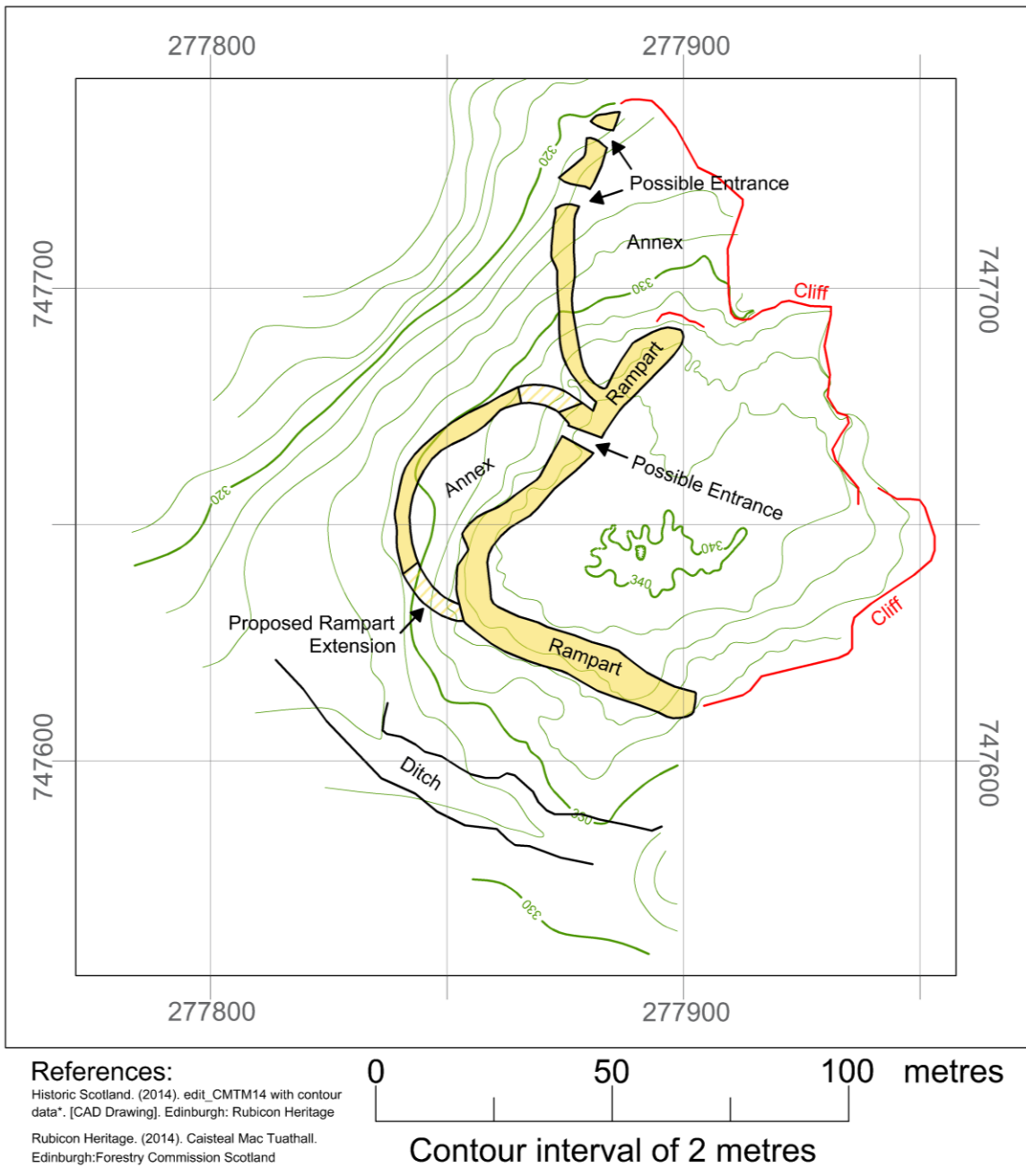
Figure 35**: Proposed structural features of Caisteal Mac Tuathal after Rubicon Heritage's 2014 surface walk and topographic survey of the site.**
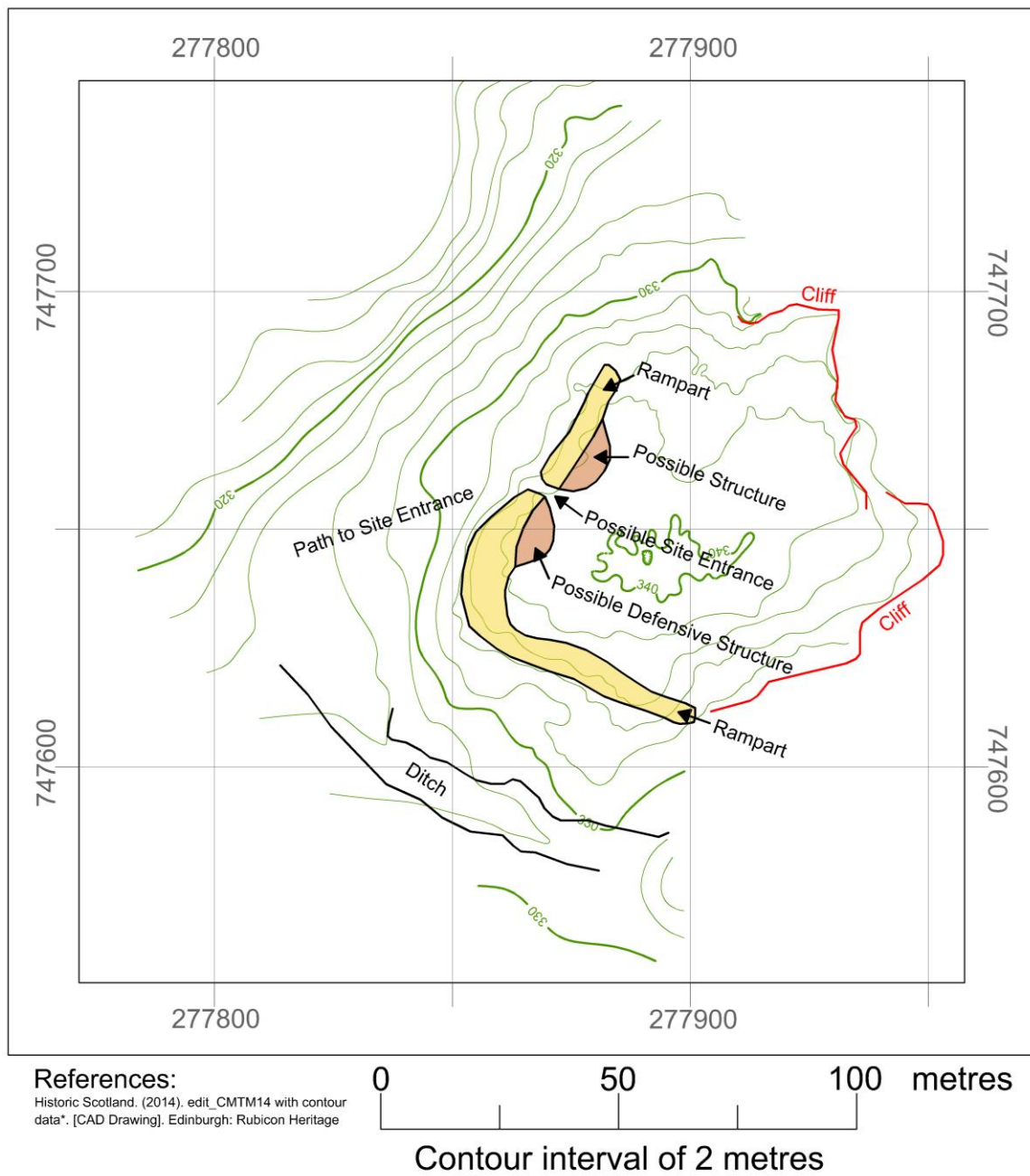
Figure 36**: Structural features proposed for Caisteal Mac Tuathal by this July 2015 multi-technique geophysical survey.**

remained *in situ* would likely be recovered from within the rubble stratum of the

collapsed ramparts, particularly around the proposed defensive tower/ structure attached

to the western rampart, and the proposed entrance between the two. One reason for this

conclusion is that the rubble would protect potential archaeological features from erosion,

if said features are indeed present.

7.2. Proposed Archaeology

Of the fortified Iron Age settlement types in the British Isles, brochs and duns are

structurally similar; the differentiation between them appears to be linguistic in origin,

with *broch* more prevalent in Norse-influenced northern Scotland and *dun* more prevalent

in Gaelic-influenced western Scotland (Romankiewicz, 2011a). Hillforts and promontory

forts, on the other hand, are geographically defined; regardless of similar structural

morphologies, the term *hillfort* is used to describe inland forts atop locally elevated

topography, and *promontory fort* is used to describe forts atop coastal cliffs (Lamb, 1980;

Cunliffe, 2005).

Caisteal Mac Tuathal is a hillfort. No evidence for a circular broch/dun structure

(e.g. those observed at Dun Ardtreck in Skye and Dun Mhadaidh in Argyll;

Romankiewicz, 2011b) confined by the upper terrace ramparts and cliff faces was

observed. Furthermore, the potential structures bordering the possible entrance through

the rampart appear to be built out from the rampart rather than pre-existing structures

being incorporated into the rampart during construction, like those at the Jarlshof

enclosed broch village in Shetland and the Midhowe broch in Orkney (cf. Fig. 30 and

MacKie, 2002:Fig.s 4.29 & 5.112). The uneven and frequently steep bedrock outcrops

within the UT would preclude the construction of stable, drystone structures therein

(Romankeiwizc, 2011a), limiting zones for potential construction to along the interior of the ramparts and small flat areas in the middle of the terrace north and south of the outcropping bedrock centered on GPR grid coordinates (26, 30). Furthermore, the proposed entrance to the site would be of practical use for the site's original occupants due to the abutting sloping terrace connecting the UT and LT, similar to that observed at the Kaimes hillfort in Midlothian (Simpson, 1969).

The Kaimes hillfort is topographically and structurally similar to the proposed archaeology of Caisteal Mac Tuathal – it is bordered by cliff faces on two sides, has an enclosed space with flat areas separated by steep terrain and exposed bedrock, and has an entrance atop a sloping terrace connecting the lower exterior landscape to the ramparts (Simpson, 1969). However, prior to modern quarrying, the Kaimes hillfort was almost four times larger (2.11 ha vs. 0.59 ha [RCAHMS, 1927; Feachem, 1963]); had a series of five and seven ramparts defending the lower and upper site areas, respectively; had visible structural remains of residences within the hillfort; and had timber constructions, at least in part, within earlier rampart contexts (Simpson, 1969).

Caisteal Mac Tuathal was built upon stable bedrock, the ramparts and two proposed structures at the site likely following the prehistoric Scottish tradition (Armit, 1990) of drystone masonry and are not timber-laced due to the distinct lack of significant forestation in the region prior to reforestation during the Victorian era (Batcheler, 1960). It is this lack of significant forestation that likely precluded the construction of Caisteal Mac Tuathal at the highest point of Drummond Hill; frequently strong winds and constant exposure to the elements would have likely rendered Caisteal Mac Tuathal unusable if it was not constructed on the more sheltered outcrop on Drummond Hill's

northern terminus. Due to the site's current state of preservation excavation is required to resolve whether or not Caisteal Mac Tuathal expresses the architectural characteristics of vitrified, rubble-and-earth-cored drystone faced, or simply a drystone hillfort (Cunliffe, 2005). Also obscured by the overlying rubble is the proposed entrance through the western rampart. The GPR data contains a distinct gap, and the magnetometry data has an anomaly that is relatively muted in comparison with the adjacent ramparts, in the western rampart where the proposed entrance is (cf. Fig.s 32 & 33). However, exact entrance morphology is not distinguishable in the geophysical data, requiring ground-truthing excavations to clarify its potential as a site entrance.

7.3. Caisteal Mac Tuathal, the Loch Tay Crannogs, and Glen Lyon

Due to Caisteal Mac Tuathal's prominent location in the local landscape, and proximity to Loch Tay, it would be unsurprising, even expected, for future investigations to reveal a temporal and/or material connection between Caisteal Mac Tuathal and the Loch Tay crannogs. If discovered during these potential future investigations of the site, this proposed connection between Caisteal Mac Tuathal and the Loch Tay crannogs would indicate the hillfort was constructed during the Early Scottish Iron Age and served primarily as a lookout and potential refuge for the Loch Tay, and possibly Glen Lyon, communities. This potential connection between Caisteal Mac Tuathal and the settlements along Loch Tay and within Glen Lyon can be tested by the following proposed future studies of Caisteal Mac Tuathal along with a thorough study of the available archaeological record from, and literature of, the Loch Tay crannogs and Glen Lyon settlements.

7.4. Future Studies at Caisteal Mac Tuathal

The geophysical surveys conducted herein did not extend to the sloping terrace connecting the northwestern rampart to the lower terrace, the northwestern annex identified by Rubicon Heritage (2014), or farther down-slope around the hillfort due to time constraints and recurring inclement weather precluding site access and use of the GPR equipment. However, additional geophysical studies utilizing magnetometry and GPR should be applied to this sloping terrace, and magnetometry surveys should be conducted along the base of the eastern and northern cliff-faces to test for archaeological materials impacted by colluvial processes and the presence of any midden outside the rampart's confines. A systematic bucket auger survey would be a logical follow-on to these additional geophysical surveys in order to confirm presence of any buried archaeological materials or features. Furthermore, a systematic remote sensing survey of the down-slope areas around the hillfort, particularly the area to the west (cf. the northwest edge of the clearing and into the forested region in Fig. 1c), should be conducted to determine said areas' potential to contain archaeological material, e.g. a LiDAR or thorough GPRS survey for a more extensive topographic survey followed by GPR, magnetometry, and, if the soil profile is sufficiently deep, resistivity surveys and ground-truthing.

Additionally, test trenches should be excavated across the proposed entrance and the two proposed structures along the western rampart to ground-truth the geophysical data and conclusions presented in this study. It would be particularly beneficial to recover material that can be radiocarbon dated as this would permit further discussion of the site in relation to the crannogs of Loch Tay; Caisteal Mac Tuathal's prominent location at the

entrance to the Tay Valley and Glen Lyon certainly requires a discussion of its use – or lack thereof – by the communities therein. Additional test trenches should be excavated across the trench separating the lower terrace from the hillfort to determine whether the trench is environmental or archaeological in origin, and to identify potential quarrying of construction material for Caisteal Mac Tuathal's ramparts from this trench.

8. Appendices

Appendix A: GPR_Slice Data Conversion, Resampling, Velocity Analysis, and 3D Volume Creation Data

Group	Process		Lines 1-20	Lines 21-77
Relative Depth	ε_r		33.28	33.28
	Velocity (m/ns)		0.052	0.052
Data Conversion	17-point gain adjust	0	1	1
		1	1	1
		2	1	1
		3	1.5	2
		4	2	2
		5	4.5	3.5
		6	3.5	2
		7	3.5	2
		8	4.5	2
		9	6.5	2
		10	8	2
		11	5.5	1.5
		12	2	2
		11	3	2
		14	2.5	1.5
		15	3.5	2
		16	1.5	1.5
	Wobble Length		52	52
Slice/Resample	# of Slices		40	40
	Samples to 0 ns		36	46
	Cuts per mark		7	7
	Resampling process		squared amplitude	squared amplitude
	% Overlap		50	50
Gridding*	Grid cell size		0.075	0.1
	X search radius		2.5	3
	Y search radius		2.5	3
	Blanking radius		2.5	2.5
Pixel	# of interpolations		4	4

*Topography Gridding Parameters: grid cell size = 0.075; search and blanking radii = 5.

Appendix B: Topographic Correction Data

X (m)	Y (m)	Z (m)	X (m)	Y (m)	Z (m)	X (m)	Y (m)	Z (m)
1	3	336.5	4	33.4	338	8	5.5	337.5
1	4.5	337	4	39.1	337.5	8	9.8	338
1	11.7	337.5	4	40	338	8	17.1	338.5
1	15.6	338	5	0	336.5	8	18.7	338
1	21.4	338.5	5	3.5	337	8	20.7	338.5
1	22.3	338	5	6.6	337.5	8	23.7	338
1	23.5	337.5	5	14	338	8	24.7	338.5
1	27	338	5	17.1	338.5	8	27.4	338
1	28.1	337.5	5	18.3	338	8	40	338.5
1	30.2	337	5	27.1	338.5	9	0	336
1	32.6	336.5	5	28.6	339	9	0.8	336.5
1	35	336	5	29.8	338.5	9	3.9	337
1	40	336.5	5	31.5	338	9	5.4	337.5
2	3	336.5	5	33.8	338.5	9	8	338
2	3.9	337	5	35.4	338	9	15.5	338.5
2	11.2	337.5	5	38.9	337.5	9	16.7	338
2	16.3	338	5	40	338	9	20.7	338.5
2	25.2	338.5	6	0	336.5	9	32.9	338
2	27.3	338	6	3.7	337	9	40	338.5
2	29.1	337.5	6	5.6	337.5	10	0	337
2	40	337	6	10.7	338	10	0.2	337.5
3	1	336.5	6	13.6	338.5	10	3.5	337
3	3.5	337	6	14.7	338	10	5.5	337.5
3	7.9	337.5	6	17.4	338.5	10	6.5	338
3	17.3	338	6	18.7	338	10	15.6	338.5
3	26.3	338.5	6	31.7	338.5	10	18.9	338
3	27.9	338	6	33.2	339	10	21.3	338.5
3	33.9	337.5	6	34.8	338.5	10	33.5	338
3	37.6	337	6	40	338	10	37.6	338.5
3	39.6	337.5	7	0	336.5	10	38.3	338
3	40	338	7	3.9	337	10	40	338.5
4	0	336.5	7	5.5	337.5	11	0	336
4	3.4	337	7	10.3	338	11	0.1	336.5
4	8	337.5	7	14.1	338.5	11	2.8	337
4	14.1	338	7	18.4	338	11	5.7	337.5
4	16.6	338.5	7	35.9	338.5	11	6.5	338
4	17.8	338	7	39	338	11	15.7	338.5
4	28	338.5	7	40	338.5	11	17.6	338
4	29.7	338	8	0	336.5	11	21.9	338.5
4	32.4	337.5	8	4	337	11	23.8	338

X (m)	Y (m)	Z (m)	X (m)	Y (m)	Z (m)	X (m)	Y (m)	Z (m)
11	26.4	338.5	14	27.9	338.5	18	21.4	339.5
11	32.2	338	14	30.2	338	18	21.5	340
11	37.4	338.5	14	39.4	338.5	18	22.4	339.5
11	38.8	338	14	40	338	18	22.9	339
11	40	338.5	15	0	337	18	24.6	338.5
12	0	336.5	15	2.8	337.5	18	25.5	339
12	2.4	337	15	4.5	338	18	27.2	339.5
12	4	337.5	15	13.8	338.5	18	28.5	339
12	5.4	337	15	14	339	18	40	338.5
12	6.1	337.5	15	26	339	19	0	336.5
12	6.8	338	15	27.4	338.5	19	2.8	337
12	21.7	338.5	15	30.5	338	19	3.8	337.5
12	23.4	338	15	39.8	338.5	19	6.5	338
12	26.6	338.5	15	40	338	19	10.4	338.5
12	29.5	338	16	27	339	19	12.9	339
12	40	338.5	16	27.2	338.5	19	17.3	339.5
13	0	336.5	16	30.2	338	19	18.3	340
13	2.3	337	16	40	338.5	19	20.8	339.5
13	2.9	337.5	16	3	337	19	22.7	340
13	4	338	16	4.6	337.5	19	24.1	339.5
13	4.2	337.5	16	7.2	338	19	27.3	340
13	5.8	337	16	13.9	338.5	19	29	339.5
13	6.5	337.5	16	17	339	19	33.8	339
13	7.3	338	17	0	336.5	19	40	338.5
13	21.8	338.5	17	2.5	337	20	0	336.5
13	24.3	338	17	4	337.5	20	3.2	337
13	25.9	338.5	17	6.7	338	20	4.1	337.5
13	27.8	338	17	10.4	338.5	20	6.8	338
13	29.3	338.5	17	21.9	339	20	10.9	338.5
13	40	338	17	27.3	338.5	20	13.3	339
14	0	336.5	17	29.2	338	20	17	339.5
14	2.3	337	17	40	338.5	20	18.8	340
14	2.9	337.5	18	0	336.5	20	21	339.5
14	3.9	338	18	2.6	337	20	23.2	340
14	4.2	337.5	18	3.8	337.5	20	23.9	339.5
14	5.9	337	18	6.5	338	20	25.6	340
14	6.5	337.5	18	10.3	338.5	20	29.2	339.5
14	7.6	338	18	13.2	339	20	34.6	339
14	22.8	338.5	18	17.9	339.5	20	40	338.5
14	25.5	338	18	20.6	339	22	0	336

X (m)	Y (m)	Z (m)	X (m)	Y (m)	Z (m)	X (m)	Y (m)	Z (m)
22	0.7	336.5	24	39.7	338.5	27	18.1	339.5
22	4.1	337	24	40	338	27	25.2	340
22	5.2	337.5	25	0	336	27	27.8	339.5
22	8.5	338	25	1.1	336.5	27	28	340
22	10.9	338.5	25	4.7	337	27	30	340.5
22	13.1	339	25	6.5	337.5	27	32	340
22	17.6	339.5	25	10.8	338	27	33	339.5
22	25.6	340	25	13.2	338.5	27	36.9	339
22	31.6	339.5	25	14.6	339	27	37.2	338.5
22	34.3	339	25	19.3	339.5	27	38.8	339
22	40	338.5	25	28.5	340	27	40	338.5
23	0	336	25	30	339.5	28	0	336.5
23	1.1	336.5	25	32	340	28	4.6	337
23	4.5	337	25	34	339.5	28	6	337.5
23	5.9	337.5	25	35.2	339	28	8.5	338
23	9.6	338	25	29.8	338.5	28	11	338
23	11.1	338.5	25	40	338	28	11.7	338.5
23	13.8	339	26	0	336	28	11.8	339
23	19.6	339.5	26	1	336.5	28	13.1	339.5
23	25.4	340	26	4.7	337	28	15.2	339
23	28.1	339.5	26	6.7	337.5	28	19.3	339.5
23	29.3	340	26	9	338	28	25	340
23	32.5	339.5	26	10	338.5	28	26.5	339.5
23	34.3	339	26	11	338.5	28	29.3	340
23	37	338.5	26	11.2	338	28	34.8	339.5
24	0	336	26	13.1	338.5	28	37	340
24	1.2	336.5	26	14.7	339	28	37.2	339.5
24	4.7	337	26	17.9	339.5	28	39	339
24	6.3	337.5	26	26.4	340	28	40	338.5
24	10.3	338	26	27.2	339.5	29	0	336
24	12.2	338.5	26	31.6	340	29	1.4	336.5
24	14.4	339	26	32.7	339.5	29	4.8	337
24	19.9	339.5	26	35.9	339	29	9.2	337.5
24	25.2	340	26	40	338.5	29	10.7	338
24	27.2	339.5	27	0	336.5	29	11.8	338.5
24	28.7	340	27	4.6	337	29	15.5	339
24	32	339.5	27	6.8	337.5	29	20.9	339.5
24	33	340	27	11.1	338	29	29.6	340
24	34.5	339.5	27	12.5	338.5	29	30	339.5
24	36	339	27	14.9	339	29	31	340

X (m)	Y (m)	Z (m)	X (m)	Y (m)	Z (m)	X (m)	Y (m)	Z (m)
29	32.2	339.5	31	33.1	340.5	28	49.5	338
29	32.8	340	31	33.9	340	28	50.6	337.5
29	33.9	340.5	31	38.7	339.5	28	52.1	337
29	36.7	340	31	40	339	28	53.7	337.5
29	37.7	339.5	23	40	338.5	28	58.2	337
29	39.9	339	23	44.1	338	28	60	336.5
29	40	338.5	23	48	337.5	29	40	339
30	0	336	24	40	338.5	29	42.8	338.5
30	1.6	336.5	24	43.6	338	29	47	338
30	5	337	24	48	337.5	29	49	338.5
30	7	337.5	24	49	338	29	51	338
30	10	338	24	50	338.5	29	56.6	337.5
30	13	338.5	24	51	338	29	57.8	337
30	13.5	339	24	51.9	337.5	29	59.5	336.5
30	14.7	339.5	24	57.3	337	29	60	337
30	16.3	339	24	60	336.5	30	40	339.5
30	21.4	339.5	25	40	338.5	30	42.2	339
30	30	340	25	43.7	338	30	47	338.5
30	31.5	341.5	25	46	337.5	30	49.5	339
30	32	341	25	49	338	30	51.5	338.5
30	34.3	340.5	25	51.3	337.5	30	52.4	338
30	35.1	340	25	57.4	337	30	57.7	338
30	38.2	339.5	25	60	336.5	30	59.9	337.5
30	40	339	26	40	339	30	60	337
31	0	335.5	26	40.3	338.5	31	40	339.5
31	0.5	336	26	43.9	338	31	44.1	339
31	1.5	336.5	26	46	337.5	31	49.3	338.5
31	5.9	337	26	49	338	31	55.6	339
31	6	337.5	26	52.2	337.5	31	58.9	338.5
31	10	338.5	26	57.4	337	31	60	338
31	13	339.5	26	60	336.5	32	40	339.5
31	13.9	340	27	40	339	32	44.8	339
31	14	339.5	27	40.8	338.5	32	48.8	338.5
31	15.1	339	27	44.4	338	32	51.6	339
31	20.5	339.5	27	50	337.5	32	52.1	339.5
31	21.2	340	27	52.4	337.5	32	59	339
31	21.9	340.5	27	56.9	337	32	60	338.5
31	29	340	27	50	336.5	33	40	339.5
31	30.5	341.5	28	40	339	33	44.9	339
31	32	341	28	42.6	338.5	33	49.7	338.5

X (m)	Y (m)	Z (m)	X (m)	Y (m)	Z (m)	X (m)	Y (m)	Z (m)
33	52.4	339	42	60	339	19	53	337.5
33	60	338.5	43	40	340	19	56	337
34	40	339.5	43	48.3	339.5	19	57	336.5
34	45	339	43	60	339	18	40	339
34	49.8	338.5	44	45	340	18	40.7	338.5
34	51.4	339	44	48.6	339.5	18	49.4	338
34	55	338.5	44	56.3	339	18	53.1	337.5
35	40	339.5	44	58.2	339.5	18	56.7	337
35	46.4	339	44	60	339	18	57	336.5
35	49.7	338.5	45	45	340	17	40	339
35	51	339	45	48.9	339.5	17	40.4	338.5
35	56	338.5	45	53.2	339	17	50.1	338
36	40	339.5	45	54.6	339.5	17	53.1	337.5
36	47.2	339	45	55.4	339	17	57	337
36	56	338.5	45	60	339.5	16	40	339
37	40	339.5	46	45	339.5	16	40.1	338.5
37	47.7	339	46	46.4	339	16	44	338
37	51.3	338.5	46	48.9	339.5	16	47.1	338.5
37	54.5	339	46	52.5	339	16	50.8	338
37	58	338.5	46	60	339.5	16	53.3	337.5
38	40	340	47	45	339.5	16	57.7	337
38	42.3	339.5	47	48	339	16	60	336.5
38	48.4	339	47	52.5	339	15	40	338.5
38	49.9	338.5	47	60	339.5	15	43	338
38	55.6	339	22	45	338.5	15	48.8	338.5
38	58	338.5	22	45.4	338	15	52.3	338
39	40	340	22	51	337.5	15	54.1	337.5
39	48.4	339.5	21	40	338.5	15	57.9	337
39	56.1	339	21	46.6	338	15	60	336.5
39	60	338.5	21	52.1	337.5	14	40	338.5
40	40	340	21	56.6	337	14	42.2	338
40	49.1	339.5	21	60	336.5	14	51	338.5
40	56.6	339	20	41	338.5	14	53.1	338
40	60	338.5	20	46	338	14	54.9	337.5
41	40	340	20	52.7	337.5	14	57.3	337
41	49	339.5	20	55.9	337	14	57.7	337.5
41	57.4	339	20	57	336.5	14	58.2	337
41	60	338.5	19	40	339	14	30	336.5
42	40	340	19	40.8	338.5	13	40	338.5
42	48.5	339.5	19	45.5	338	13	41.1	338

X (m)	Y (m)	Z (m)	X (m)	Y (m)	Z (m)	X (m)	Y (m)	Z (m)
13	48	338.5	8	52.8	338.5	4	52.4	337.5
13	50	339	8	53.6	338	4	54.5	337
13	51.4	338.5	8	55.4	337.5	4	55.2	336.5
13	53.8	338	8	59.8	337	4	55.5	336
13	54.8	337.5	8	60	336.5	4	60	335.5
13	56.3	337	7	40	339	3	40	338.5
13	58.3	337.5	7	41.6	338.5	3	42.8	338
13	59.4	337	7	50.8	339	3	48.8	337.5
13	60	336.5	7	53	338.5	3	51.4	337.5
12	40	339	7	53.7	338	3	52.5	337
12	51.6	338.5	7	55.3	337.5	3	53.4	336.5
12	53.7	338	7	59.8	337	3	54.2	336
12	54.8	337.5	7	60	336.5	3	57.3	335.5
12	57.4	337	6	40	338.5	3	60	335
12	58.5	337.5	6	40.3	338	2	40	337.5
12	60	337	6	45.4	338.5	2	40.6	337
11	40	339	6	50	339	2	43.8	337.5
11	48.4	338.5	6	51.7	338.5	2	47.2	337
11	50.1	339	6	52.7	338	2	50.4	337.5
11	52.6	338.5	6	55	337.5	2	51.6	337
11	54.6	338	6	56.5	337	2	52.1	336.5
11	56.4	337.5	6	59.2	336.5	2	52.8	336
11	60	337	6	60	336	2	56.5	335.5
10	40	339	5	40	338.5	2	59.1	335
10	47.1	338.5	5	41.4	338	2	60	334.5
10	50.5	339	5	42.4	338.5	1	40	337
10	53.7	338.5	5	45.3	338	1	41.6	336.5
10	54.5	338	5	50.3	338.5	1	45.5	337
10	57.1	337.5	5	50.8	338	1	46.7	336.5
10	60	337	5	54	337.5	1	50.7	337
9	40	339	5	55.3	337	1	51.4	336.5
9	45.2	338.5	5	56.1	336.5	1	52.2	336
9	51	339	5	56.5	336	1	54.8	335.5
9	52.8	338.5	5	60	336	1	59.1	335
9	53.6	338	4	40	338.5	1	60	334.5
9	55.9	337.5	4	44.2	338			
9	60	337	4	45.6	337.5			
8	40	339	4	48.1	338			
8	41.8	338.5	4	49.7	338.5			
8	51.3	339	4	50.1	338			

Appendix C: Potential Data Impairment Locations along GPR Lines

Line #	File #	Location from S60°W Baseline (m)	Description
4	237	20	Antenna swung around SIR-2000 control unit
8	243	15	Log
9	245	15	Log
11	250	5	Antenna lifted
		15	Possible tree throw
		30	Stump
13	252	17	Tree throw
14	252	10	Stump
		20	Antenna lifted over stump
17	258	15	Antenna lifted
19	260	14	Cable yank
20	261	30	Antenna lowered
		39	Antenna lifted
21	266	10	Antenna lifted
		22	Antenna swung around obstacle
		35	Antenna lifted and swing around obstacle
22	267	37	Antenna snagged on obstacle
23	268	10	Antenna lifted
24	270	18	Antenna lifted
		25	Antenna lowered
		36	Cable yank
25	272	2	Antenna snagged on obstacle
		17	Antenna lifted
		25	Antenna lifted
26	274	12	Antenna lifted
27	276	25	Antenna swung around SIR-2000 control unit
28	278	10	Antenna between bedrock outcrops
		12	Antenna lifted
29	280	19	Antenna lifted over rock
29			Maximum site elevation in line break 2
32	287	44	Antenna lifted
33	289	4	Antenna passed over stump
34	291	44	Antenna lifted
35	293	46	Antenna lifted

Line #	File #	Location from S60°W Baseline (m)	Description
36	294	46	Antenna lowered
		54	Antenna lifted
37			Treefall in line break
38			Treefall in line break
39	299	49	Tree throw
40	300		SIR-2000 control unit just past line terminus
41	301	55	Antenna swung around obstacle
			SIR-2000 control unit just past line terminus
42	302		SIR-2000 control unit just past line terminus
43	303	50	Antenna swung around obstacle
44	304	50	Antenna lifted
48	308	45	Antenna lifted
55	315	47-49	Antenna lifted over boulder
56	316		Path between two bedrock outcrops
57	317	62	Antenna lowered
		64	Antenna lifted
63	323	49-50	Treefall
		59	Antenna lifted over foliaged stump/rock
64	324	49-50	Antenna swung around treefall
65	325	49-50	Antenna over treefall
66	327	47	Antenna lifted
		49	Antenna swung around obstacle
		51	Antenna lowered
68	329	43	Antenna over stump
69	330	45	Antenna lifted
70	331	40-50	Antenna lifted
71	332	46	Antenna lifted
72	333	50	0.5 m drop over obstacle
73	334	40	Antenna lowered
74	335	41	Operator lost footing; antenna cattywompus
75	336	56	Antenna lifted
76	337	44-46	Antenna lifted over stumps
77	338	45-47	Antenna swung around obstacles
		49	Operator lost footing
		53	Antenna lifted

9. Plans

9.1. Topography

Caisteal Mac Tuathal with Selected Topography

Plan 1

Caisteal Mac Tuathal UT with Selected Topography
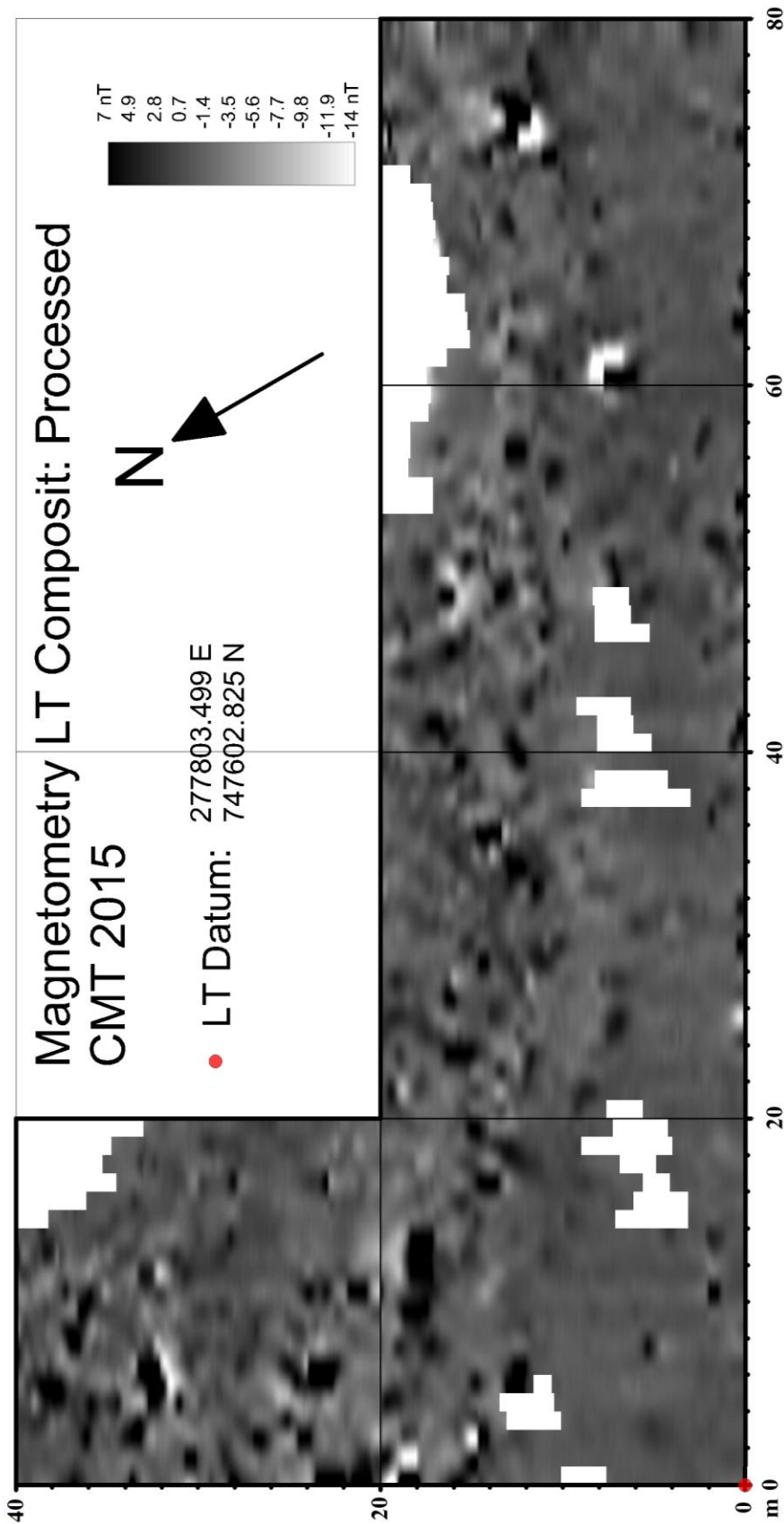

747700

277900

747700

747600

277900
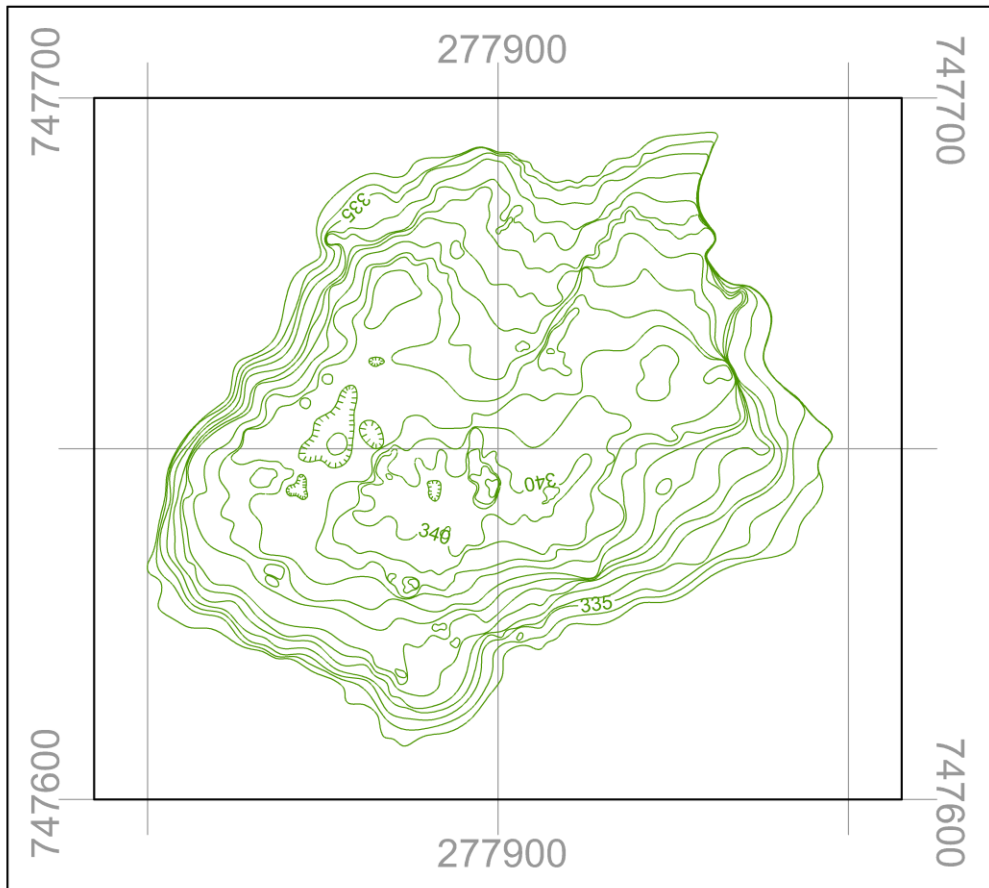
747600

References:

Historic Scotland. (2014). edit_CMTM14
with contour data*. [CAD Drawing].
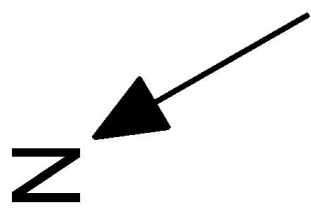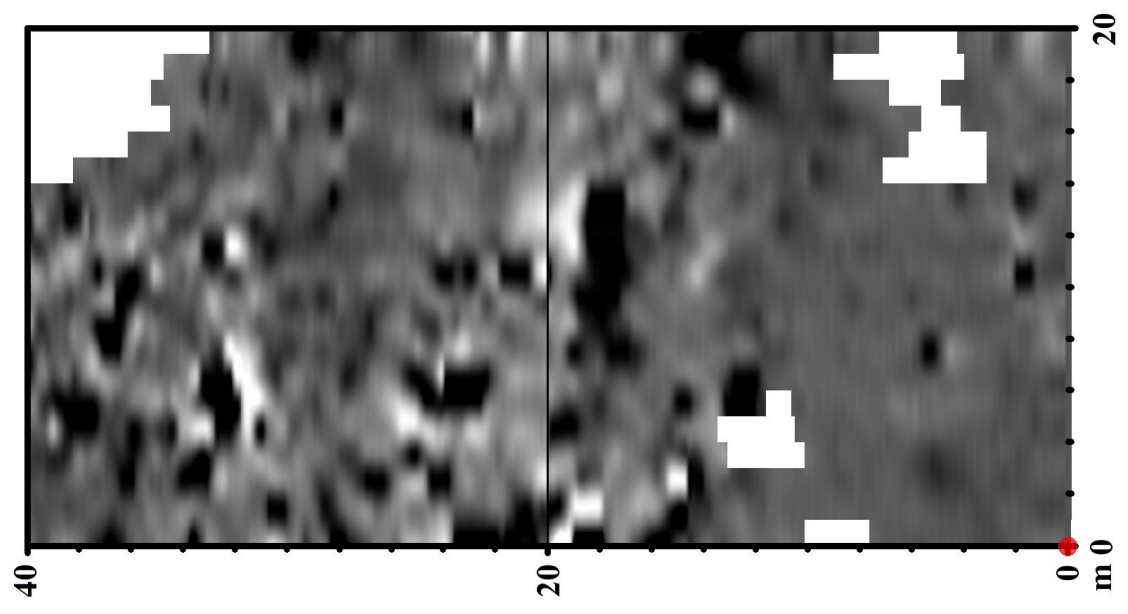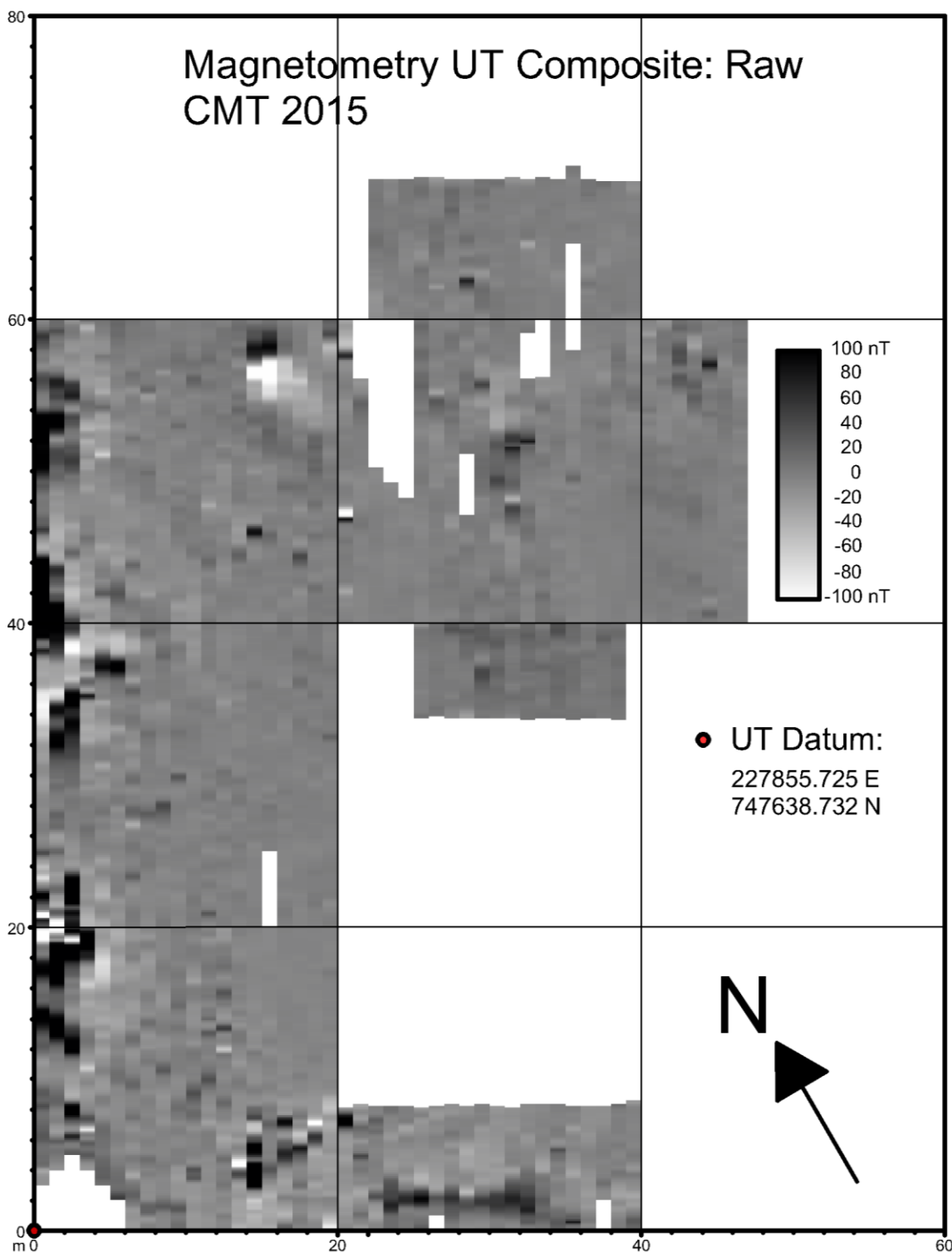Edinburgh: Rubicon Heritage

0   50 metres

Contour interval of 0.5 metres

Plan 2

9.2. Magnetometry

Magnetometry LT Composit: Raw
CMT 2015

● LT Datum: 277803.499 E
747602.825 N

N

100 nT
80
60
40
20
0
-20
-40
-60
-80
-100 nT

Plan 3

Magnetometry LT Composit: Processed
CMT 2015

• LT Datum: 277803.499 E
            747602.825 N

7 nT
4.9
2.8
0.7
-1.4
-3.5
-5.6
-7.7
-9.8
-11.9
-14 nT

N
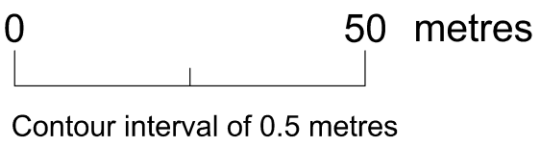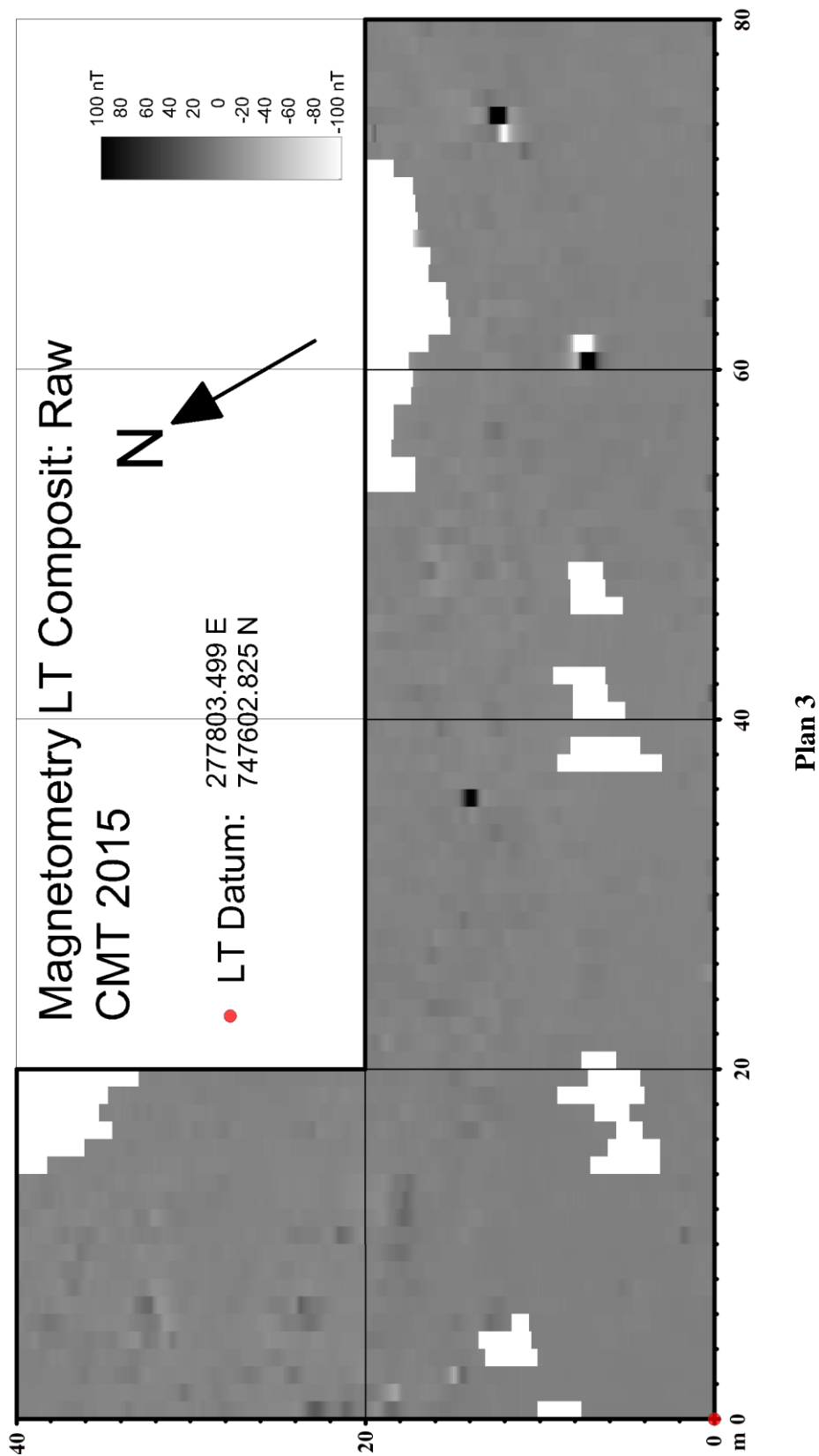
Plan 4

Magnetometry Western
LT and Swale Composite
CMT 2015

● LT Datum:
277803.499 E
747602.825 N

5 nT
3.6
2.2
0.8
-0.6
-2
-3.4
-4.8
-6.2
-7.6
-9 nT

Plan 5

Magnetometry UT Composite: Raw
CMT 2015

UT Datum:
227855.725 E
747638.732 N

N

Plan 6

Plan 7

CMT 2015 UT Circular Anomalies

Plan 8

UT Datum:
277855.725 E
747638.732 N

N

15 nT
8.5
2
-4.5
-11
-17.5
-24
-30.5
-37
-43.5
-50 nT

a   b   c

Plan 9

9.3. GPR

Gain-adjusted   **Plan 10**

r7: 1.8-2.41m
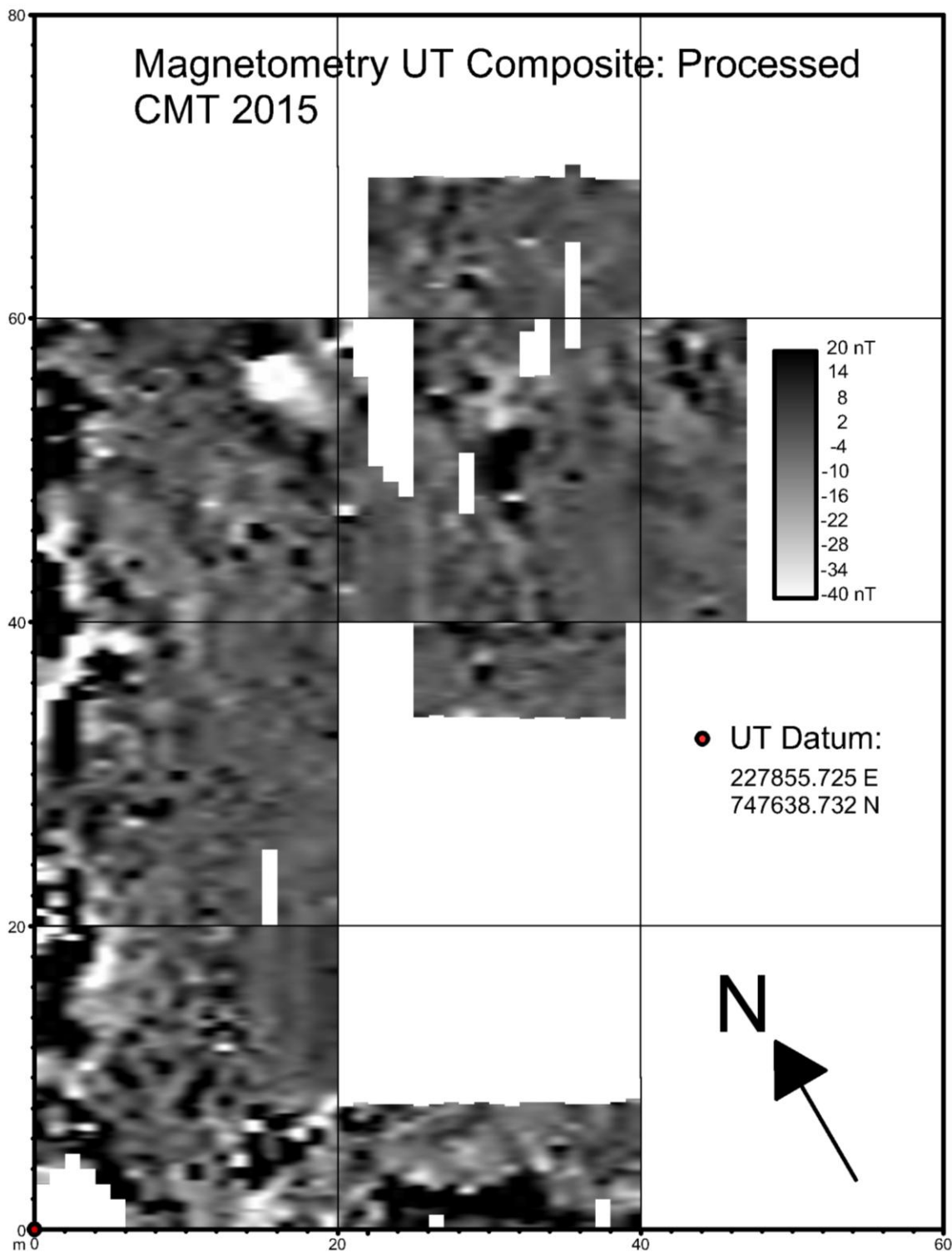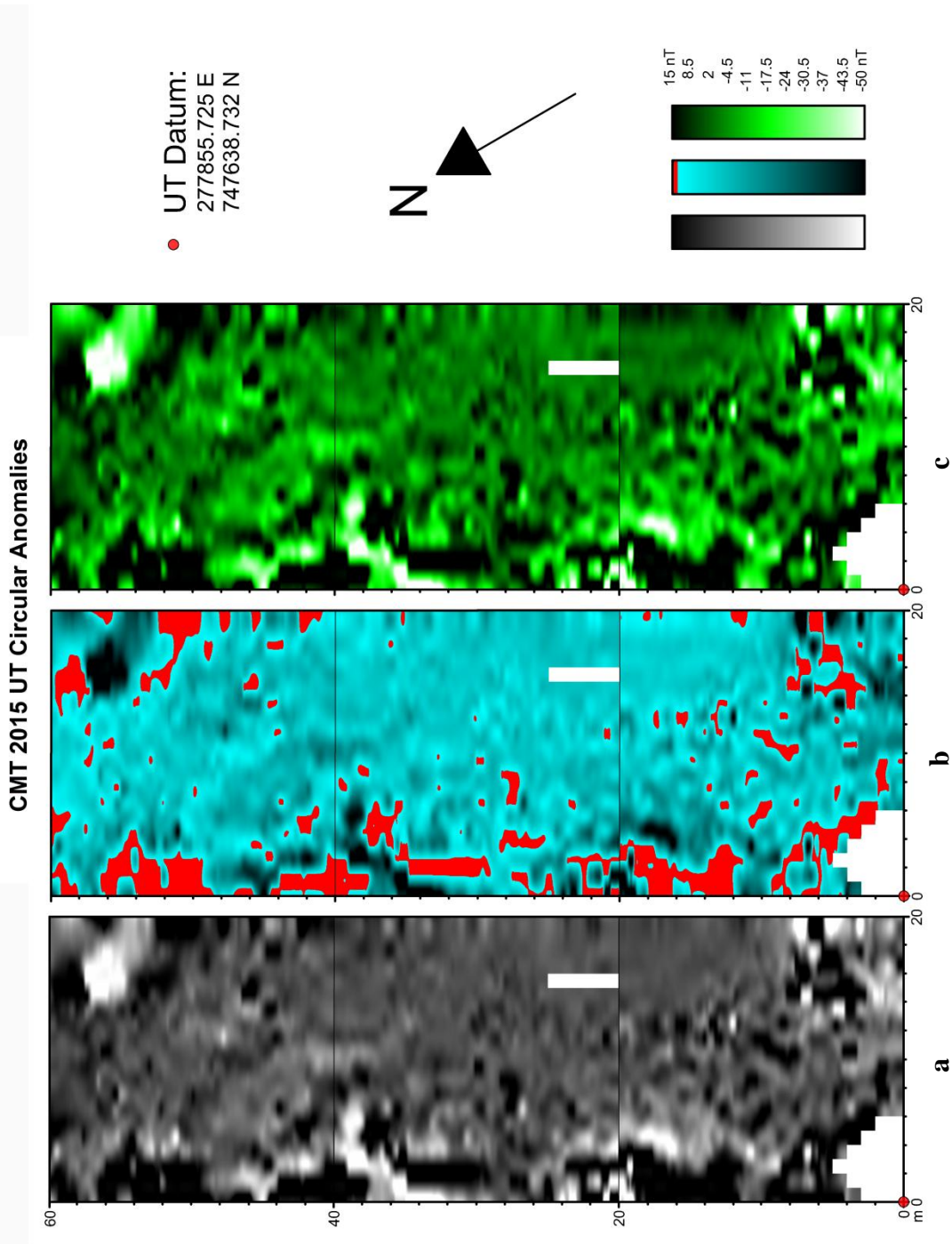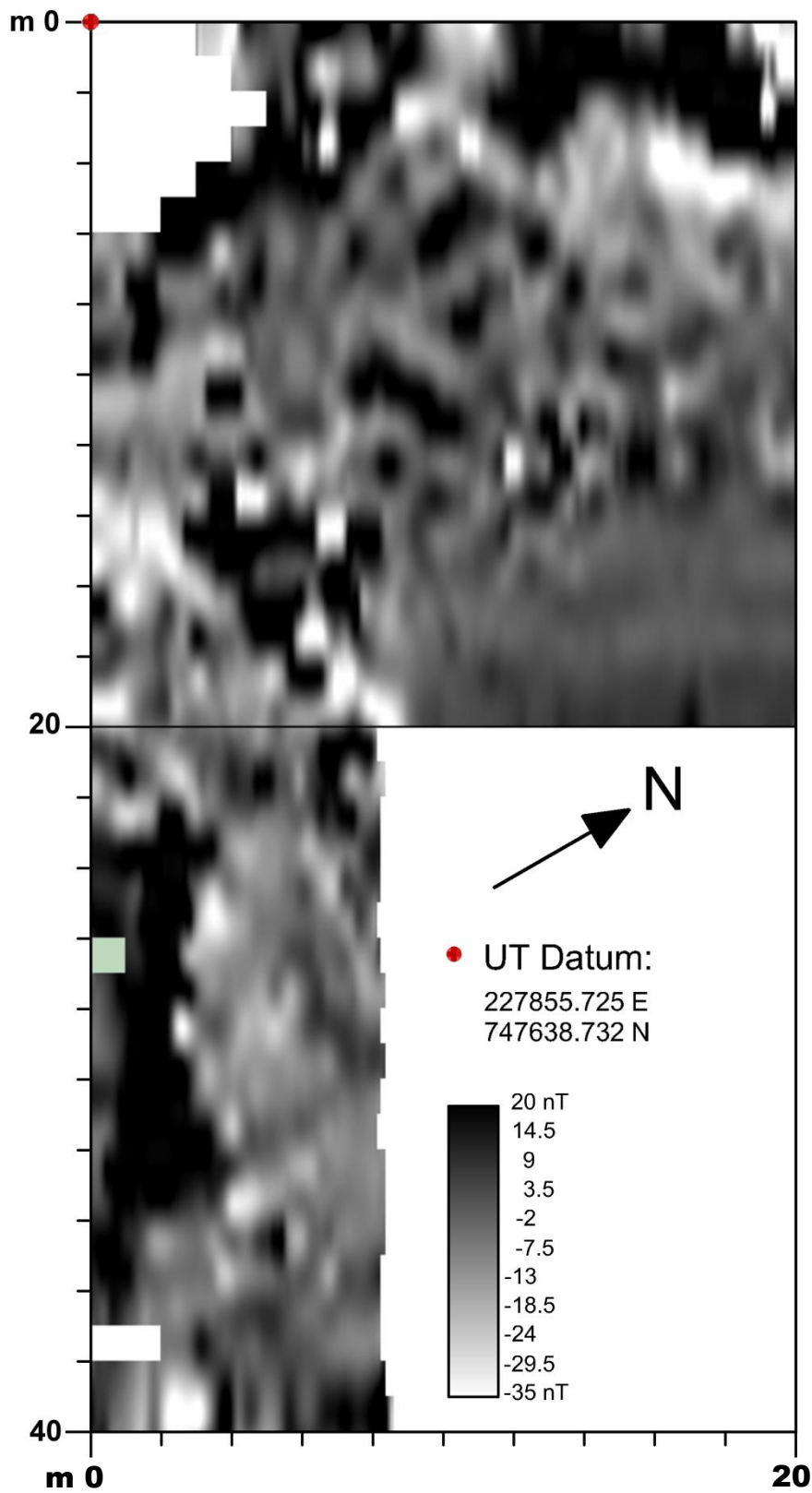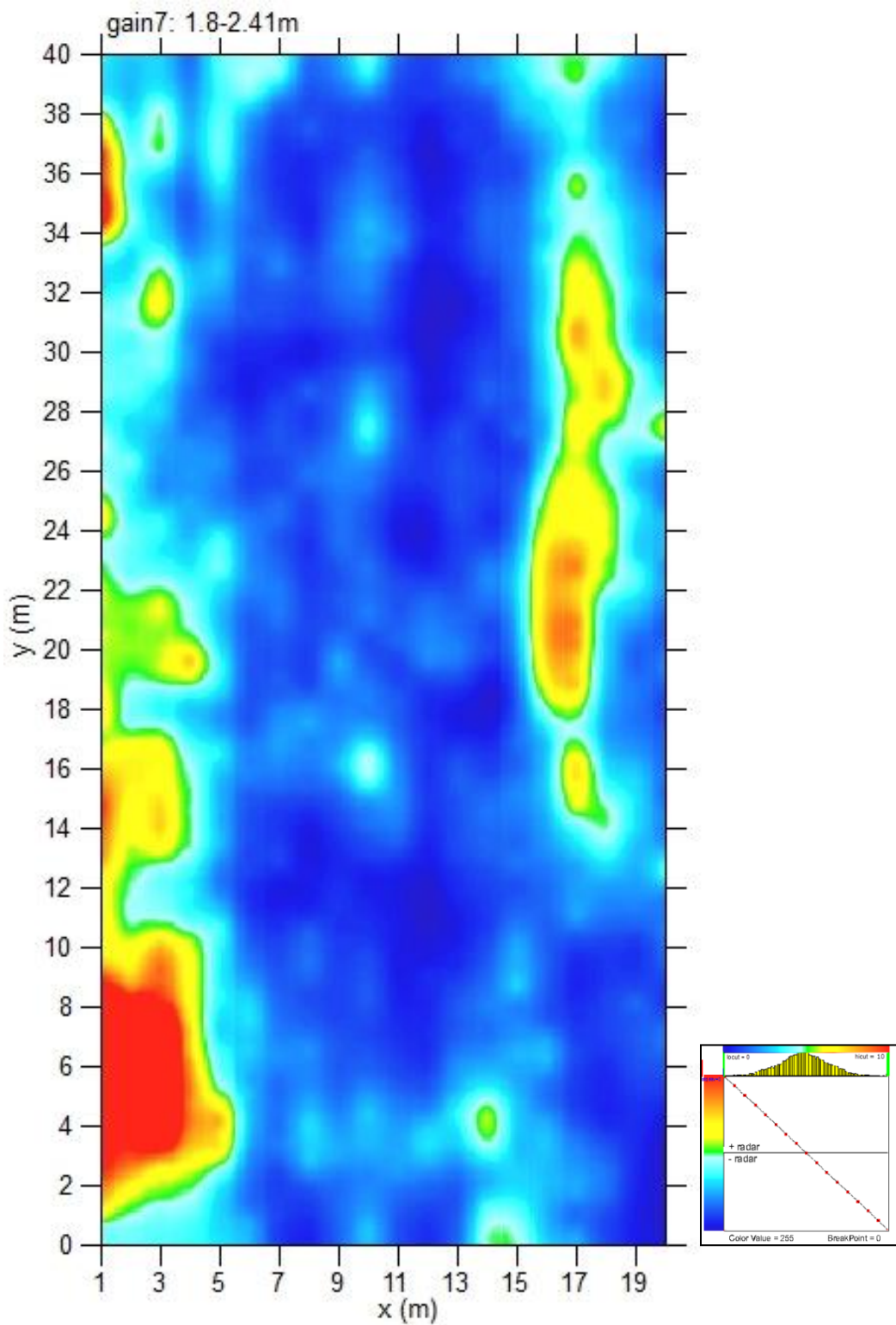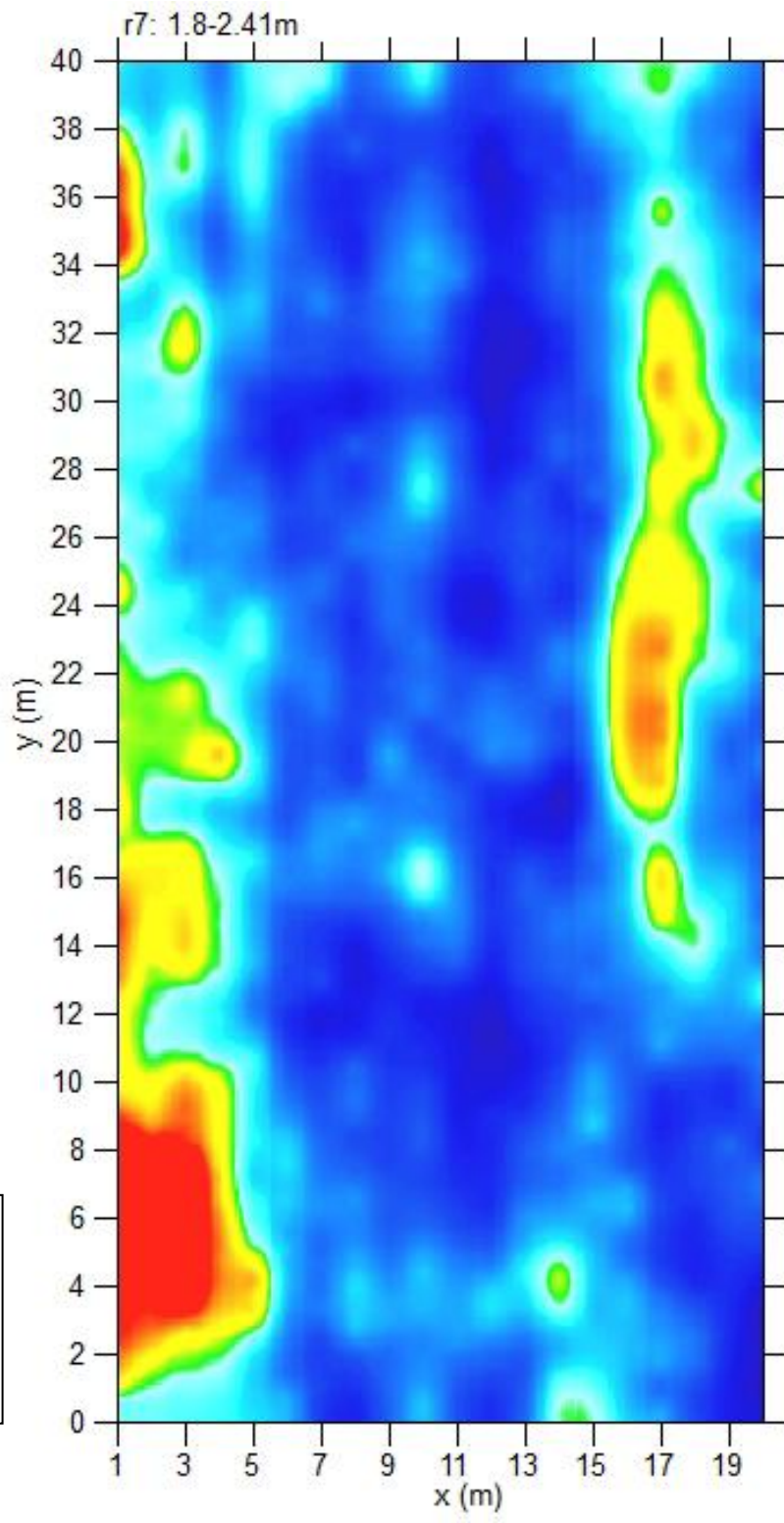
Plan 11

Gain-adjusted / Resampled

rf7: 1.8-2.41m
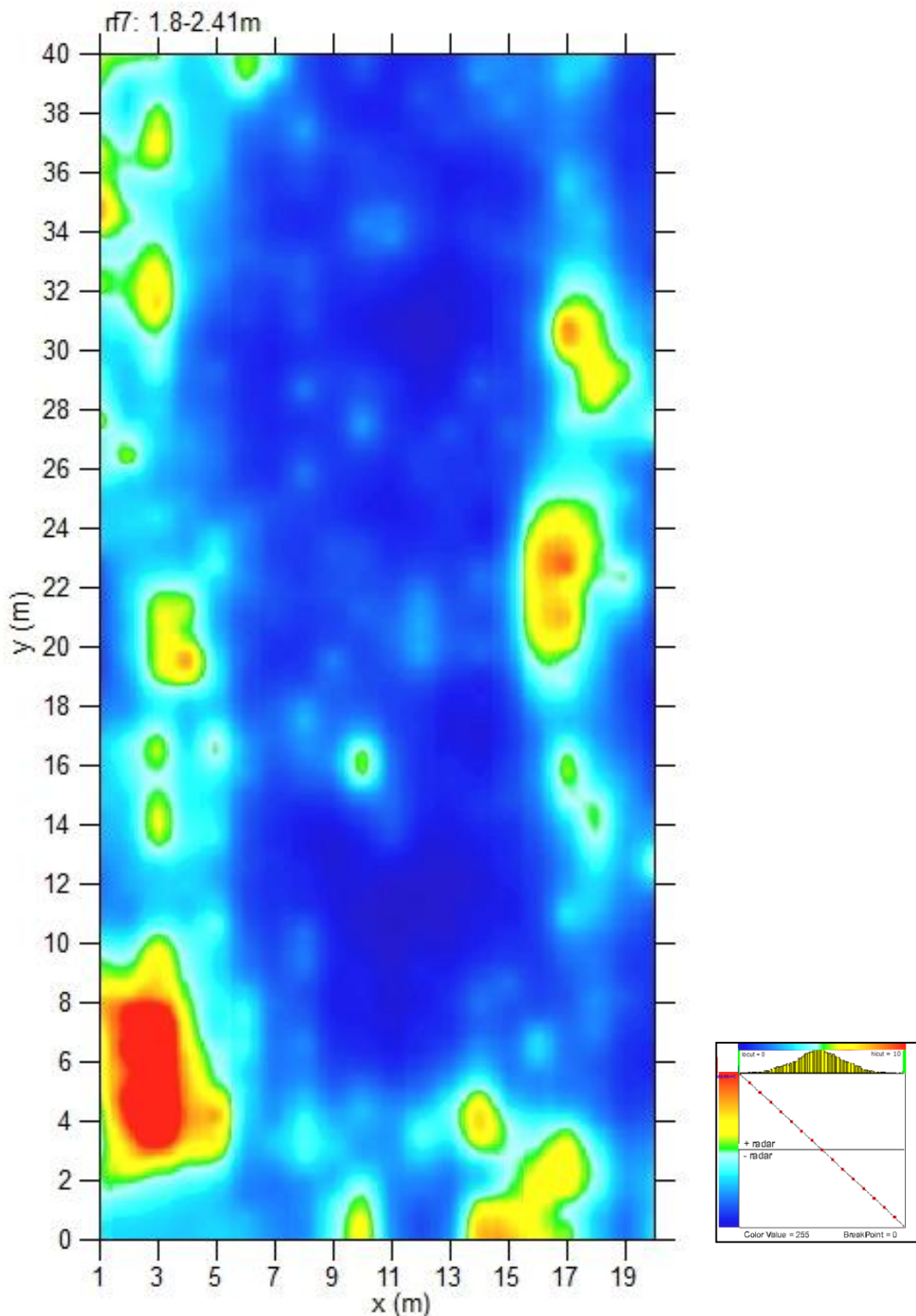
**Gain-adjusted / Resampled /
Background Filtered**
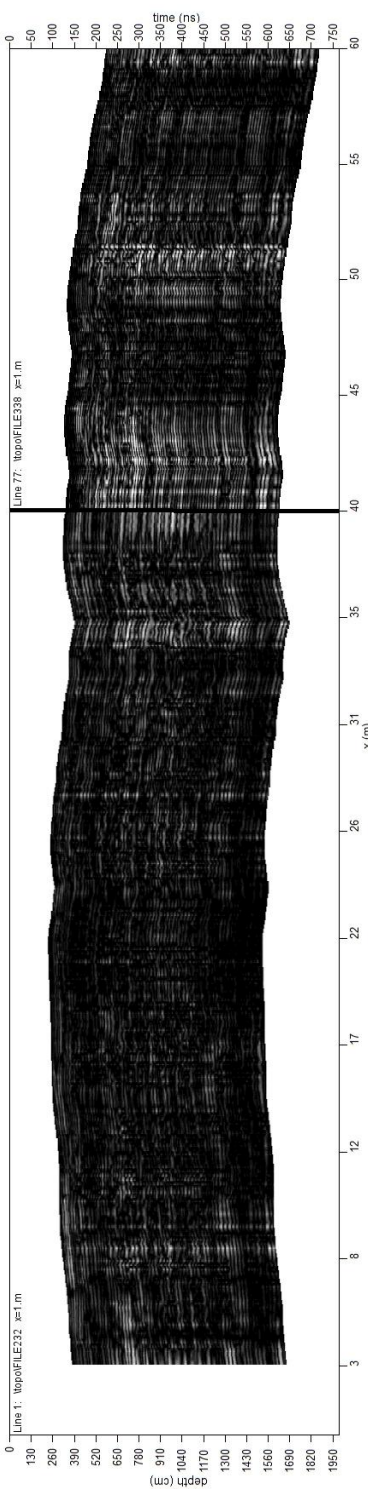
Plan 12

ez-topo-rf-i3d54: 3.85-4.57m
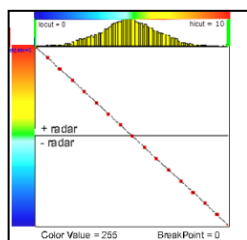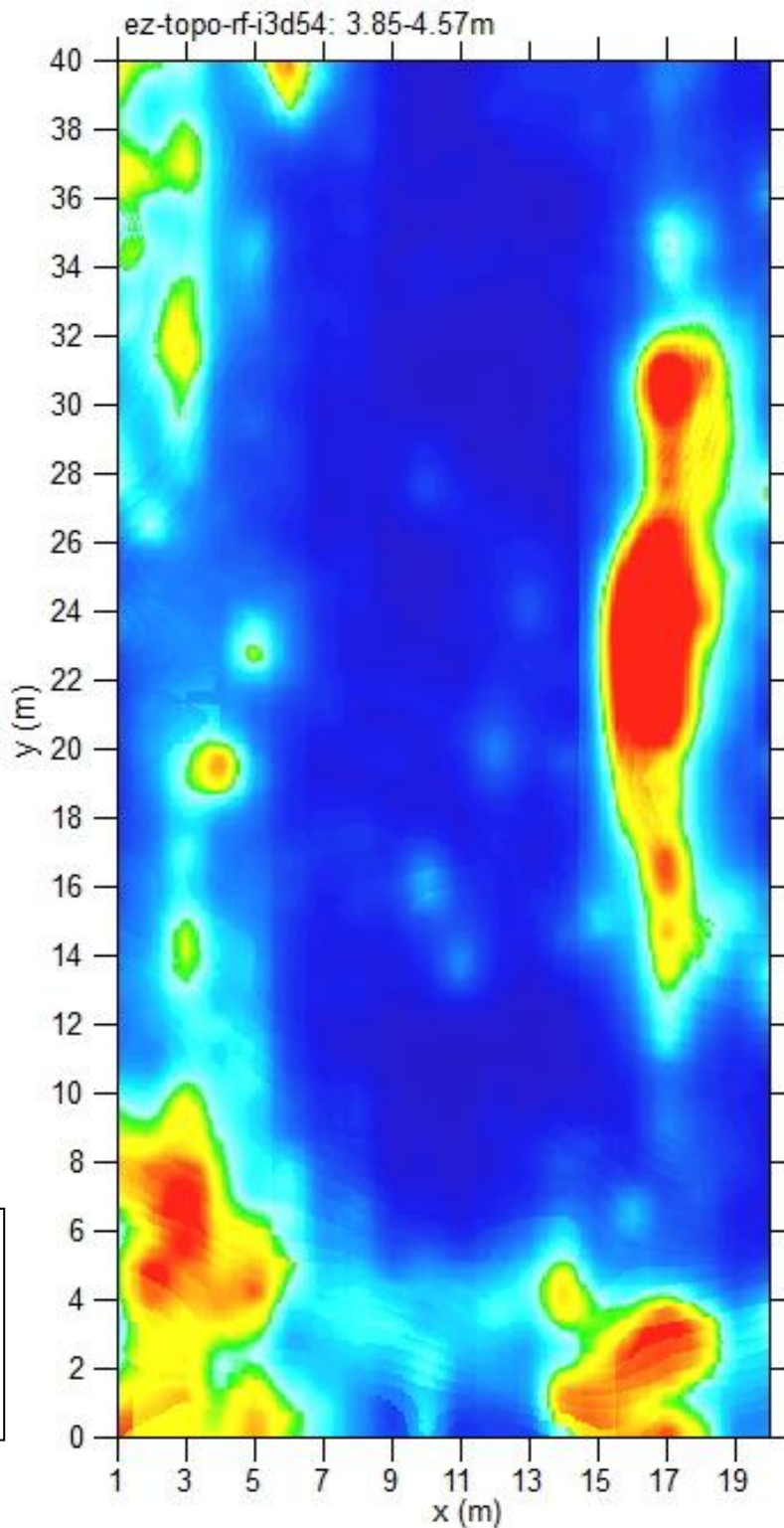
Plan 13

**Gain-adjusted / Resampled /
Background Filtered /
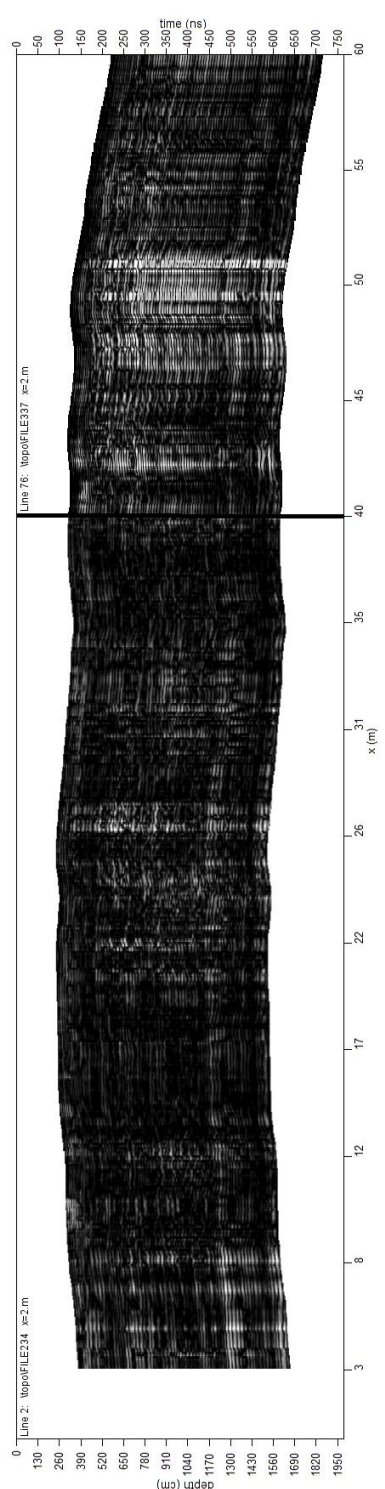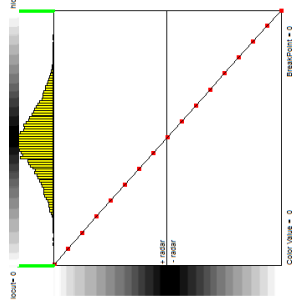Topographically Corrected**
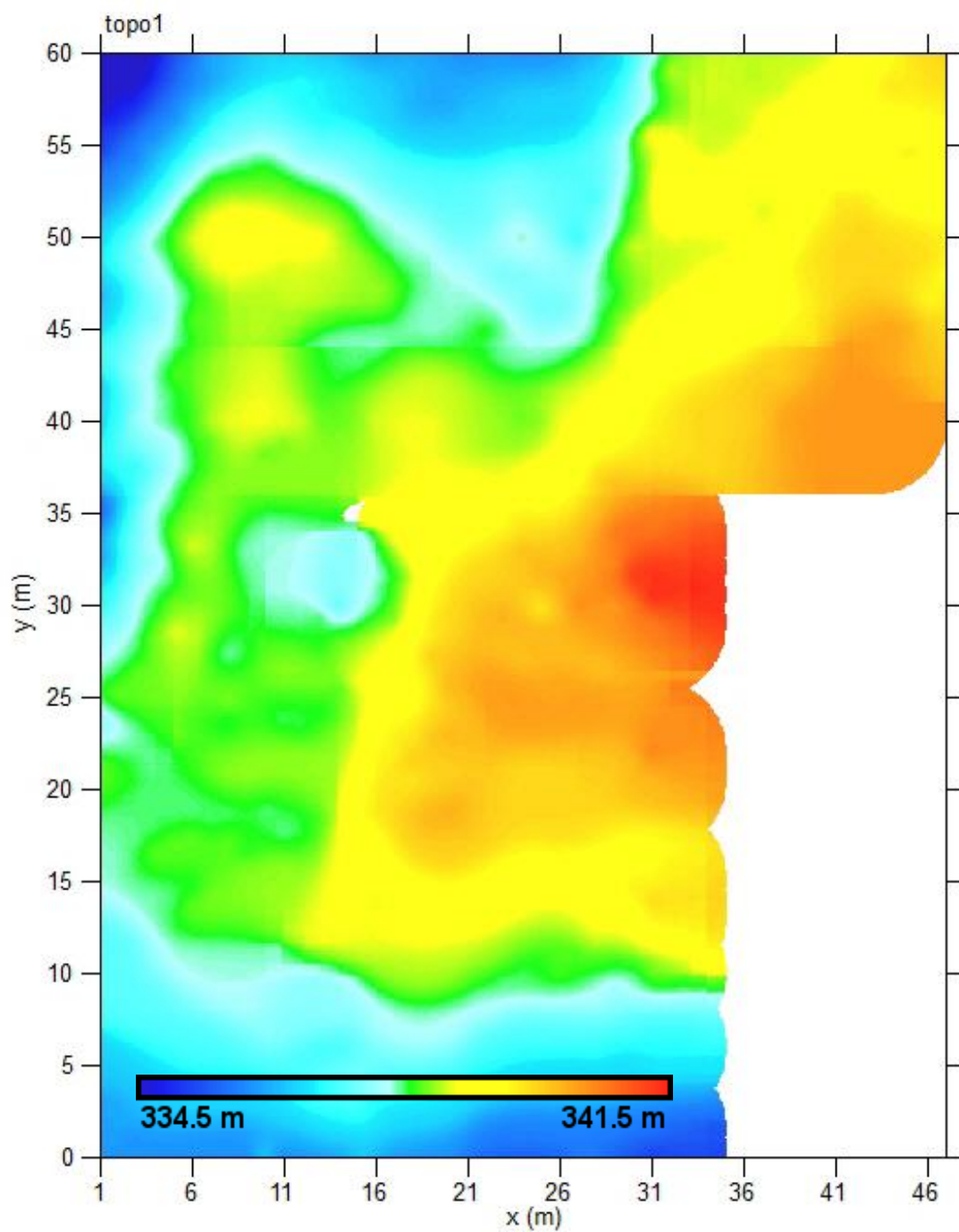
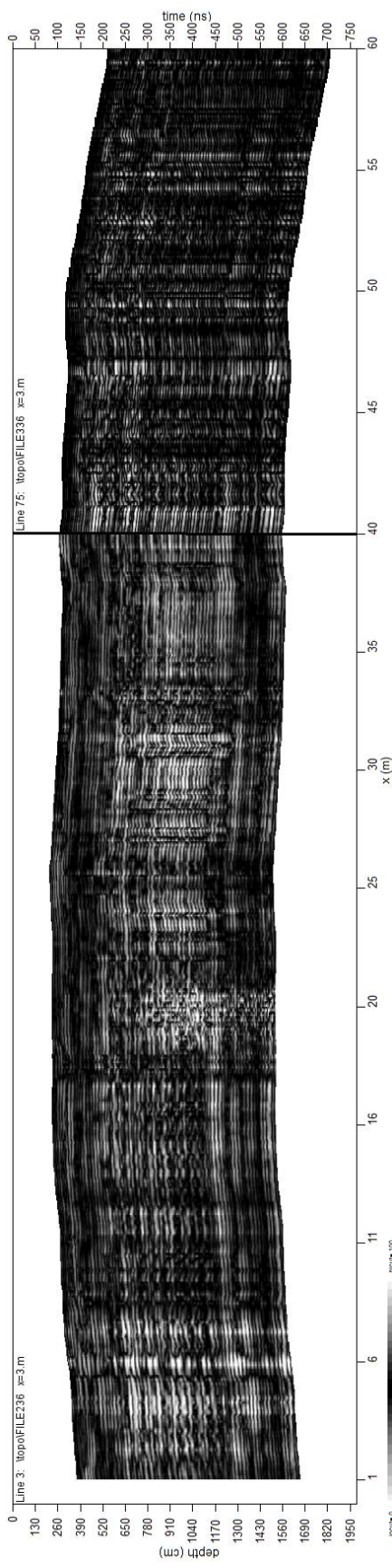**GPR Topographic Correction Data**

Plan 14

10. Compiled Topo-Corrected Radargrams of the UT Semi-circular Anomalies

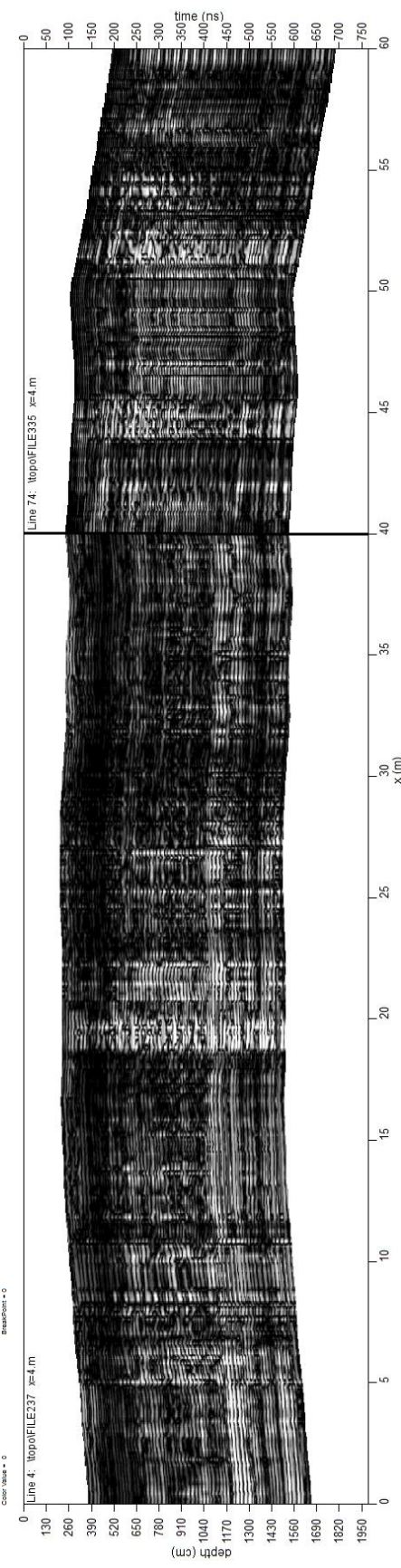**Radargram 1: Lines 1 & 77 composite.**
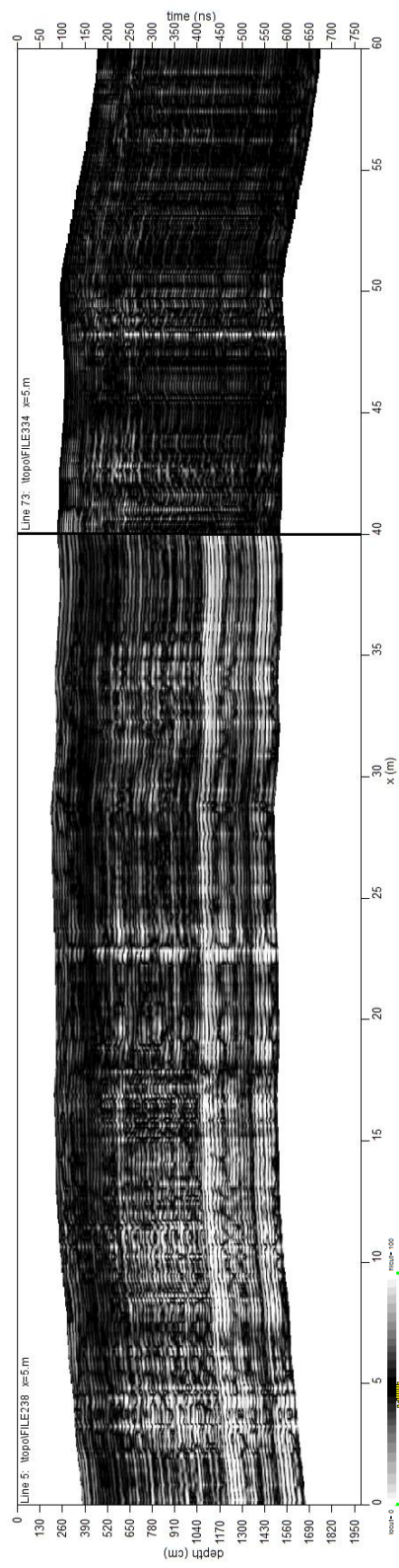
Radargram 2: Lines 2 & 76 composite.

Radargram 3: Lines 3 & 75 composite.

Radargram 4: Lines 4 & 74 composite.

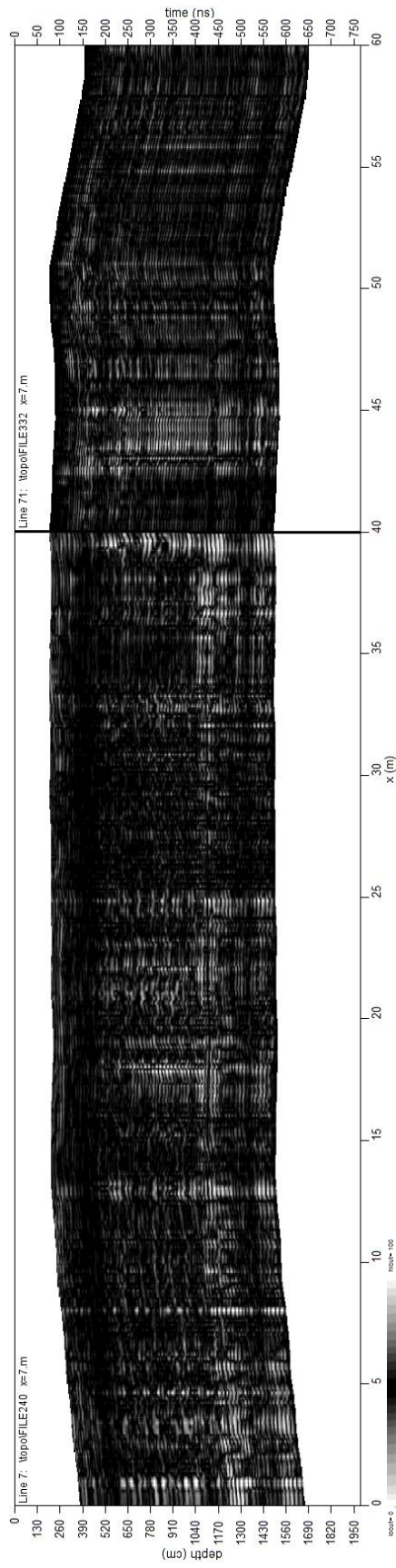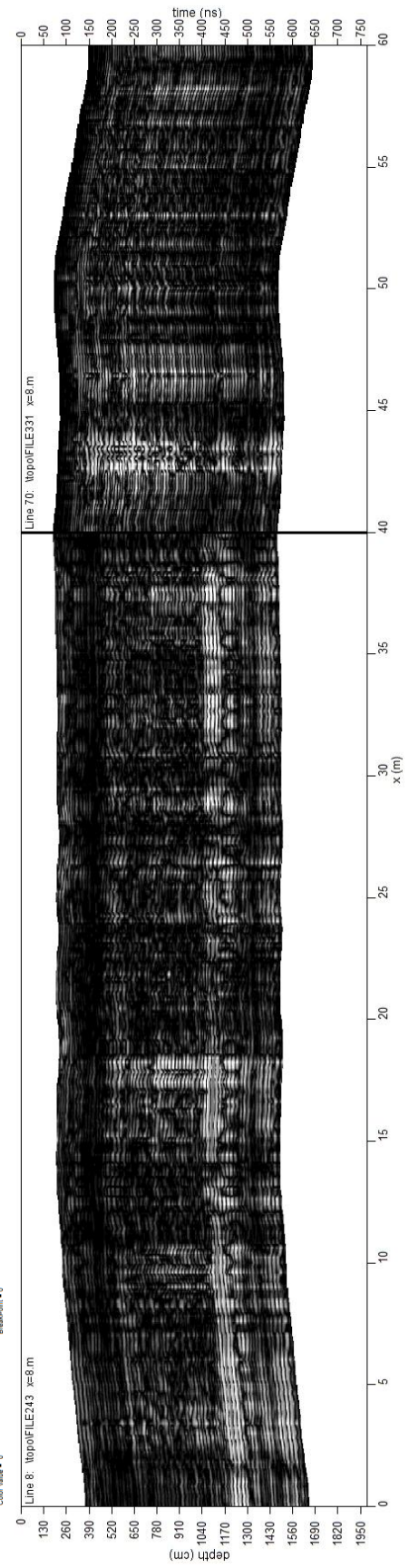**Radargram 5: Lines 5 & 73 composite.**
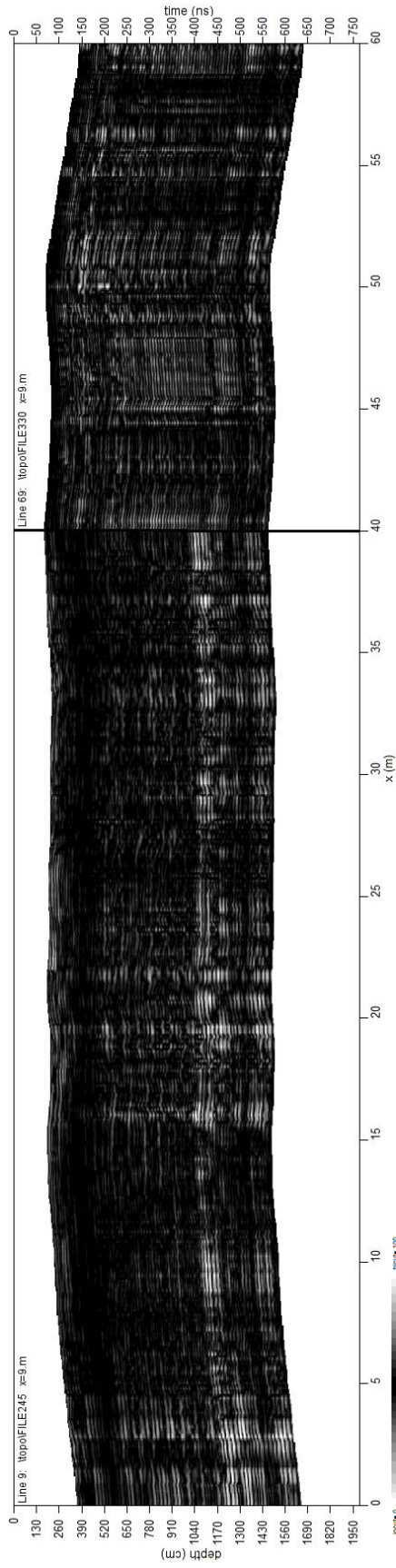
Radargram 6: Lines 6 & 72 composite.
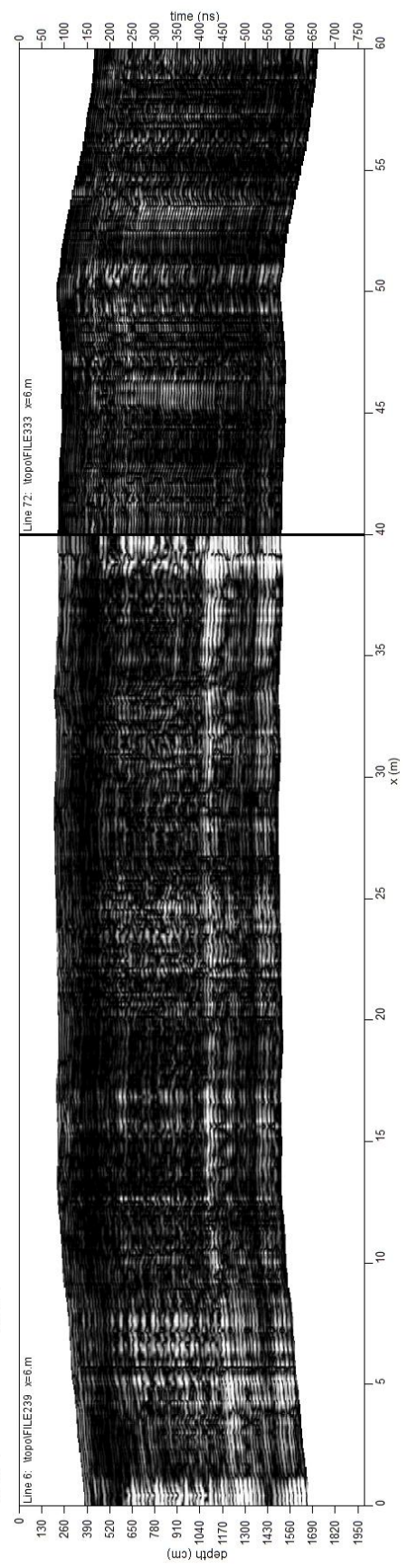
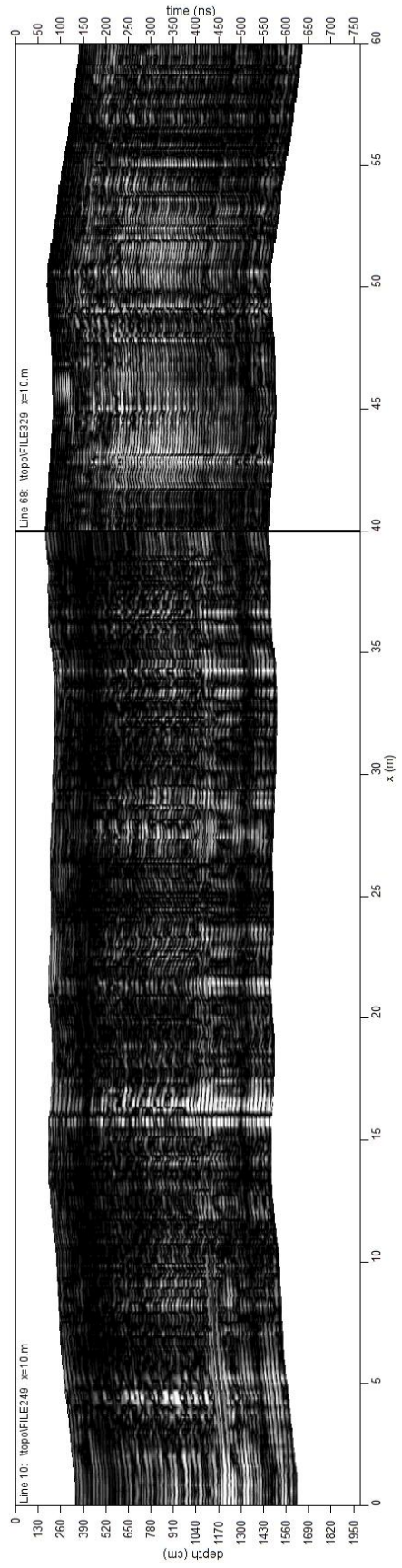**Radargram 7: Lines 7 & 71 composite.**

Radargram 8: Lines 8 & 70 composite.

Radargram 9: Lines 9 & 69 composite.

Radargram 10: Lines 10 & 68 composite.

11. Archive Location

The Laboratory for Geoarchaeology, Department of Geology, The University of Georgia,

210 Field Street, Athens, GA, 30602, USA.

12. Bibliography

Armit, I. (1990). Broch building in northern Scotland: The context of innovation. *World Archaeology, 21*(3), 435-445. doi:10.1080/00438243.1990.9980118

Armit, I. (1992). The Atlantic Scottish Iron Age: five levels of chronology. *Proceedings of the Society of Antiquaries of Scotland, 121*, 181-214.

Armit, I. (1999). The abandonment of souterrains: evolution, catastrophe or dislocation? *Proceedings of the Society of Antiquaries of Scotland, 129*, 577-596.

Armit, I. (2003). *Towers in the North: the Brochs of Scotland.* Stroud: Tempus.

Armit, I. (2005). *Celtic Scotland: Iron Age Scotland in its European Context.* London: B T Batsford & Historic Scotland.

Armit, I. (2007). Hillforts at War: From Maiden Castle to Taniwaha Pā. *Proceedings of the Prehistoric Society, 73*, 25-37.

Asăndulesei, A. (2011). Geophysical Prospecting Techniques Used in Archaeology: Magnetometry. *Studia Antiqua et Archaeologica, 17*, 5-17.

Batayneh, A., Khataibeh, J., Alrshdan, H., Tobasi, U., & Al-Jahed, N. (2007). The Use of Microgravity, Magnetometry, and Resistivity Surveys for the Characterization and Preservation of an Archaeological Site at Umm er-Rasas, Jordan. *Archaeological Prospection, 14*, 60-70.

Batcheler, C. L. (1960). A Study of the Relations Between Roe, Red and Fallow Deer, with Special Reference to Drummond Hill Forest, Scotland. *Journal of Animal Ecology, 29*(2), 375-384.

Bernardini, F., Sgambati, A., Kokelj, M. M., Zaccaria, C., Micheli, R., Gragiacomo, A., . . . De Min, A. (2013). Airborne LiDAR application to karstic areas: the example of Trieste province (north-eastern Italy) from prehistoric sites to Roman forts. *Journal of Archaeological Science, 40*, 2152-2160.

Birch, J. (2010). Coalescence and Conflict in Iroquoian Ontario. *Archaeological Review from Cambridge, 25.1*, 29-48.

Böniger, U., & Tronicke, J. (2010, July-August). Integrated data analysis at an archaeological site: A case study using 3D GPR, magnetic, and high-resolution topographic data. *Geophysics, 75*, B169-B176.

British Geological Survey. (2000). Schiehallion. Scotland Sheet 55W. Solid Geology. 1:50 000. [Map]. Keyworth, Nottingham: British Geological Survey.

Caesar, J. (1982). *The Conquest of Gaul.* (S. A. Handford, Trans.) New York: Penguin Books.

CFR. (2015, December 22). *Subpart F - Ultra-Wideband Operation.* (e-CFR, Ed.) Retrieved December 24, 2015, from U.S. Government Publishing Office: http://www.ecfr.gov/cgi-bin/text-idx?SID=f6cdbeb9c58acfa5ac9cc4d377b256fb&mc=true&node=sp47.1.15.f&rgn=div6

Challis, K., Forlin, P., & Kincey, M. (2011). A Generic Toolkit for the Visualization of Archaeological Features on Airborne LiDAR Elevation Data. *Archaeological Prospection, 18*, 279-289.

Chianese, D., Lapenna, V., Di Salvia, S., Perrone, A., & Rizzo, E. (2010). Joint geophysical measurements to investigate the Rossano of Vaglio archaeological site (Basilicata Region, Southern Italy). *Journal of Archaeological Science, 37*, 2237-2244.

Christison, D. (1900). The forts, "camps", and other field-works of Perth, Forfar and Kincardine. *Proceedings of the Society of Antiquaries of Scotland, 34*, 69-71.

Clark. (1970). Weem, Castle Menzies, cist, pit with quern stones. *Discovery and Excavation in Scotland*, 40.

Conyers, L. B. (2013). *Ground-Penetrating Radar for Archaeology.* Plymouth: AltaMira Press.

Cook, M. (2011). New evidence for the activities of Pictish potentates in Aberdeenshire: the hillforts of Strathdon. *Proceedings of the Society of Antiquaries of Scotland, 141*, 207-229.

Cook, M. (2012). The altered earth: excavations at Hill of Barra, Oldmeldrum, Aberdennshire. *Tayside and Fife Archaeological Journal*, 27-40.

Cowen, J. D. (1967). The Hallstatt sword of bronze: on the continent and in Britain. *Proceedings of the Prehistoric Society, 33*, 377-454.

Craig, G. Y. (Ed.). (1991). *Geology of Scotland* (3rd ed.). London: The Geological Society.

Crow, P. (2008). *Historic Environment Surveys of woodland using LiDAR.* Farnham: Forest Research.

Cunliffe, B. (1999). *The Ancient Celts.* London: Penguin Books Ltd.

Cunliffe, B. W. (2005). *Iron Age communities in Britain: an account of England, Scotland and Wales from the seventh century BC until the Roman conquest.* London: Routledge.

Dalland, M., & Wessel, J. V. (2011). Drummond Hill / Dun-da-Lamb / Dun Deardail / Torr Dhuin / Craig Phadrig, Highland / Perth and Kinross (Abertarff, Boleskine, Inverness and Bona, Kilmallie, Laggan / Dull parishes), survey. *Discovery and Excavation in Scotland, 12*.

Davidson, D. A., & Jones, R. L. (1990). The environment of Orkney. In C. Renfrew (Ed.), *The Prehistory of Orkney* (pp. 10-35). Edinburgh: Edinburgh University Press.

De Smedt, P., Saey, T., Lehouck, A., Stichelbaut, B., Meerschman, E., Islam, M. M., . . . Van Meirvenne, M. (2013). Exploring the potential of multi-receiver EMI survey for geoarcheological prospection: A 90 ha dataset. *Deoderma, 199*, 30-36.

Dirix, K., Muchez, P., Degryse, P., Kaptijn, E., Mušič, B., Vassilieva, E., & Poblome, J. (2013). Multi-element soil prospection aiding geophysical and archaeological survey on an archaeological site in suburban Sagalassos (SW-Turkey). *Journal of Archaeological Science, 40*, 2961-2970.

Dixon, N. (1982). Excavation of Oakbank Crannog, Loch Tay Interim Report. *International Journal of Nautical Archaeology, 11*(2), 125-132.

Dixon, T. N. (1981). Radiocarbon dates for crannogs in Loch Tay. *International Journal of Nautical Archaeology and Underwater Exploration, 10*, 346-7.

Dixon, T. N., Cook, G. T., Adrian, B., Garety, L. S., Russell, N., & Menard, T. (2007). Radiocarbon dating of the crannogs of Loch Tay, Perthshire (Scotland). *Radiocarbon, 49*(2), 673-684.

Dumayne, L. (1994). The Effect of the Roman Occupation on the Environment of Hadrian's Wall: A Pollen Diagram from Fozy Moss, Northumbria. *Britannia, 25*, 217-224.

Dumayne-Peaty, L. (1998). Human impact on the environment during the Iron Age and Romano-British times: palynological evidence for three sites near the Antonine Wall, Great Britain. *Journal of Archaeological Science, 25*, 203-214.

FCC. (2002, May 16). 47 CFR Part 15. *Federal Register, 47*(95), 34852-34860.

FCC. (2004, July 6). *GPR Service Providers Coalition 6516485331.* Retrieved December 24, 2015, from Federal Communications Commission: http://apps.fcc.gov/ecfs/document/view?id=6516485331

Feachem, R. (1963). *A guide to prehistoric Scotland.* London: Held at RCAHMS E.2.FEA.

Fojut, N. (1982). Towards a geography of Shetland brochs. *Glasgow Archaeological Journal, 9*, 37-59.

Gaffney, C. (2008). Detecting trends in the prediction of the buried past: A review of geophysical techniques in archaeology. *Archaeometry, 50*, 313-336.

Garrison, E. (2015, October). Personal Communication: Geophysical prospection at Caisteal Mac Tuathal. Athens, GA.

Gillies, W. A. (2005). *In Famed Breadalbane: The story of the antiquities, lands and people of a highland district.* Ellon: Famedram Publishers Ltd.

Goodman, D., & Piro, S. (2013). *GPR Remote Sensing in Archaeology.* New York: Springer.

Goodman, D., Nishimura, Y., Hongo, H., & Higashi, N. (2006). Correcting for Topography and the Tilt of Ground-penetrating Radar Antennae. *Archaeological Prospection, 13*, 157-161.

Google Inc. (2014). *Google Earth (Version 7.1.2.2041) [Software]*. Retrieved from https://www.google.com/earth/

Grant, R. (1981). Eastern Scotland. Soil Survey of Scotland. Sheet 5. 1:250 000. [Map]. Aberdeen: The Macaulay Institute for Soil Research.

Green, S., Bevan, A., & Shapland, M. (2014). A comparative assessment of structure from motion methods for archaeological research. *Journal of Archaeological Science, 46*, 173-181.

GSSI. (2001). *SIR System-2000 Operation Manual.* North Salem: Geophysical Survey Systems, Inc.

GSSI. (2009). *SIR System-3000 Manual.* North Salem: Geophysical Survey Systems, Inc.

Hale, A. (2000). Marine crannogs: previous work and recent surveys. *Proceedings of the Society of Antiquaries of Scotland, 130*, 537-558.

Harding, D. W. (2004). *The Iron Age in Northern Britain: Celts and Romans, natives and invaders.* New York: Routledge.

Historic Scotland. (2001). *Entry in the Schedule of Monuments, Re: The Monument known as Caisteal Mac Tuathal, fort 1200m NNW of Taymouth Castle in the Parish of Dull and County of Perth.* Historic Scotland. County of Perth: Registers of Scotland.

Historic Scotland. (2014). edit_CMTM14 with contour data*. [CAD Drawing]. Edinburgh: Rubicon Heritage.

Hughes, A. L., Clark, C. D., & Jordan, C. J. (2014). Flow-pattern evolution of the alst British Ice Sheet. *Quaternary Science Reviews, 89*, 148-168.

Hunter, F. (1997). Iron Age hoarding in Scotland and northern England. In A. Gwilt, & C. Haselgrove, *Reconstructing Iron Age Societies; New Approaches to the British Iron Age* (pp. 108-33). Oxbow: Oxbow Monographs.

Hutcheson, A. (1889). Notes on the stone circle near Kenmore and of some hill forts in the neighbourhood of Aberfeldy, Perthshire. *Proceedings of the Society of Antiquaries of Scotland, 23*, 147.

Lamb, R. G. (1980). *Iron Age Promontory Forts in the Northern Isles.* Oxford: British Archaeological Reports.

Lane, A., & Campbell, E. (2000). *Dunadd: an early Dalriadic capital.* Oxford: Oxbow.

LeBlanc, S. A. (1999). *Prehistoric Warfare in the American Southwest.* Salt Lake City: The University of Utah Press.

Lenfert, R. (2013). Integrating Crannogs and Hebridean Island Duns: Placing Scottish Island Dwellings Into Context. *Journal of Island and Coastal Archaeology, 8*, 122-143. doi:10.1080/15564894.2013.766912

Leopold, M., Gannaway, E., Völkel, J., Haas, F., Becht, M., Heckmann, T., . . . Zimmer, G. (2011). Geophysical Prospection of a Bronze Foundry on the Southern Slope of the Acropolis at Athens, Greece. *Archaeological Prospection, 18*, 27-41.

Leopold, M., Plöckl, T., Forstenaicher, G., & Völkel, J. (2010). Integrating pedological and geophysical methods to enhance the informative value of an archaeological prospection - The example of a Roman villa rustica near Regensberg, Germany. *Journal of Archaeological Science, 37*, 1731-1741.

Macinnes, L. (1984). Brochs and the Roman occupation of lowland Scotland. *Proceedings of the Society of Antiquaries of Scotland, 114*, 235-249.

MacKie, E. W. (1982). Excavations at Leckie broch, Stirlingshire, 1970-78: an interim report. *GAJ, 9*, 60-72.

MacKie, E. W. (2002). *The Roundhouses, Brochs and Wheelhouses of Atlantic Scotland c. 700 BC - AD 500: Architecture and Material Culture - Part 1.* Oxford: British Archaeological Reports.

Main, L. (1998). Excavation of a timber round-house and broch at the Fairy Knowe, Buchlyvie, Stirlingshire, 1975-8. *Proceedings of the Society of Antiquaries of Scotland, 128*, 293-418.

Malyshkin, G. S., Timofeev, V. N., & Turkalova, O. I. (2013). Resolution of Weak Signals and Estimation of Their Parameters in the Presence of Interfering Sources

in the Fresnel Zone Using Modern Adaptive Algorithms. *Acoustical Physics, 59*(4), 464-473.

McCormick, F. (2009). Ritual Feasting in Ireland. In G. Cooney, K. Becker, J. Coles, M. Ryan, & S. Sievers (Eds.), *Relics of Old Decency: Archaeological Studies in Later Prehistory: Festschrift for Barry Raftery* (pp. 405-412). Dublin: Wordwell.

Met Office. (2013, February 18). *Temperature, rainfall and sunshine time-series*. Retrieved November 2014, from Met Office: http://www.metoffice.gov.uk/climate/uk/summaries/actualmonthly

Milsom, J. (2003). *Field Geophysics.* West Sussex: John Wiley & Sons Ltd.

MISR. (1984). *Organization and Methods of the 1:250 000 Soil Survey of Scotland.* Aberdeen: The Macaulay Institute for Soil Research.

Munro, R. (1882). *Ancient Scottish Lake Dwellings.* Edinburgh: David Douglas.

Murdie, R. E., Goulty, N. R., White, R. H., Barratt, G., Cassidy, N. J., & Gaffney, V. (2003a). Comparison of Geophysical Techniques for Investigating an Infilled Ditch at Bury Walls Hill Fort, Shropshire. *Archaeological Prospection, 10*, 265-276.

Murdie, R. E., White, R. H., Barratt, G., Gaffney, V., & Goulty, N. R. (2003b). Geophysical Surveys of Bury Walls Hill Fort, Shropshire. *Archaeological Prospection, 10*, 249-263.

Murray, J. M. (1935). Drummond Hill. *Forestry, 9*, 17-33.

Noble, G., Gondek, M., Campbell, E., & Cook, M. (2013). Between prehistory and history: the archaeological detection of social change among the Picts. *Antiquity, 87*, 1136-1150.

NSA. (1834-35). *The new statistical account of Scotland by the ministers of the respective parishes under the superintendence of a committee of the society for the benefit of the sons and daughters of the clergy* (Vol. 10). Edinburgh: The New Statistical Account.

Parkhomenko, E. I. (1967). *Electrical Properties of Rocks.* (G. V. Keller, Trans.) New York: Plenum Press.

Piggott, S. (1951). Excavations in the broch and hill-fort of Torwoodlee, Selkirkshire, 1950. *Proceedings of the Society of Antiquaries of Scotland, 85*, 92-117.

Raven, J. A., & Shelley, M. (2003). South Uist and Benbecula duns (South Uist parish), survey. *Discovery and Excavation in Scotland, 4*, 136.

RCAHMS. (1927). *Plan of Kaimes Hill fort [map]*. Retrieved February 29, 2016, from Canmore: https://canmore.org.uk/collection/376692

RCAHMS. (1950-9). *Marginal Land Survey.* Held at RCAHMS A.1.1.MAR: (unpublished typescripts).

RCAHMS. (1956). Marginal Land Survey. *(unpublished typescripts), 3v*. Held at RCAHMS A.1.1.MAR.

RCAHMS. (1957). *Machair Leathann. Excavation photograph. Site B fully excavated, looking S. PRINTED IN REVERSE-*. Retrieved from Canmore: https://canmore.org.uk/collection/518388

RCAHMS. (1979). *The archaeological sites and monuments of Stirling District, Central Region. The archaeological sites and monuments of Scotland, series no. 7.* Edinburgh: The Royal COmmission on the Ancient and Historical Monuments of Scotland.

RCAHMS. (2009, December 5). *Oblique aerial view centred on the Broch of Gurness, taken from the NE.* Retrieved 2015, from Canmore: https://canmore.org.uk/collection/1144045

RCAHMS. (2015a). Retrieved from Royal Commision on the Ancient and Historical Monuments of Scotland: http://www.rcahms.gov.uk/

RCAHMS. (2015b). *Woden Law Hill Fort, Scottish Borders*. Retrieved from Royal Commission on the Ancient and Historical Monuments of Scotland: http://www.rcahms.gov.uk/index.php?option=com_rcahmsimagebank&view=ima gebank&Itemid=32&imageId=194

RCAHMS. (2016). Retrieved from Canmore: https://canmore.org.uk

Rego, J. P., & Cegielski, W. H. (2014, June). Gradiometry survey and magnetic anomaly testing of Castros de Neixón, Galicia, Spain. *Journal of Archaeological Science, 46*, 417-427.

Reynolds, D. M. (1982). Aspects of later prehistoric timber construction in south-east Scotland. In D. W. Harding, *Later Prehistoric Settlement in South-East Scotland* (pp. 44-56). Edinburgh: Edinburgh University.

Reynolds, J. M. (2011). *An Introduction to Applied and Environmental Geophysics* (2nd ed.). Oxford: John Wiley & Sons.

Richards, C. (Ed.). (2005). *Dwelling among the monuments: the Neolithic village of Barnhouse, Maeshowe passage grave and surrounding monuments at Stenness, Orkney.* Cambridge: McDonald Institute for Archaeological Research.

Romankiewicz, T. (2011a). *The Complex Roundhouses of the Scottish Iron Age* (Vol. I). Oxford: British Archaeological Reports.

Romankiewicz, T. (2011b). *The Complex Roundhouses of the Scottish Iron Age* (Vol. II). Oxford: British Archaeological Reports.

Rubicon Heritage. (2014). *Caisteal Mac Tuathall.* Edinburgh: Forestry Commision Scotland.

Ruffell, A., Geraghty, L., Brown, C., & Barton, K. (2004). Ground-penetrating Radar Facies as an aid to Sequence Stratigraphic Analysis: Application to the Archaeology of Clonmacnoise Castle, Ireland. *Archaeological Prospection, 11*, 247-262.

Shukla, M. K. (2014). *Soil Physics: An Introduction.* New York: CRC Press.

Simmons, G., Caruso, L., & Miller, F. (1981, January 29). Complex Dielectric Properties of Several Igneous and Metamorphic Rocks. *Defense Technical Information Center, AD A094301*.

Simpson, D. D. (1969). Excavations at Kaimes Hillfort, Midlothian, 1964-1968. *Glasgow Archaeological Journal, 1*, 7-28.

Simpson, D., Van Meirvenne, M., Lück, E., Bourgeois, J., & Rühlmann, J. (2010). Prospection of two circular Bronze Age ditches with multi-receiver electrical conductivity sensors (North Belgium). *Journal of Archaeological Science, 37*, 2198-2206.

Sinopoli, C. M. (1994). The Archaeology of Empires. *Annual Review of Anthropology, 23*, 159-180.

Tacitus, C. (1942). *Agricola.* (W. J. Brodribb, Trans.) New York: The Modern Library.

Taylor, J. D. (2012). American and European Regulations on Ultrawideband Systems. In J. D. Taylor (Ed.), *Ultrawideband Radar: Applications and Design* (pp. 105-158). Boca Raton: CRC Press.

Teixidó, T., Artigot, E. G., Peña, J. A., Molina, F., Nájera, T., & Carrión, F. (2013). Geoarchaeological Context of the Motilla de la Vega Site (Spain) Based on Electrical Resistivity Tomography. *Archaeological Prospection, 20*, 11-22.

Ulrich, B., Günther, T., & Rücker, C. (April 2-6, 2007). Electrical Resistivity Tomography Methods for Archaeological Prospection. In A. Posluschny, K. Lambers, & I. Herzog (Ed.), *Layers of Perception. Proceedings of the 35th International Conference on Computer Applications and Quantitative Methods in Archaeology (CAA)* (pp. 25 + CD-ROM). Berlin: Kolloquien zur Vor- und Frühgeschiechte, Vol. 10.

Verhoeven, G., Taelman, D., & Vermeulen, F. (2012). Computer Vision-Based Orthophoto Mapping of Complex Archaeological Sites: The Ancienct Quarry of Pitaranha (Portugal-Spain). *Archaeometry, 54*(6), 1114-1129.

Warner, R. (1980). Irish souterrains: Later Iron Age Refuges. *Archaeologica Atlantica, 3*, 81-99.

Watkins, T. F. (1980). Excavation of an Iron Age open settlement and souterrain at Newmill, near Bankfoot, Perthshire. *Proceedings of the Society of Antiquitaries of Scotland, 110*, 165-208.

Watson, W. J. (1915). Circular forts in Lorn and north Perthshire; with a note on the excavation of one at Borenich, Loch Tummel. *Proceedings of the Society of Antiquaries of Scotland, 49*, 17.

Woodbridge, J., Fyfe, R. M., Roberts, N., Downey, S., Edinborough, K., & Shennan, S. (2014). The imapct of the Neolithic agriculture transition in Britain: a comparison of pollen-based land-cover and archaeological 14C date-inferred population change. *Journal of Archaeological Science, 51*, 216-224.